

ENZYME-BASED DETOXIFICATION OF ORGANOPHOSPHORUS
NEUROTOXIC PESTICIDES AND CHEMICAL WARFARE AGENTS

A Dissertation

by

RORY JAMES KERN

Submitted to the Office of Graduate Studies of
Texas A&M University
in partial fulfillment of the requirements for the degree of

DOCTOR OF PHILOSOPHY

December 2007

Major Subject: Toxicology

ENZYME-BASED DETOXIFICATION OF ORGANOPHOSPHORUS
NEUROTOXIC PESTICIDES AND CHEMICAL WARFARE AGENTS

A Dissertation

by

RORY JAMES KERN

Submitted to the Office of Graduate Studies of
Texas A&M University
in partial fulfillment of the requirements for the degree of

DOCTOR OF PHILOSOPHY

Approved by:

Chair of Committee,
Committee Members,

James R. Wild
Melinda Wales
Kirby C. Donnelly
Timothy Phillips
Robert Burghardt

Chair of Toxicology Faculty,

December 2007

Major Subject: Toxicology

ABSTRACT

Enzyme-based Detoxification of Organophosphorus Neurotoxic

Pesticides and Chemical Warfare Agents. (December 2007)

Rory James Kern, B.S., Texas A&M University

Chair of Advisory Committee: Dr. James Wild

There are some 15,000 known organophosphorus chemicals. Some of these OP's, including VX and paraoxon, demonstrate an acute neurotoxicity due to the inhibition of cholinergic enzymes. Organophosphorus chemical warfare agents and pesticide neurotoxins are subject to hydrolysis by OP degrading enzymes. To be useful as a bioremediation or anti-chemical warfare agent, the enzyme must be tailored for, and integrated into, a practical application platform. Several studies have established enzyme-based countermeasures, describing such diverse applications as decontaminating foams for surface remediation, encapsulating enzyme with liposome for in vivo therapy, enzyme attachments to surfaces for biosensors and development of a corn expression system for large-scale enzyme production. The goal of the research described here is to select, investigate and improve the operational potential of organophosphate-degrading enzymes including Organophosphorus Hydrolase (OPH, 3.1.8.1) and Organophosphorus Acid Anhydrolase (OPAA, 3.1.8.2). Using saturation kinetics, the catalytic efficiencies of these two major detoxification enzymes were characterized with substrates representing each class of OP neurotoxin, phosphotriester, phosphothioate and

phosphofluoridate. OPH presents superior kinetic parameters with each OP class tested. Variants of OPH were created to increase the operational effectiveness of OP hydrolytic enzymes against phosphorothioates. An H254S/H257L mutation in the active site resulted in an improvement in the kinetics (k_{cat}/K_M) for the phosphorothioate, demeton-S. To screen potential vascular protection therapies, an in vitro protocol was developed to predict enzymatic effectiveness for protection of acetylcholinesterase from acute OP-inhibition. The protection abilities of the enzymes were directly related to their second order rate constants as inhibitory levels of OP are below the K_M of the enzymes. Consideration of contaminant nature concentration and enzyme kinetic parameters, k_{cat} and K_M , is critical to understanding decontamination and effective use of enzyme technology. These technologies continue to develop and provide promising new decontamination tools for OP compounds.

DEDICATION

To Stephanie

ACKNOWLEDGMENTS

I would like to thank my committee chair, Dr. Jim Wild, for his mentorship, enthusiasm and encouragement throughout my graduate career. I would also like to thank my committee members, Dr. KC Donnelly, Dr. Tim Phillips and Dr. Melinda Wales. Their classroom instruction, free and abundant advice, and genuine interest in my education has been paramount to my study here.

I would also like to acknowledge the laboratory researchers and all my fellow researchers I toiled along side, Dr. Janet Grimsley, Dr. Boris Novikov, Dr. David Armstrong, Dr. Tony Reeves, Dr. Mauricio Rodriguez, Dr. Scott Pinkerton, Dr. Shane Gold and Leamon Viveros. I have enjoyed and benefited greatly from their friendship and advice.

Lastly I would like to thank my family, especially my wife, Stephanie, for their support, encouragement, devotion and food. Without Dad, Mom, Pat, Toni, Barry, Linda, Kim and especially Cosmo, my efforts would be far less important.

TABLE OF CONTENTS

| | Page |
|--|------|
| ABSTRACT | iii |
| DEDICATION | v |
| ACKNOWLEDGMENTS..... | vi |
| TABLE OF CONTENTS | vii |
| LIST OF FIGURES..... | ixx |
| LIST OF TABLES | xi |
| CHAPTER | |
| I INTRODUCTION | 1 |
| Development of Organophosphorus Agents | 1 |
| Toxicokinetics of Organophosphates | 3 |
| Organophosphate Poisoning Treatment | 10 |
| OP Neurotoxin Mitigating Enzymes | 14 |
| Organophosphate Decontaminating Strategies | 24 |
| II DETAILED CATALYTIC CHARACTERIZATION OF ORGANOPHOSPHORUS HYDROLASE AND ORGANOPHOSPHORUS ACID ANHYDROLASE | 32 |
| Materials and Methods | 38 |
| Results | 42 |
| Discussion | 45 |
| III RATIONAL DESIGN OF OPH FOR TARGETED ENZYME EFFICACY | 51 |
| Materials and Methods | 59 |
| Results | 67 |
| Discussion | 69 |

| CHAPTER | Page |
|---------|--|
| IV | ANALYSIS OF THE IN VITRO PROTECTION OF ACETYLCHOLINESTERASE FROM INHIBITION BY OP NEUROTOXINS 85 |
| | Materials and Methods 91 |
| | Results 93 |
| | Discussion 103 |
| V | SUMMARY OF APPLICATIONS AND CONCLUSIONS 108 |
| | Dermal Protection with Enzyme Towelettes 108 |
| | Enhanced Enzyme Stability 110 |
| | Aerosol Fogging Decontamination 111 |
| | Conclusions 112 |
| | REFERENCES 115 |
| | VITA 128 |

LIST OF FIGURES

| FIGURE | | Page |
|--------|---|------|
| 1.1 | Organophosphate Compounds and Their Associated Physical Characteristics | 4 |
| 1.2 | Schematic of Neurotransmitters at Nerve Ending..... | 6 |
| 1.3 | Acetylcholinesterase Inhibition Reaction..... | 7 |
| 1.4 | Aging of Acetylcholinesterase | 9 |
| 1.5 | Oxime Reactivation of Unaged Acetylcholinesterase..... | 13 |
| 1.6 | Cholinesterase Structure..... | 17 |
| 1.7 | PON1 and Squid-type DFPase Structures..... | 20 |
| 1.8 | OPH Structure | 23 |
| 1.9 | Active Site of OPH..... | 25 |
| 1.10 | OPH Reaction..... | 26 |
| 2.1 | Enzyme Kinetics for OPH and OPAA | 43 |
| 2.2 | Substrate Saturation Curves | 47 |
| 3.1 | Molecular Description of the Active Site of OPH | 52 |
| 3.2 | Stereoisomers of Soman..... | 54 |
| 3.3 | Representative Binding of Demeton-S into WT OPH | 71 |
| 3.4 | Cut Away of the Wild Type and the F306L OPH Variant Active Sites | 74 |
| 3.5 | Energy Minimization of the F306L Variant..... | 76 |
| 3.6 | Hydrophobicity Change in the H254L Variant..... | 78 |

| FIGURE | | Page |
|--------|---|------|
| 3.7 | Representative Binding of the Demeton-S Hydrolysis Product into OPH..... | 81 |
| 4.1 | Reaction Scheme of Acetylcholinesterase Inhibition, Reactivation and Protection | 90 |
| 4.2 | Counteracting AChE Inhibition | 95 |
| 4.3 | Comparison of the Protection Potential (P_{50}) and Kinetic Character of OPH and OPAA..... | 98 |
| 4.4 | Comparison of the Protection Potential (P_{50}) and Kinetic Character of OPH Variants with the OP Compound, Demeton-S | 100 |
| 4.5 | Counteracting AChE Inhibition by Demeton-S | 102 |

LIST OF TABLES

| TABLE | | Page |
|-------|--|------|
| 1.1 | Enzyme Use of Substrate | 15 |
| 1.2 | Current United States Stockpile Status | 29 |
| 2.1 | Highest Reported Kinetic Values for the <i>B. diminuta</i> OPH and the <i>Altermonas sp JD6.5</i> OPAA..... | 34 |
| 2.2 | Correlation of OPH Activity with Metal Content | 36 |
| 2.3 | Kinetic Constants for OPH and OPAA with Paraoxon and DFP..... | 44 |
| 2.4 | Intravascular OP Levels. | 49 |
| 3.1 | OPH Stereoselectivity with Chiral Substrates..... | 56 |
| 3.2 | OPH Variants with Improved Demeton-S Activity | 58 |
| 3.3 | Design Rational for the Variants..... | 60 |
| 3.4 | Mutagenic Primers | 61 |
| 3.5 | Kinetic Values of the OPH Variants | 68 |
| 3.6 | WT Docking of Paraoxon and Demeton-S | 73 |
| 3.7 | Demeton-S Docking Energies and Positions | 84 |
| 4.1 | Concentration of Protectants (μM) and Inhibitors (μM) of AChE | 94 |
| 4.2 | AChE Protective Index (P_{50}) of Enzymatic Bioscavengers | 96 |
| 4.3 | AChE Protective Index (P_{50}) of Enzymatic Bioscavengers with Demeton-S..... | 101 |

CHAPTER I

INTRODUCTION

Development of Organophosphorus Agents

Organophosphorus (OP) compounds are esters of phosphoric acid; the first described organophosphate was tetra-ethyl pyrophosphate (TEPP) and is thought to have been made in 1854 by Wurtz (1). In 1937, a group of German scientists led by Gerhard Schrader at Farbenfabriken Bayer AG began the development of OP compounds as insecticides. Many of their initial compounds proved to be exceedingly toxic and were subsequently developed into the first nerve agent chemical weapons by the Nazis (2). The designation “G” arose from the markings on German chemical weapons found after the war: GA for tabun (ethyl N,N-dimethylphosphoramidocyanidate), GB for sarin (O-isopropyl methylphosphonofluoridate), GD for soman, (O-pinacolyl methylphosphonofluoridate) and GF for cyclosarin, (O-Cyclohexyl methylphosphonofluoridate). O-ethyl S-(2-diisopropylaminoethyl) methylphosphonothioate (VX) was created by the British in the 1950’s and adopted by

This dissertation follows the style of *Biochemistry*.

the United States for its burgeoning arsenal. The O-isobutyl S-(2-diethylamino) methylphosphonothioate (RVX) isomer has been produced by, and included in, the Russia stockpile. These compounds are termed V-agents and have increased toxicity over the G-agents (3). Subsequently, V and G organophosphate nerve agents have been produced as chemical warfare agents by several countries including Germany, the United States, Britain, Russia, Egypt, Iran, Libya, North Korea, Syria and Iraq (3). In response to the horrors of World War I, the Geneva Protocol of 1925 prohibited the use of asphyxiating, poisonous or other gases for chemical warfare, and the Chemical Weapons Convention (CWC) of 1997 called for the destruction of the signatory's military capacity to use chemical weapons (4, 5). In 1988, the first recorded use of a chemical agent by a government against its own civilian population occurred when Saddam Hussein used sarin against Kurdish villages in northern Iraq. This was followed, in 1994 and 1995, by the use of sarin by the Aum Shinrikyo terrorists against the Japanese civilian population, including an attack in the Tokyo subway, which killed a total of 19 people (4). In intervening years, there has been increased concern about these chemicals as a perceived threat to national security.

In addition, OP compounds have long been used for many agricultural purposes, most commonly as insecticides and pesticides, although there are some OP herbicides as well. Since the removal of organochlorine insecticides from use in the early 1970's, organophosphate insecticides have become the most widely used insecticides available today. More than forty OP active ingredients are currently registered for use today and all may induce acute and subacute toxicity (6). Today, many brands of OP pesticides are

available in the United States for agricultural and industrial purposes, with parathion being both most frequently used and involved in accidental poisonings (4, 7). Although most OP's are toxic to humans, they exhibit relatively low ecological toxicity, due to rapid microbial degradation, chemical and UV hydrolysis (8). OP compounds remain a popular method of pest control because they tend to be labile in the environment, lasting from hours to months, depending on the OP and environmental conditions (9).

Toxicokinetics of Organophosphates

OP compounds are esters of phosphoric acid and include phosphorothioates (P-S), phosphorfluoridates (P-F), phosphonates (P-CH₃), phosphorocyanidates (P-CN) and thion (P=S) moieties (10-14) (Figure 1.1). They tend to be lipophilic, which facilitates dermal absorption. This is especially true for the chemical warfare agents VX and RVX, for which the primary route of toxic exposure is dermal absorption. The nerve agents VX and RVX have a volatility of 10.5 mg/m³ and 8.9 mg/m³, respectively, and act primarily as a liquid via the percutaneous route (13, 15). Upon dermal contact, they easily pass through the skin into the vascular serum (15). Other OP's have a high volatility, such as sarin at 22,000 mg/m³, and act primarily via the respiratory route (15, 16). Ingestion is an important route of exposure in the case of suicides and accidental consumption. OP compounds are distributed by the vascular system, ultimately passing through the blood brain barrier to the target of their toxicity.

Chemical warfare agents are chiral at the phosphorus center and soman also contains a chiral pinacolyl group branched from the phosphorus. The S_P enantiomers of the G agents are more toxic, while the VX stereoisomers have similar toxicities (15).

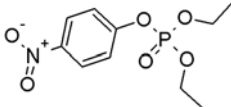
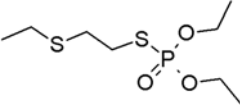
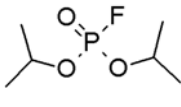
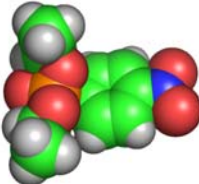
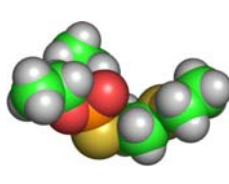
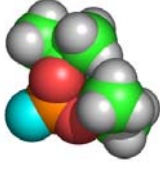
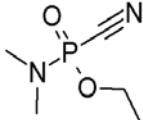
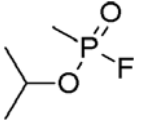
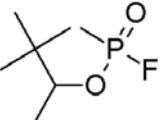
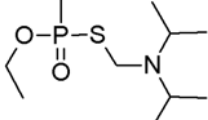
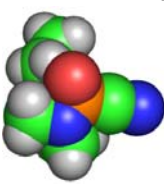
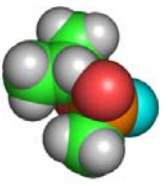
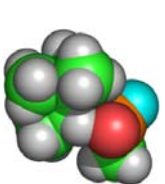
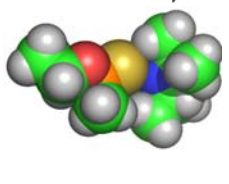
| | Pesticides | | | |
|-------------------------------------|---|---|--|---|
| | Paraoxon | Demeton-S | DFP | |
| |  |  |  | |
| |  |  |  | |
| Molecular Weight (C) | 275.2 | 258.36 | 184.15 | |
| Freezing Point (C) | | -25 | -82 | |
| Boiling Point (C) | 420 | 134 | 62 | |
| Vapor Pressure (mbar) | | 0.000255 | 0.579 | |
| Liquid Density (g/cm ³) | 1.274 | 1.132 | 1.055 | |
| Solubility (%) | | 0.2 | 1.54 | |
| LD ₅₀ (mg/kg) | 0.33 | 4.2 | 7.0 | |
| | Chemical Warfare Agents | | | |
| | Tabun (GA) | Sarin (GB) | Soman (GD) | VX |
| |  |  |  |  |
| |  |  |  |  |
| Molecular Weight (C) | 162 | 140 | 182 | 267 |
| Freezing Point (C) | -50 | -56 | -42 | -39 |
| Boiling Point (C) | 220-246 | 158 | 198 | 298 |
| Vapor Pressure (mbar) | 0.07 | 2.1 | 0.4 | 0.0007 |
| Volatility (mg/m ³) | 610 | 22,000 | 3,900 | 10.5 |
| Vapor Density (air=1) | 5.6 | 4.9 | 6.3 | 9.2 |
| Liquid Density (g/cm ³) | 1.073 | 1.102 | 1.022 | 1.008 |
| Solubility (%) | 10.5 | inf | 2.1 | 3.0 |
| Persistency Sunny, 15 C | 1-4 days | .25-4 hrs | 2.5-5 days | 3 days-3 weeks |
| Windy and rainy, 10 C | .5-6 hrs | .25-1 hrs | 3 hrs-1.5 days | 1-12 hrs |
| Calm, sunny, snow, -10 C | 1 day-2 weeks | 1-2 days | 1-6 weeks | 1-16 weeks |
| Ageing Half-life | 40 hrs | 5 hrs | 2 min | 40 hrs |
| LD ₅₀ (mg/kg) | 0.6 | 0.05 | 0.14 | 0.008 |
| Skin Penetration (min) | | 10-15 min | 10-15 min | 5-7 min |

Figure 1.1: Organophosphate Compounds and Their Associated Physical Characteristics.

For soman, the chirality of the phosphorus, rather than the chirality of the pinacolyl group, influences toxicity. For the chemical warfare agents, the S_P enantiomer is 20- to 130-fold more toxic than its R_P isomer (17).

The nature of OP neurotoxicity is determined by the reactivity of the phosphoryl center, as they bind to and inactivate acetylcholine esterases of target organisms (18). Acetylcholine (ACh), the synaptic transmitter released by cholinergic neurons, is synthesized by choline acetyltransferase (ChAT) and catabolized by acetylcholinesterase (AChE, E.C. 3.1.1.7) (Figure 1.2). Once produced in the pre-synaptic nerve ending, ACh is exported to the extracellular matrix between neurons where it interacts with muscarinic and nicotinic membrane receptors on the post-synaptic nerve ending, which in turn opens ion channels into the post-synaptic cell. The nonspecific cholinesterase, butylcholinesterase (BChE), also possesses the capacity to hydrolyze ACh, but is lower in concentration in the brain tissue than AChE (19). AChE is responsible for termination of impulse transmissions at synaptic junctions by cleaving the neurotransmitter ACh. The phosphoryl center of the neurotoxic OP covalently binds to the active site serine in AChE. This transient intermediate complex is then hydrolyzed with the loss of the leaving group, leaving a stable, phosphorylated, and largely, inhibited enzyme (Figure 1.3). Upon inactivation of AChE, ACh builds up between the neurons, causing an incessant signal. This overwhelms the nicotinic and muscarinic receptors, leading to continual stimulation of electrical activity. This in turn can lead to the acute effects of respiratory failure, central and peripheral nervous damage, loss of muscle control, cardiac arrest, and death.

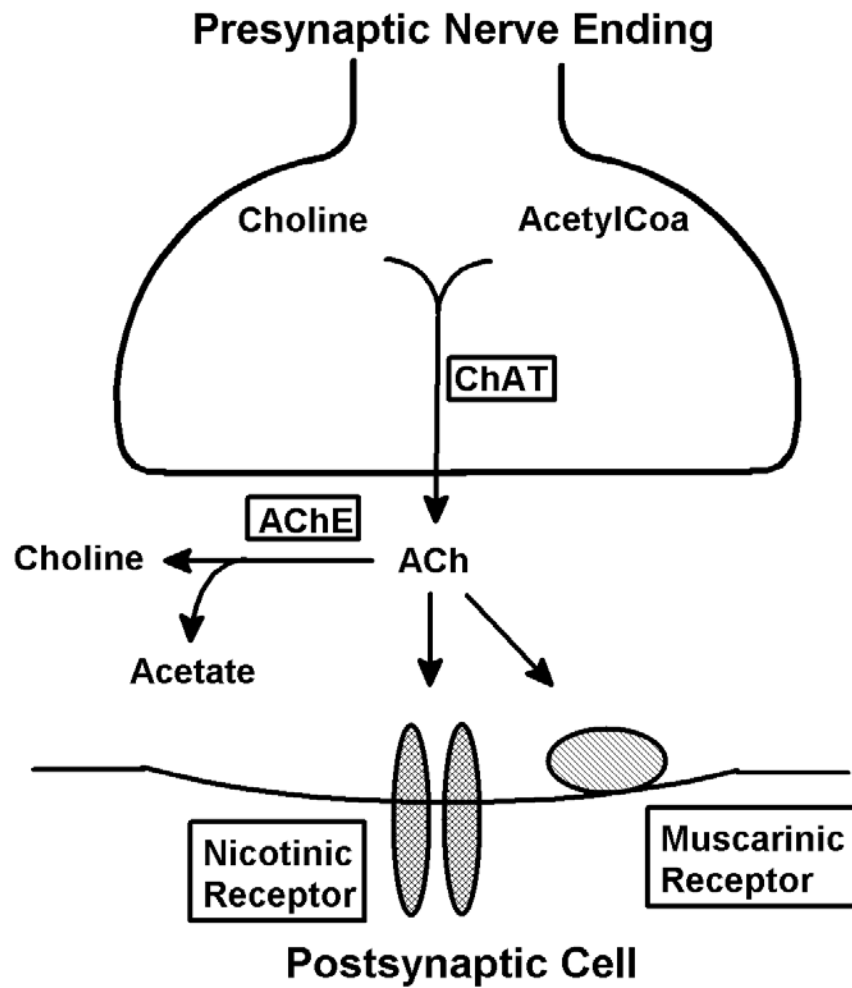


Figure 1.2: Schematic of Neurotransmitters at Nerve Ending. ChAT is Choline acetyl transferase, ACh is acetylcholine, AChE is acetylcholinesterase

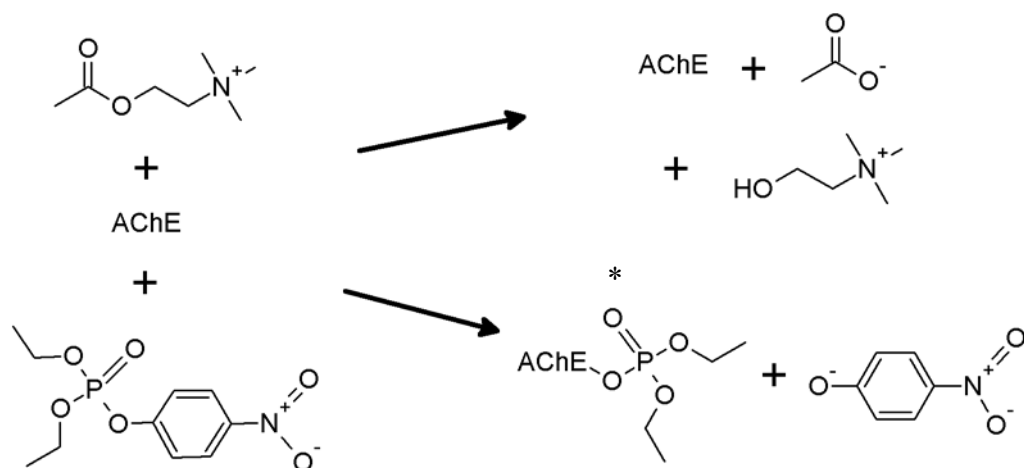


Figure 1.3: Acetylcholinesterase Inhibition Reaction. AChE hydrolyzes ACh to choline and acetate. The presence of an OP, in this case paraoxon, results in the phosphorylated and inactive AChE. The toxic endpoint for OP poisoning is represented by *.

The phosphorylated enzyme can also undergo an irreversible process called aging (Figure 1.4). This process, usually attributed to the loss of an alkyl group from the phosphoryl alkoxy substituent, is most pronounced for those compounds with branched alkyl groups, such as soman (20). The aging process of the phosphorylated AChE prevents treatment and exacerbates the effects of OP intoxication (21). Soman, with a pinacoyl group, has an ageing half-life of 2 minutes, while VX and tabun with ethyl groups have an ageing half-life of 40 hours. With many OP compounds, an irreversibly inhibited enzyme is formed. The signs and symptoms of intoxication are prolonged and persistent, lasting from weeks to years, and require vigorous medical intervention, including the reactivation of the enzyme with specific chemical antidotes (6).

The body metabolizes OP compounds with phase I and II enzymes, including the cytochrome P450's (P450) and glutathion-S transferases (GST). The compounds can undergo oxidative biotransformation at a number of atoms and/or bonds on the molecule, and the dominant pathways in each species determine sensitivity to OP compounds. For example, oxidative desulfuration of phosphorothioate (parathion, methyl parathion, fenitrothion, etc.) and phosphorodithioate (azinophos methyl, malathion, etc.) esters, results in a significant increase in toxicity of the products. In mammals, these oxon metabolites can then be hydrolyzed by an aryldialkylphosphatase, such as PON1. This is a major obligatory pathway in OP detoxification in mammals equipped with tissue aryl and aliphatic hydrolases. In contrast, insects can desulfonate the OP's, but are deficient in the hydrolases, making them more susceptible to OP poisoning (22). The P450 system can also facilitate dealkylation, dearylation, aromatic ring hydroxylation,

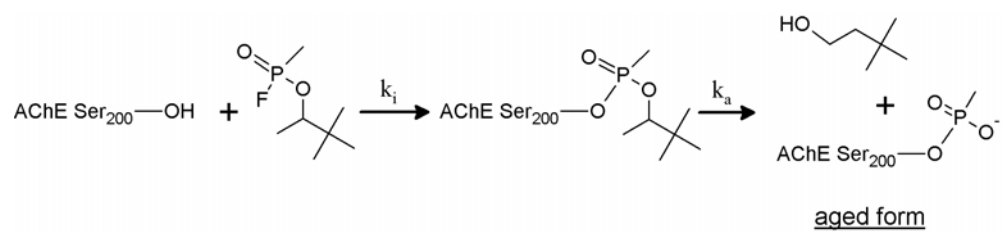


Figure 1.4: Aging of Acetylcholinesterase. Example used is soman.

thioether oxidation, and deamination. Phase II glutathion conjugative detoxification can occur with O-methyl and O-aryl groups on OP compounds, with some requiring previous modification from phase I enzymes. These pathways produce more hydrophilic metabolites that can be excreted more efficiently than the parent OP compound.

A less well-known feature of some neurotoxic organophosphates, such as mipafox and sarin, is their propensity to cause a delayed neuropathy that has been termed organophosphate-induced delayed neurotoxicity (OPIDN). OPIDN is a progressive neurological condition characterized by weakness, ataxia and subsequent paralysis of the limbs. The major neuropathological hallmark of OPIDN is degeneration of the long axons of the spinal cord and peripheral neurons (23). One postulated mechanism of action for OPIDN is the inhibition and aging of neuropathy target esterase (neurotoxic esterase, NTE, EC 3.1.1.1). OP compounds that both inhibit NTE by 70-90% and modify its structure by ageing result in OPIDN (24). Inhibition alone does not result in OPIDN, and the link between NTE aging and OPIDN is not absolute. It is postulated that other phosphorylated proteins are important in the acute and delayed effects of OP compounds (23). Candidates abound and a few, such as key protein kinases (protein kinase A, calcium/calmodulin-dependant protein kinase II), components of the cytoskeleton and transcription factors, have recently been implicated in the development of OPIDN (25-27). There remains controversy over this issue.

Organophosphate Poisoning Treatment

As previously described, OP compounds cause cholinergic overstimulation, leading to unique and highly characteristic poisoning symptoms which onset within

minutes to hours after exposure. Signs of OP poisoning can be grouped into 3 categories: muscarinic, nicotinic, and central. Muscarinic signs, which usually appear first, include hypersalivation, miosis (constriction of the pupil), frequent urination, diarrhea, vomiting, colic, and dyspnea due to increased bronchial secretions and bronchoconstriction. Subsequent nicotinic effects include muscle fasciculations and weakness. The long term central effects include nervousness, ataxia, apprehension, and seizures. Some OP neurotoxins (eg, amidothioates) do not enter the brain easily, so that CNS signs are mild. Onset of signs after exposure is usually within minutes to hours, but may be delayed for days depending on route of exposure. Severity and course of intoxication is influenced principally by the dosage and route of exposure. In acute poisoning, the primary clinical signs may be respiratory distress and collapse, followed by death due to respiratory muscle paralysis.

Traditional treatment of OP poisoning utilizes three categories of drugs: 1) muscarinic blocking agents, 2) cholinesterase reactivators, and 3) emetics, cathartics, and adsorbants to decrease further absorption. For example, diazepam acts as an anticonvulsant, while atropine is used as a muscarinic antagonist to affect release of ACh from the receptor (28). In moderately severe poisoning, defined as hypersecretion and other end-organ manifestations without central nervous system depression, adults and children over 12 years old receive 2.0-4.0 mg of atropine, repeated every 15 minutes until pulmonary secretions are controlled. Children under 12 years old receive 0.05-0.1 mg/kg body weight, with a minimum dose of 0.1 mg, repeated every 15 minutes until atropinization is achieved. Severely poisoned individuals may exhibit remarkable

tolerance to atropine, requiring two or more times these recommended dosages.

Reversal of muscarinic manifestations, rather than a specific dosage, is the objective of atropine therapy. Atropine does not alleviate the nicotinic cholinergic effects, such as muscle fasciculations and muscle paralysis, so that death from OP overdose can still occur. Atropine can be quite toxic itself, with fever, muscle fibrillations, and delirium presenting as the main indicators of atropine toxicity (6).

In some cases, oximes are employed as cholinesterase reactivators in an attempt to release active cholinesterase from the organophosphate-cholinesterase conjugates (29, 30) (Figure 1.5). One of the most commonly used oximes, pralidoxime chloride (2-PAM), is used in cases of severe poisonings. It is delivered either intramuscularly or by slow IV. Adults and children over 12 years old receive 1.0-2.0 g by intravenous infusion at a rate of no more than 0.2 g per minute. Children under 12 years old receive 20-50 mg/kg body weight (depending on severity of poisoning) intravenously. The currently available oximes cannot pass the blood-brain barrier, and so their action is limited to serum cholinesterase. Response to cholinesterase reactivators decreases with time after exposure; therefore, treatment with oximes must be instituted as soon as possible (within 24-48 hr) (6). The rate at which the organophosphate-cholinesterase conjugates become unresponsive to activators varies with the particular OP. The negatively charged oxygen atom is the oxime's nucleophile. The strength of the nucleophile, its orientation with respect to the phosphate conjugated to the active center serine, and aging of the organophosphate conjugate are three factors known to affect reactivation. Focusing on the nucleophilic strength and orientation considerations, various oximes have been

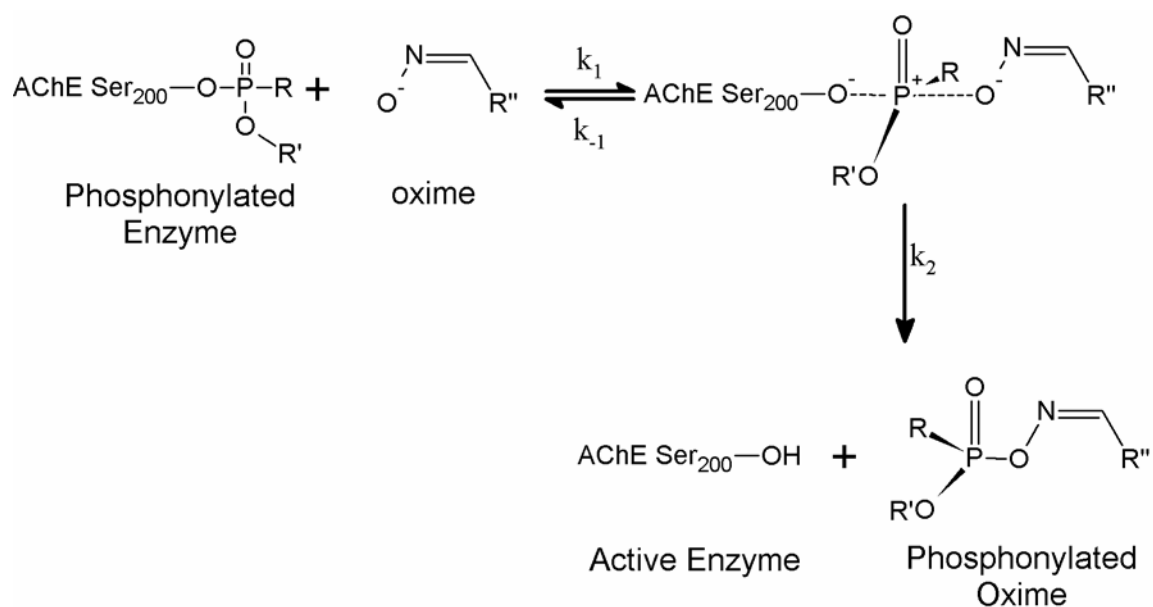


Figure 1.5: Oxime Reactivation of Unaged Acetylcholinesterase. R = O-CH₃, O-CH₂CH₃, CH₃, or CH₂CH₃ group. R' = CH₃, CH₂CH₃, or alkyl group, R'' = various oxime structures.

developed as cholinesterase reactivators (29), although one of the limitations to their use remains the relatively slow rate of reactivation they elicit. In contrast, ageing, which arises from cleavage of the carbon-oxygen bond on one of the alkoxy constituents of the conjugated organophosphate, results in an anionic phosphorylated conjugate that is resistant to all oximes (31).

OP Neurotoxin Mitigating Enzymes

Research has been conducted on the development of biological scavengers as an alternative therapeutic approach to the conventional treatment described above, as well as environmental applications. Their mode of action is to either sequester or hydrolyze the nerve agent (32, 33). The specificity and high catalytic rates of biological catalysts make them appropriate for decommissioning nerve agent stockpiles, counteracting nerve agent attacks, remediating pesticide spills and treatment of organophosphate exposures (33). There are several families of enzymes involved with OP mitigation: the cholinesterases, which are generally non-catalytic and can function as OP sponges, and the phosphotriesterases, which are usually categorized by their bond type hydrolysis. The phosphotriesterases are given the E.C. 3.1.8 designation and are further divided as aryl dialkyl phosphatases (E.C. 3.1.8.1) or DFPase (E.C. 3.1.8.2), even though some enzymes, such as OPH and PON1, could be placed in either category (11, 12, 34-49) (Table 1.1). DFPases were originally further segregated by molecular weight into squid-type DFPases (<40 kDa) and Mazur-type DFPases (40 to 96 kDa).

Cholinesterases. AChE, the neurotoxic target of OP compounds, could be used as a bioscavenger of an OP hazard (50). Human AChE is secreted into culture medium

Table 1.1: Enzyme Use of Substrate.

| | Paraoxon | | Demeton-S | | DFP | |
|--------------|----------|-------|-----------|------------|-----|-----|
| AChE | - | | - | | - | |
| BChE | - | | - | | - | |
| PON1 | + | | - | | + | |
| Squid DFPase | - | | - | | + | |
| OPAA | + | | - | | + | |
| OPH | + | | + | | + | |
| | Tabun | Sarin | Soman | Cyclosarin | VX | RVX |
| AChE | - | - | - | - | - | - |
| BChE | - | - | - | - | - | - |
| PON1 | + | + | + | + | - | - |
| Squid DFPase | + | + | + | + | - | - |
| OPAA | + | + | + | + | - | - |
| OPH | + | + | + | + | + | + |

as a mixture of monomers, dimers and tetramers (51, 52). The enzyme monomer is an alpha/beta protein that contains 537 amino acids (Figure 1.6A). It consists of a 12-stranded mixed beta sheet surrounded by 14 alpha helices and bears a striking resemblance to several hydrolase structures, including diene lactone hydrolase, serine carboxypeptidase-II, three neutral lipases, and haloalkane dehalogenase (53). The active site of AChE consists of two major subsites, the “esteratic” and “anionic” subsites, corresponding to the catalytic machinery and the choline binding pocket, respectively (29). AChE is catalytically efficient for the substrates ACh and acetylthiocholine (ASCh). The k_{cat}/K_M for ACh is $> 10^8 \text{ M}^{-1} \text{ sec}^{-1}$ and the k_{cat}/K_M for ASCh is $4.2 \times 10^9 \text{ M}^{-1} \text{ sec}^{-1}$ (54). Elucidation of the three-dimensional structure of *Torpedo californica* AChE showed that the active site contains a catalytic triad, consisting of S200, H440, and E327, similar to that present in other serine hydrolases (53, 55). This triad is located near the bottom of a 20 Å deep, and narrow, cavity named the “aromatic gorge”, since it is lined by the rings of 14 highly conserved aromatic residues (55, 56). AChE, in addition to its role in nerve signal transduction, can also be found in the blood stream and so provides a vascular target for OP compounds. Additional functions for AChE are based on the high levels of AChE observed in non-neuronal tissues such as blood cells, notably erythrocytes and megakaryocytes (57-59). The hematopoietic role of AChE is to reduce proliferation of multipotent erythropoietic and megakaryocytotpoietic stem cells and macrophages and promote apoptosis in the progeny of the stem cells (60).

Butylcholinesterase (BChE, EC 3.1.1.8) is found in the serum of mammals. The overall structure of human BChE is very similar to that of AChE. BChE is 529 amino

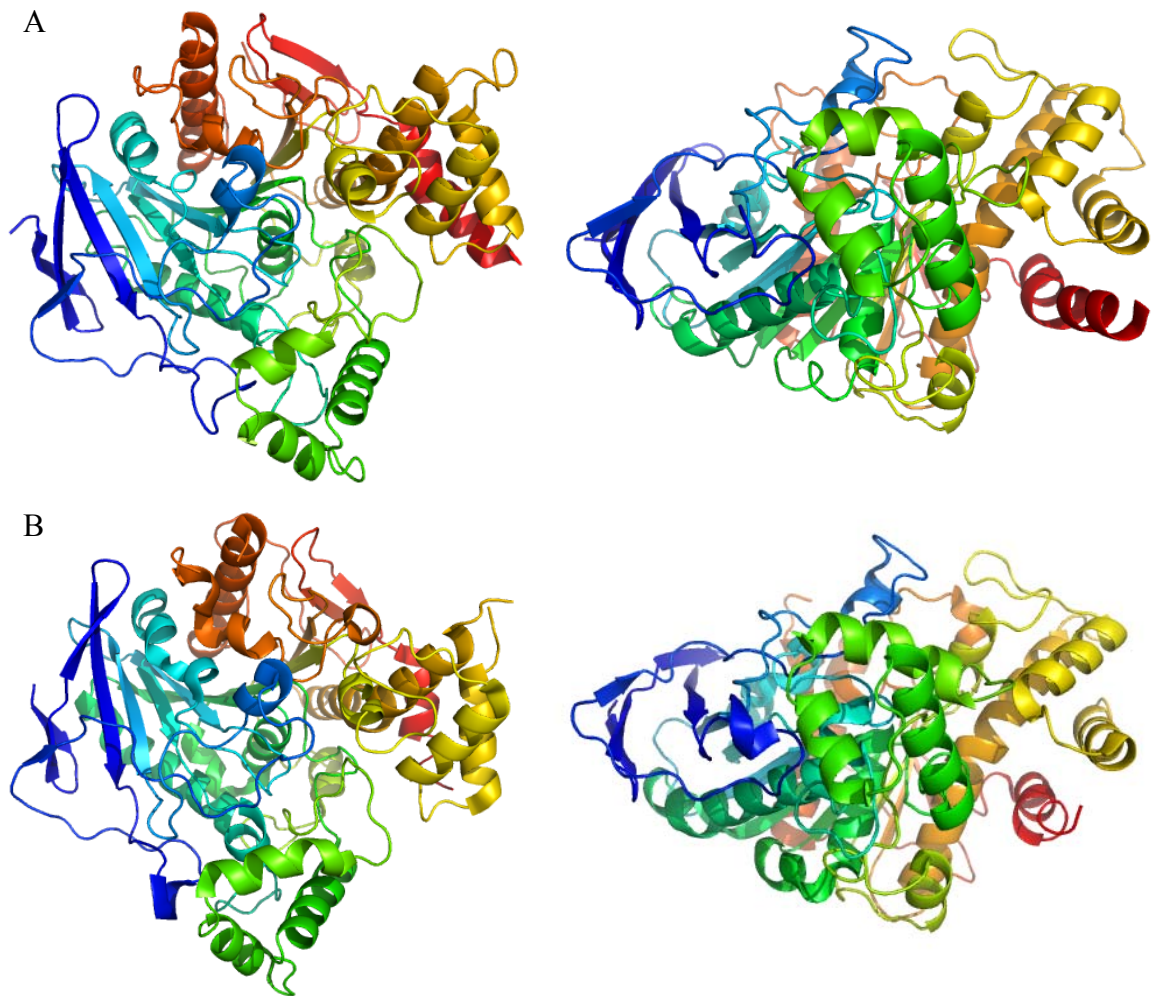


Figure 1.6: Cholinesterase Structure. A) AChE and B) BChE.

acids long and does not form a dimer or tetramer as has been observed in structures of AChE (52, 53, 61) (Figure 1.6B). Most of the amino acid differences between BChE and AChE are confined to the residues lining the aromatic gorge, where aromatic groups of AChE have been replaced by hydrophobic residues. Replacements of Phe288 and Phe290 of AChE by Leu286 and Val288, respectively; in the acyl-binding pocket make binding of the bulkier butyrate substrate moiety possible in BChE (61). The BChE k_{cat}/K_M with BSCh is $1.7 \times 10^7 \text{ M}^{-1} \text{ sec}^{-1}$ (62). Low levels of BChE, either through naturally occurring deficiencies or due to exposure to cholinesterase inhibitors, may cause reduction of hematopoietic levels of early megakaryocytes, suggesting the requirement of the BChE protein for megakaryopoiesis (63).

Substitution of Gly 117 with His (G117H) endowed BChE with the ability to catalyze the hydrolysis of organophosphate esters. Wild-type BChE is irreversibly inhibited by echothiophate and paraoxon, but G117H regains 100% activity within 2-3 min following reaction with these compounds. Echothiophate and paraoxon were hydrolyzed with the same k_{cat} of 0.75 min^{-1} . (64). A G117H/E197Q variant catalyzes soman hydrolysis, as well as sarin and VX. Reactions with VX and sarin regained 95% of initial BChE activity within 48 hours for sarin and 72 hours for VX. Rates were not determined for sarin and VX. Reactions with soman are stereospecific. Wild type BChE and the single substitutions G117H and E197Q had less than $0.000001 \text{ sec}^{-1}$ activity with soman, which is at the lower limit of detection. The double mutant of the histidine and glutamine residues created an enzyme capable of reactivation with rates of 0.0001, 0.0013, and 0.0021 sec^{-1} for the $P_{R/S}C_R$, $P_S C_S$, and $P_R C_S$ soman stereoisomers,

respectively. The protein design converted an archetypal “irreversible inhibitor” into a slow substrate for the target enzyme (62).

Phosphotriesterases. PON1 (aryldialkylphosphatase, E.C.3.1.8.1 or aromatic esterase E.C. 3.1.1.2) is a member of the PON family of proteins, which consist of PON1, PON2 and PON3. PON1 and PON3 reside in high-density lipoproteins and appear to prevent lipid oxidation in low-density lipoprotein, thus reducing levels of oxidized lipids involved in the initiation of atherosclerosis. PON2 and PON3 share a 60% sequence identity with PON1, but demonstrate no paraoxonase activity. PON1 takes the shape of a 45 kDa, 355 amino acid β -propeller with 2 Ca^{2+} ions in the center channel required for catalysis and a disulfide bridge between Cys42 and Cys353 (65-67) (Figure 1.7A). PON1 hydrolyzes homocysteine thiolactone, a compound formed as a result of editing reactions of some aminoacyl-tRNA synthetases. Because reactions of thiolactone with proteins are potentially harmful, the ability to detoxify homocysteine thiolactone is essential. Substrate specificity studies suggest that homocysteine thiolactone is a possible natural substrate of this enzyme with a k_{cat} of 0.95 sec^{-1} , a K_{M} of 23 mM and a $k_{\text{cat}}/K_{\text{M}}$ of $4.1 \times 10^1 \text{ M}^{-1} \text{ sec}^{-1}$.

The PON1 gene contains 2 polymorphic sites at amino acid positions L55M and R192Q. These variants affect gene expression and OP hydrolysis activity, with the LR variant, having a k_{cat} of 45 sec^{-1} , a K_{M} of 0.9 mM and a $k_{\text{cat}}/K_{\text{M}}$ of $5 \times 10^5 \text{ M}^{-1} \text{ sec}^{-1}$ with paraoxon (34). Insecticide and nerve gas hydrolysis by serum paraoxonase is a major factor determining OP toxicity to vertebrates and PON1 is the mammalian enzyme capable of hydrolyzing these OP's. PON1's activity was initially detected in rabbit,

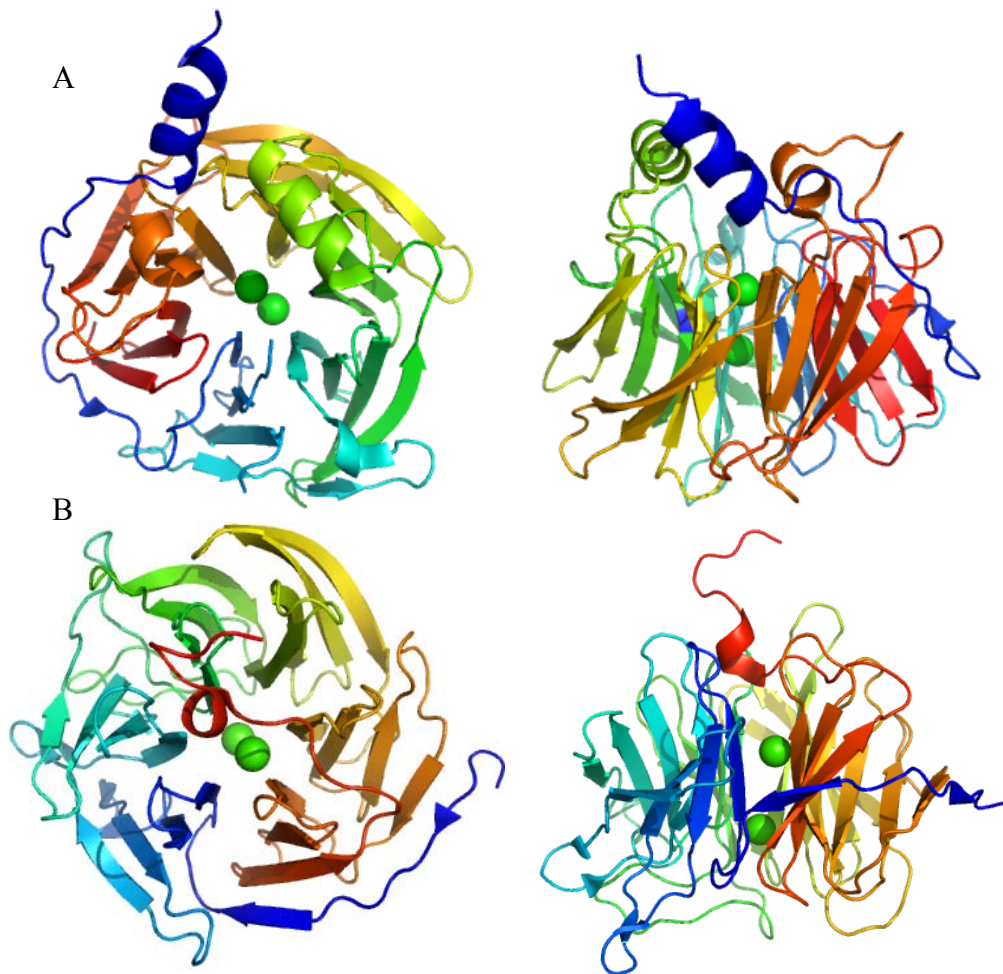


Figure 1.7: PON1 and Squid-type DFPase Structures. Top-down and side views of the A) PON1 and B) Squid-type DFPase β -propeller proteins. The green spheres represent the Ca^{2+} ions required for activity.

human and monkey plasma and red blood cells (35), and characterized as a Mazur type DFPase, named after its discoverer. This enzyme is responsible for hydrolyzing the oxidized thioate moieties produced by the P450 system and can hydrolyze the P-O, P-F, and P-CN bonds.

Diisopropylfluorophosphatases (DFPase, E.C. 3.1.8.2), also known as squid type DFPase (*Loligo vulgaris*), are capable of cleaving the P-F bond of fluorophosphates. As a 35 kDa, 314 amino acid β -propeller, DFPase's structure is similar to PON1 (Figure 1.7B) (68, 69). Squid type DFPase was purified from brain and ganglia of squid *Loligo vulgaris* (68, 70). Although squid type DFPase has substrate preference for DFP, it is also able to hydrolyze soman and sarin at approximately 1/10 that of DFP. The hydrolytic activity toward paraoxon is very low compared with P-F substrates (36).

Organophosphorus Acid Anhydrolase (OPAA, E.C. 3.1.8.2 or 3.4.13.9), originally characterized as a DFP hydrolyzing enzyme, was cloned and purified from *Alteromonas sp*, and later found to be a proline dipeptidase that cleaves a dipeptide bond with a prolyl residue at the carboxy terminus (Xaa-Pro) (71, 72). The enzyme is a 60 kDa monomer metalloprotease with manganese in its native form. The crystal structure of OPAA has not yet been elucidated. Many organisms have a form of this enzyme, which may or may not have OP hydrolyzing activity and seems to have a role in amino acid or protein metabolism. The activity of the proline dipeptidase with organophosphorus compounds has been proposed to be due to the similarity of the physical and chemical properties shared by these compounds and the dipeptide substrates (38, 72, 73). However, this seems unlikely, as OPAA's substrates, DFP and a

C-terminal proline dipeptide for example, are very dissimilar. OPAA is well documented in its ability to hydrolyze the P-F bonds of DFP, sarin and soman, but has slow P-O or P-CN and no P-S, hydrolysis activity (71). The K_{MS} reported for DFP, GB, GD, and GF were 2.99, 1.57, 2.48 and 0.63 mM and k_{cat} s of 230, 442, 151 and 652 sec^{-1} , respectively. It was also shown that OPAA from *Alteromonas sp. JD6.5* hydrolyzes paraoxon at 2% the rate of DFP (72).

Organophosphorus Hydrolase (OPH, E.C. 3.1.8.1) is found in only a few organisms and was originally isolated as identical plasmid-borne genes from *Brevundamonas (Pseudomonas) diminuta* and *Flavobacterium sp. (ATCC 27551)* (74-77). OPHs have also been found in *Flavobacterium bulustinum*, *Chryseobacterium bulustinum*, *Deinococcus radiodurans* and *Agrobacterium radiobacter* with a homology of 94.6%, 94.6%, 94.6%, and 87.7% at the protein level, respectively. OPH is an $(\alpha\beta)_8$ member of the TIM Barrel-fold family of hydrolases. The enzyme is a homodimer with a molecular weight of 72 kDa and has a large conformational stability contributed, at least in part, by the protein's organization at the tertiary and quaternary level (78, 79) (Figure 1.8). A carboxylated lysine and four histidine residues, which coordinate the two divalent cations, are required in the active-center for activity. The metals in turn coordinate an activated hydroxyl that functions as the nucleophile in the OP hydrolysis reaction. Although the identity of the divalent metal ions in the active-center influences the activity and stability of the enzyme, Zn^{2+} (the native), Co^{2+} , Cd^{2+} , Ni^{2+} or Mn^{2+} all support the catalytic activity of the enzyme (80-84). A two Zn^{2+} center has the greatest effect on stability, while a two Co^{2+} center increases the activity (300%) of the enzyme

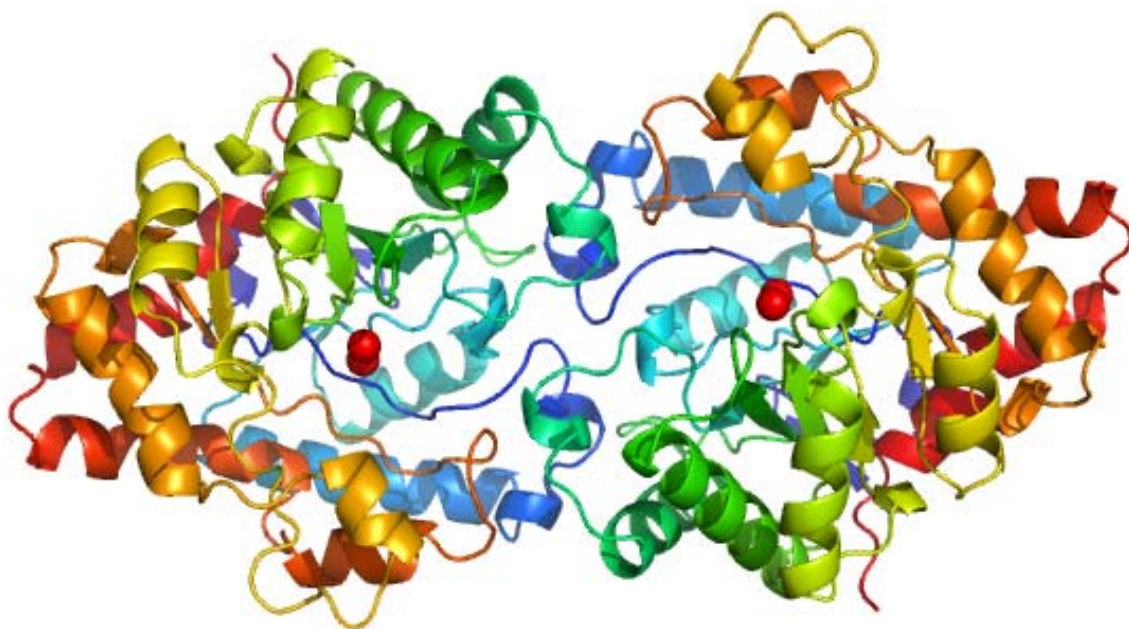


Figure 1.8: OPH Structure. The red spheres represent the Zn²⁺ ions present in the active site.

at the expense of stability (60%) (85). The active site is composed of a small and a large pocket for the substrate, which brackets the activated hydroxyl (10, 86) (Figure 1.9). It has been proposed that the large hydrophobic end of substrates such as VX and demeton-S reside in the leaving group pocket during cleavage. There are several residues that make up this pocket including H254, H257 and F306 (81).

The enzyme-mediated hydrolysis of phosphotriesters has been shown to occur through a S_N-2 like mechanism where an activated water molecule attacks the phosphorous center of the substrate. This results in the cleavage of the P-O bond (87). OPH is currently known to be capable of hydrolyzing the phosphotriester P-O bond of paraoxon (Figure 1.10), the phosphonofluoride bond P-F of DFP, sarin and soman, and the phosphorothioate bond P-S of demeton-S and VX and the phosphoramidocyanide bond P-CN of tabun (49, 79). OPH's preferred substrate, paraoxon, is hydrolyzed ($10^8 M^{-1} sec^{-1}$) approaching diffusion-controlled rates ($10^{10} M^{-1} sec^{-1}$) while the hydrolysis of the P-S and P-F bonds occurs at much slower rates.

Organophosphate Decontamination Strategies

Decontamination strategies can fall into at least two formats, personal protection and environmental decontamination. Personal protection includes medical treatment or prophylaxis, dermal decontamination and person protective equipment (PPE). Environmental decontamination includes chemical warfare agent stockpile destruction, building and surface decontamination, and low-level, agriculture and household related, pesticide mitigation.

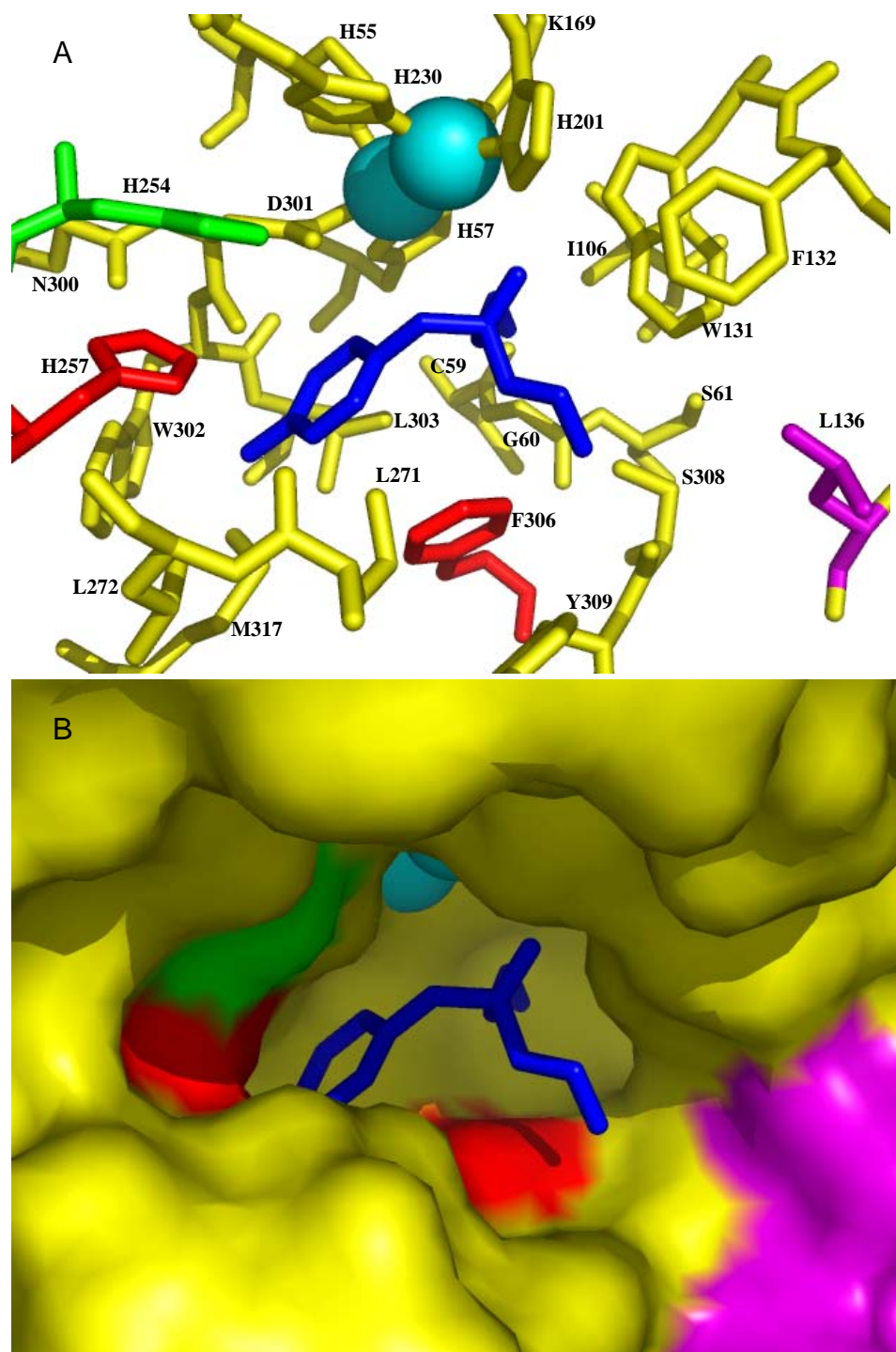


Figure 1.9: Active Site of OPH. Cyan spheres represent metals, the blue sticks represent the inhibitor. The green surface is H254. The red surfaces are the H257 and F306 residues. The purple surface is the contribution from the adjacent subunit. A: Stick representation. B: Surface representation.

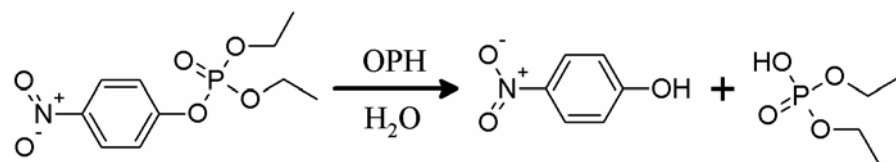


Figure 1.10: OPH Reaction. Schematic representation of the reaction catalyzed by the enzyme OPH on paraoxon.

Personal Treatment or Protection. Mission Oriented Protective Posture

(M.O.P.P.) gear is the military's PPE to be used in a toxic environment. It consists of a protective mask, overgarments, which are clothing equipped with a charcoal lining to absorb agents and worn over the normal uniform, and gloves and overboots made of butyl rubber. This equipment can be worn in appropriate combinations determined by the threat. For non-military personnel, a Hazmat suit is most commonly used. It is a fully encapsulating garment combined with a breathing apparatus used by researchers, firefighters and other emergency personnel. Levels of protection range from A (the highest) to C. In addition, topical systems for pre-exposure dermal protection have been in use since the Army introduced the M-5 ointment at the end of World War II (88, 89). However, poor barrier effectiveness, which included reduced efficacy when subjects perspired and only a retardation of the absorption of the chemical agents, resulted in a recall of this product. PEG-based topical skin protectants (TSP) are being developed that act by either slowing the absorption of or sequestering target compounds; however, they do not actively decontaminate. Thus, there is a push for a reactive TSP that would protect by decontaminating the toxicant before it is dermally absorbed (88, 89). Reactive Skin Decontamination Lotion (RSDL) is a patented, broad spectrum skin decontamination product intended to remove or neutralize chemical warfare agents from the skin. Originally developed for the Canadian Department of National Defense (DND), RSDL has since been adopted by several military services around the world, and is currently undergoing final configuration testing by the U.S. Department of Defense for eventual deployment with U.S. troops. Dermal decontamination of an individual

exposed to chemical warfare agents typically would use a cloth wetted in the undiluted household bleach followed by washing with lukewarm soapy water and rinsing with clear lukewarm water (90). Currently there are no practical models for the decontamination of mass casualties in a healthcare response (91, 92). As previously discussed the current treatment for an OP exposure is a drug therapy, consisting of oxime, atropine and anticonvulsant. Enzymes have been introduced as an alternative or addition to this therapy. Vascular treatments have been proposed using AChE and BChE as bioscavengers of OP's (50). OPAA and OPH have been encapsulated within erythrocytes and liposomes for vascular drug delivery (14, 93, 94).

Environmental Decontamination. As agreed to in the Chemical Weapons Convention of 1997, there are 30,000 tons of weapons material, including sarin nerve agent, VX nerve agent, and mustard gas, that must be destroyed. The storage and destruction of these agents takes place at the U.S. Army's Chemical Materials Agency (CMA) storage facilities. To destroy the vast U.S. arsenal and come into compliance with the treaty, the army uses two techniques: incineration and neutralization (95, 96) (Table 1.2). At all facilities, the chemical agents are drained from their containers (usually a munition) and then pumped to the treatment area. In those facilities which utilize neutralization, the agent is diluted with either hot water, in the case of mustard agents, or sodium hydroxide, in the case of V-agents. The liquid mixture is processed, treated, and products released into the public water system. The Newport, IN facility uses a neutralization process, which involves a two-stage supercritical water oxidation. The Army originally planned to transport the wastewater produced in Indiana to a

Table 1.2: Current United States Stockpile Status.

| | Agents | Disposal Process | Tons Remaning | % Destroyed |
|----------------|------------|---------------------|------------------|----------------|
| Tooele, UT | HD | Incineration | 6,263 | 63 |
| Johnston Atoll | None | Incineration | 0 | 100 |
| Anniston, AL | VX, HD | Incineration | 1,826 | 27 |
| Hermiston, OR | VX, GB, HD | Incineration | 3,197 | 26 |
| Pine Bluff, AR | VX, GB, HD | Incineration | 3,657 | 13 |
| Newport, IN | VX | Neutralization | 1,117 | 54 |
| Edgewood, MD | None | Neutralization | 0 | 100 |
| Pueblo, CO | HD | Neutralization | 2,611 | 0 |
| Richmond, KY | VX, GB, HD | Neutralization | 523 | 0 |

DuPont hazardous-waste treatment facility in New Jersey for secondary treatment.

Because of opposition from the states of Delaware and New Jersey and several environmental groups, the Army has not transferred the wastewater and is instead storing it on-site. Without secondary treatment, OPCW doesn't consider the nerve agent destroyed and the United States, therefore, receives no credit for the first stage of the destruction process and cannot apply the quantity of VX now rendered less toxic toward meeting the deadline (97). Recently, the Army signed a \$49 million contract with Veolia Environmental Services, a hazardous waste treatment facility based in Port Arthur, Texas. On April 16, the Army began trucking containers of the caustic wastewater, called hydrolysate, across eight states. Veolia began incinerating the hydrolysate on April 20 (98).

In those facilities that utilize incineration, furnaces separately heat the chemical agents and the containers to 2000°F. The fumes pass through a pollution abatement system, and post-incineration remnants are disposed of as hazardous wastes (95). For the remediation of OP contaminated buildings, the EPA has recommended the use of several chemical decontaminants, two household chemicals, hypochlorite and hydrogen peroxide, and two commercial grade decontaminants, Sandia and Cascad. Although each is effective at decontaminating OP compounds to varying extents, there are secondary issues with each that must be considered. For example, hypochlorite is a corrosive oxidant and waste products should be managed and disposed of as hazardous waste. Hydrogen peroxide is an oxidant and breaks down to water and oxygen after treatment and may be used in vapor form. Sandia foam will rust bare steel and the foam

requires removal and may be contaminated. Cascad foam requires removal and also may be contaminated (99) In addition to the CWA, agricultural pesticide use and indoor residential pest control contribute to the low level environmental OP contamination. Children, more than adults, have been the target of toxicity due to their higher surface area to volume ratio and higher soil intake, yet there is no common method for agriculture pesticide clean up other than soap or bleach and water (100).

It was the goal of this research to explore the strengths and limitations of OP-degrading enzymes for use in operationally feasible applications. Representatives of the two major families of OP degrading enzymes were screened to select for application-oriented suitability. An in vitro screening method was developed to facilitate in vivo evaluation of enzymes for potential efficacy in vascular OP treatment.

CHAPTER II

DETAILED CATALYTIC CHARACTERIZATION OF ORGANOPHOSPHORUS HYDROLASE AND ORGANOPHOSPHORUS ACID ANHYDROLASE

Eukaryotic OP degrading enzymes are difficult to produce and are less efficient than their prokaryotic counterparts. Production of enzyme is most efficient in bacterial expression systems and the production of the eukaryotic enzymes can require more complex cellular machinery than prokaryotic enzymes. Therefore, only the prokaryotic enzymes OPH and OPAA were compared. There exist discrepancies in the literature as to the kinetic capabilities of these bacterially-derived enzymes. This is primarily due to variation in the enzyme preparations and assays, which includes differences in purification, buffer conditions, metal content, measurement device and substrate range. For example, OPH's reported k_{cat} with paraoxon varies from 0.76 sec^{-1} to $15,000 \text{ sec}^{-1}$ and OPH's reported k_{cat} with DFP varies from 41 sec^{-1} to $3,500 \text{ sec}^{-1}$ (11, 37, 48, 101). OPAA's reported k_{cat} with DFP varies from 230 sec^{-1} to $1,820 \text{ sec}^{-1}$ (38, 72). K_{MS} can vary similarly. OPH with DFP ranges from 0.012 mM to 1.42 mM and OPAA with DFP ranges from 0.54 mM to 3.0 mM . A literature review of OPAA and OPH follows, with particular attention paid to preferred substrates for the enzymes, paraoxon and DFP.

The Mauzer and squid type enzymes were the first OP hydrolases discovered. A standard assay was established for the monitoring of enzymatic P-F bond hydrolysis. The buffer was potassium chloride and sodium chloride in bis-tris propane, pH 7.2 with

manganese supplement at 25°C (43). OPAA was first reported and characterized from the obligately halophilic *Alteromonas sp* JD6.5, isolated from a warm salt spring. The enzyme has been purified 1,300 fold, indicating that OPAA was approximately 0.01% of total protein in the native host. When assayed in the standard assay conditions, OPAA was reported to hydrolyze 357 μ moles DFP per mg of protein (102). The gene encoding OPAA from *Alteromonas sp* JD6.5 was cloned into *E. coli*, resulting in an improved expression such that OPAA made up 0.4% of the total protein (72). Modifications to the standard assay conditions resulted in new ammonium based assay buffers, which enhanced the activity approximately 5-fold (38, 103). However, a maximum 3 mM of DFP was used in the aforementioned studies, and yet K_M 's of 3 mM were reported. Determination of K_M at the maximal substrate concentration tested indicates that the enzyme was not saturated, and that the reported K_M 's are not reliable. Comparisons between enzymes at a sub-saturating substrate level can be valid and valuable, yet the determination of the kinetic constants, k_{cat} , K_M and k_{cat}/K_M is optimistic at best. OPAA has been tested with other substrates, including P-O, P-CN, P-S and other P-F bond OP's, including chemical warfare agents (11, 12, 37, 38, 45, 47, 48) (Table 2.1). OPAA has also been purified from *A. undina* and *A. haloplanktus*. The enzymes from these strains had DFP hydrolysis activity at 3 mM comparable to the *A. sp* JD6.5 OPAA at 77% and 38%, respectively (38). A crystallographic structure for OPAA has not been solved.

Table 2.1: Highest Reported Kinetic Values for the *B. diminuta* OPH and the *Altermonas sp JD6.5* OPAA.

| | Paraoxon | Demeton-S | DFP | Tabun | Sarin ^a | Soman ^a | VX |
|--|----------|-----------|------|-----------------|--------------------|--------------------|-----------------|
| OPH k_{cat} (s ⁻¹) | 15000 | 4.8 | 3500 | 360 | 56 | 5 | 0.3 |
| <i>B. diminuta</i> K_M (mM) | 0.12 | 4 | 2.81 | NA ^b | 0.7 | 0.5 | 0.44 |
| OPAA k_{cat} (s ⁻¹) | 4.64 | 0.028 | 1820 | 85 | 611 | 3145 | NA ^b |
| <i>A. sp.JD6.5</i> K_M (mM) | 0.6 | 3.5 | 1.42 | NA ^b | 3 | 3 | NA ^b |

^a These values were obtained with the Zn²⁺ liganded OPH, all others used Co²⁺

^b NA = Not reported in the literature

Pseudomonas diminuta, re-named to *Brevundamonas diminuta*, was isolated from an American soil that had demonstrated rapid hydrolysis of parathion (104). The gene encoding the enzyme was identified and cloned into *E. coli* (76). OPH was purified from *E. coli* 1,760-fold as 0.08% of the total protein. Standard assay conditions for paraoxon hydrolysis by OPH were originally reported as CHES buffer at pH 9.0 and 25°C (78, 105). Paraoxonase assays are still performed in these conditions. The first crystal structure for OPH was solved without metal present; structures have subsequently been solved with various metal, including Cd^{2+} , Zn^{2+} and Co^{2+} , in the active site (80-82, 85). As discussed previously, OPH requires metals in the active site for activity. OPH activity has been explored with a variety of divalent cations, with Co^{2+} demonstrating the most favorable activity (Table 2.2). OPH has also been isolated from a *Flavobacterium sp.* and *Agrobacterium sp.*, with 100% and 90% amino acid sequence homology, respectively, to the *B. diminuta* gene (77, 101). OPH has been tested with other substrates, including P-O, P-CN, P-S and other P-F bonded OP's, which includes the chemical warfare agents (Table 2.1). It is important to note, especially for the chemical warfare agents and P-F bond substrates, that the values reported may not have been determined under saturating conditions. The potential utility of enzymes for a particular substrate can be preliminarily assessed in this manner, but fixed and limited substrate concentration constrains the reported kinetic values to estimations. Together, these examples illustrate that the kinetic parameters of OPAA and OPH can vary wildly depending on buffer systems, metal used and even detection method. There exists a cacophony of data and sources for OPH and OPAA with a host of substrates.

Table 2.2: Correlation of OPH Activity with Metal Content.

| | Zn ^a | Co ^b | Co/Zn ^c | Cd ^d | Mn ^e | Ni ^e | None ^f |
|-------------------------------------|-----------------|-----------------|--------------------|-----------------|-----------------|-----------------|-------------------|
| k_{cat} (s ⁻¹) | 2100 | 15000 | 3170 | 6000 | 1750 | 5970 | 0.76 |
| K_M (mM) | 0.048 | 0.12 | 0.058 | 0.46 | 0.08 | 0.15 | 0.225 |

^a (78)

^b (11)

^c (106)

^d (107)

^e (84)

^f (101)

At substrate concentrations well above K_M , the enzyme is saturated and the catalyzed reaction is pseudo first order:

$v = k_{\text{cat}} [E]$ where v is the reaction velocity and k_{cat} is the turnover rate in sec^{-1} of the enzyme or the first order rate constant. When the substrate concentration is at or below the K_M of the enzyme, the catalyzed reaction becomes second order:

$$v = k_{\text{cat}} / K_M [E][OP]$$

where v is the reaction velocity and k_{cat}/K_M is the catalytic efficiency in $M^{-1} \text{sec}^{-1}$ of the enzyme, the second order rate constant or the bimolecular rate constant. At saturating OP concentrations the k_{cat} is indicative of the hydrolysis rate. As substrate concentration decreases below saturation, the K_M of the enzyme becomes increasingly important to determining hydrolysis rate. If the inverse of the reaction velocity is plotted with respect to the inverse of the substrate concentration, the resulting curve, a Lineweaver-Burke Reciprocal Plot, can be used to determine the kinetic values, V_{max} and K_M . However, when a Lineweaver-Burke is used to calculate these parameters, the substrate concentration necessarily should be near the K_M . If concentrations used are very high compared to K_M , the curve will be essentially horizontal. This will allow for the calculation of V_{max} , but the K_M will be determined inaccurately. If substrate concentrations are chosen well below the K_M , the curve will intercept too closely to both axes to calculate either K_M or V_{max} (108). Each of these studies used Lineweaver-Burke plots to determine enzyme kinetics with DFP. While use of a Lineweaver-Burke Plot can be appropriate, care must be taken during analysis because the required saturating conditions are not obvious from observing the plot.

For an improved comparison, the kinetic parameters k_{cat} , K_M , and k_{cat}/K_M of wild type OPH and OPAA were determined in identical assays with representatives of the bond-types of the major classes of OP, paraoxon (phosphotriesters, P-O), demeton-S (phosphothioate, P-S) and DFP (phosphofluoridates, P-F). The Co^{2+} -liganded form of OPH and the Mn^{2+} -form of OPAA were used, as these enzyme forms exhibit the highest relative activity (84, 102).

Materials and Methods

Materials. Paraoxon and demeton-S were purchased from ChemService (West Chester, PA). OPAA was a generous gift from the laboratory of T.C. Cheng, US Army Edgewood Chemical & Biological Center, Aberdeen Proving Ground, MD and stored at $-70^{\circ}C$ in 1 μM DTT. All other chemicals were purchased from Sigma–Aldrich (St. Louis, MO).

Purification of OPH. The pUC19 plasmid containing the wild type OPH gene (pOP419) was transformed into competent *E. coli* DH5 α cells, prepared using a $CaCl_2$ method (106). A single colony was used to inoculate four 5 mL cultures of LB broth containing 50 $\mu g/mL$ of ampicillin, which were allowed to grow overnight at $37^{\circ}C$ in a tube roller. The overnight cultures were used to inoculate four 1.0 L Fernbach flasks of Difco Terrific Broth (BD, Sparks, MD) media containing 1.0 mM $CoCl_2$ and 50 $\mu g/mL$ ampicillin (107). The cobalt-supplemented growth medium was incubated at $30^{\circ}C$ and 180-200 rpm. After 20 hours of incubation, another 50 $\mu g/mL$ ampicillin was added to each flask. The cells were harvested by centrifugation 40 hours after inoculation. The cells were lysed by sonication with five 60 second pulses at $4^{\circ}C$ with a model W-225R

ultrasonic (Heat System Ultrasonics, Inc.), and OPH was purified according to published procedures (84). In brief, following lyses, centrifugation was utilized to pellet the cell debris and allow separation of the soluble cytoplasmic fraction as the supernatant. The nucleic acids were removed by slowly adding streptomycin sulfate to 1 % (w/v) and stirring at 4°C for 15 minutes, followed by centrifugation at 22,770 x g for 40 minutes. Solid ammonium sulfate was added to the supernatant to a saturation of 45 %, stirred for at least 4 hours and again centrifuged for 70 minutes at 22,770 x g, to collect the pellet. The pellet was resuspended in K₂HPO₄/KH₂PO₄ buffer (10 mM potassium phosphate buffer, pH 6.7, 50 μM CoCl₂) and dialyzed for at least 6 hours at 4°C with two fresh 2 L buffer exchanges. The dialyzed resuspension was loaded onto a 5.0 x 150 cm ion exchange column containing Sephadex SP sepharose. OPH was eluted with a 0 to 0.5 M KCl gradient over 400 ml at a flow rate of 3.0 mL/min and collected as 6 ml fractions. Ten μl of each fraction was analyzed using a 10% sodium dodecyl sulfate-polyacrylamide gel. The fractions that contained OPH were visualized using Commassie stain, and were pooled and concentrated to between 10-20 ml. This OPH fraction was dialyzed against 6 L K₂HPO₄/KH₂PO₄ + KCl buffer (10 mM potassium phosphate buffer, pH 8.3, 50 μM CoCl₂, 20 mM KCl) overnight at 4°C. A DEAE-Sephadex column was equilibrated in the buffer and the protein pooled from the previous column was run at 4 °C. The purity of the protein was verified by SDS-PAGE and the protein concentration was determined spectrophotometrically at 280 nm with a Nanodrop ND-1000 Spectrophotometer and calculated using the extinction coefficient of

$58,000 \text{ M}^{-1} \text{ cm}^{-1}$. OPH was stored at a concentration of no less than 1.0 mg/ml in 10 mM potassium phosphate buffer, pH 8.3, 50 μM CoCl_2 , 20 mM KCl at 4°C.

Determination of DFP Kinetics. The hydrolysis of DFP results in the release of free fluoride, which was monitored in a continuously stirred 2 ml reaction. The reaction buffer was 50 mM NH_4Cl , 100 mM NaCl and 0.1 mM MnCl_2 , pH 8.5. A standard curve was established with known concentrations of sodium fluoride from 10 to 10,000 μM and plotted as signal in millivolts vs. $\log[\text{F}^-]$. This was fit to the equation $y = a + b \log[\text{F}^-]$, in which $[\text{F}^-]$ was the concentration of fluoride in μM , a is the signal at 0 μM F^- , b was the change signal (mV)/change in $\log[\text{F}^-]$, and y was the signal (mV), the plot representing signal as a function of fluoride concentration. DFP was dissolved into isopropanol at each concentration for the substrate saturation assay and added as a constant volume to start the reaction. Fluoride release was monitored over three minutes using an Orion 96-09 ionplus fluoride specific electrode (Thermo Electron Corporation). Each reaction was prepared individually with 1860 μl of reaction buffer and 100 μl of appropriately diluted enzyme defined as that amount of enzyme which results in a linear change in $[\text{F}^-]$ over the course of the 2-3 minute reaction interval. Forty μl of the isopropanol diluted DFP was added to the stirred mixture to initiate the reaction. The electrode and stir bar were rinsed between uses with 20% methanol.

The $[\text{F}^-]$ vs. time was plotted and the linear portion of the graph was used to calculate a velocity. The k_{cat} , K_M , and k_{cat}/K_M of the wild type OPH enzyme from *B. diminuta* and the wild type OPAA enzyme from *Alteromonas sp.* were determined from the Michaelis Menton equation (Equation 1), where V_o is the initial velocity, V_{max} in the

maximum velocity, $[S]$ is substrate concentration and K_M is the substrate specificity or substrate concentration at $\frac{1}{2} V_{\max}$.

$$V_o = \frac{v_{\max} \times [S]}{K_M + [S]} \quad (1)$$

The kinetic parameters, K_M and k_{cat} , were determined from Equation 1 fit to the plot of the velocity vs. DFP concentration. To obtain a K_M the substrate concentration must saturate the enzyme; since the K_{MS} of the enzymes vary, the proper DFP concentration saturation range must be found empirically.

Determination of Paraoxon Kinetics. The hydrolysis of paraoxon releases *p*-nitrophenol, which can be detected spectrophotometrically at 405 nm ($\epsilon = 17,000 \text{ M}^{-1} \text{ cm}^{-1}$). The paraoxon assay was performed in 1 ml total volume in 20 mM CHES, pH 9.0 as a substrate saturation experiment in a Ultrospec 3300 pro UV/Vis Spectrophotometer. To obtain the saturation curve, the velocities at each substrate concentration must be linear over the course of the reaction. The appropriate dilution of pure enzyme which produced a linear response over one minute, was determined empirically. As with DFP, to obtain a K_M the substrate concentration must saturate the enzyme. Since the K_{MS} of the enzymes vary, the paraoxon concentration saturation range must be found empirically for each enzyme. For OPH a constant for substrate inhibition, K_i , was added to more appropriately fit the kinetics curve to the data (Equation 2).

$$V_o = \frac{v_{\max} \times [S]}{K_M + [S](1 + ([S]/K_i))} \quad (2)$$

To obtain the kinetic parameters K_M , k_{cat} and K_i , Equation 2 was fit to the data obtained from the plot of the reaction velocity as a function of paraoxon concentration

Determination of Demeton-S Kinetics. The hydrolysis of demeton-S releases a product with a free thiol which reacts with 2,2'-dithiodipyridine (2-DTP, $\epsilon_{343} = 7060 \text{ M}^{-1} \text{ cm}^{-1}$). The demeton-S assay was performed as a substrate saturation experiment in tripart buffer (50 mM MES, 25 mM N-ethylmorpholine, 25 mM diethanolamine) pH 8.0 with 1% methanol and 1 mM 2-DTP as a substrate saturation experiment in a Ultrospec 3300 pro UV/Vis Spectrophotometer in 1 ml cuvettes. To obtain the saturation curve, the velocities must be linear over the course of the reaction. An appropriate dilution of pure enzyme was selected to produce a linear reading in a spectrophotometer over one minute at maximum velocity. As with the other substrates, to obtain K_M the substrate concentration must saturate the enzyme; since the K_{MS} of the enzymes vary, the proper demeton-S concentration saturation range must be found empirically. To obtain the kinetic parameters, K_M and k_{cat} , Equation 1 was fit to the data obtained from the plot of the reaction velocity as a function demeton-S concentration

Results

The kinetic comparison of the OPH and OPAA enzymes was performed with DFP, paraoxon and demeton-S (Figure 2.1, Table 2.3).

The two enzymes demonstrated a similar rate with DFP as a substrate, with a k_{cat} of 3748 sec^{-1} for OPH and 3780 sec^{-1} for OPAA. Although OPAA had a similar k_{cat} , the assay required more than 40 mM DFP to saturate the enzyme, resulting in a K_M of 15.3 mM. In contrast OPH had a much lower K_M of 2.8 mM. The k_{cat}/K_M for OPH and OPAA is $1.34 \times 10^6 \text{ M}^{-1} \text{ sec}^{-1}$ and $2.48 \times 10^5 \text{ M}^{-1} \text{ sec}^{-1}$, respectively. It is important to note that for each enzyme tested the DFP concentration range used extended well below

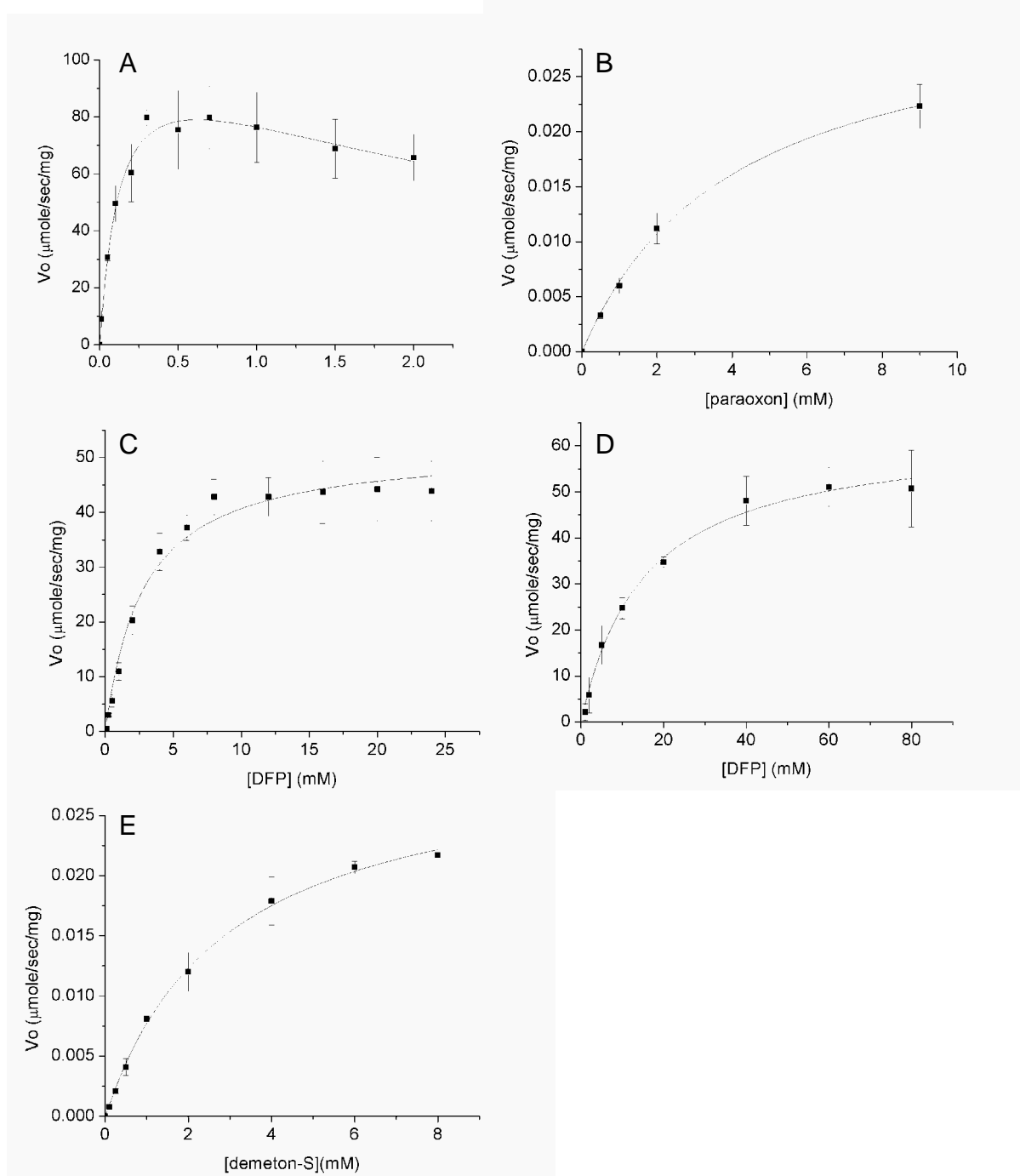


Figure 2.1: Enzyme Kinetics for OPH and OPAA. A) OPH with paraoxon, B) OPAA with paraoxon, C) OPH with DFP D) OPAA with DFP, E) OPH with demeton-S.

Table 2.3: Kinetic Constants for OPH and OPAA with Paraoxon and DFP.

| | | OPH | OPAA |
|----------------------|--------------------------------|--------------------|--------------------|
| Paraoxon | | | |
| k_{cat} | sec^{-1} | 7751 ± 1427 | 1.94 ± 0.07 |
| K_M | mM | 0.12 ± 0.01 | 4.1 ± 0.3 |
| K_{cat}/K_M | $\text{M}^{-1}\text{sec}^{-1}$ | 6.46×10^7 | 4.80×10^2 |
| DFP | | | |
| k_{cat} | sec^{-1} | 3748 ± 370 | 3780 ± 560 |
| K_M | mM | 2.8 ± 0.5 | 15.3 ± 3.9 |
| K_{cat}/K_M | $\text{M}^{-1}\text{sec}^{-1}$ | 1.34×10^6 | 2.48×10^5 |
| Demeton-S | | | |
| k_{cat} | sec^{-1} | 2.2 ± 1.0 | ND |
| K_M | mM | 2.9 ± 0.5 | ND |
| K_{cat}/K_M | $\text{M}^{-1}\text{sec}^{-1}$ | 7.50×10^2 | ND |

ND = not detected

and above the K_{MS} of either enzyme. Therefore, determination of the enzymatic parameters is more accurate than those previously described.

Paraoxon is hydrolyzed by OPH at 7751 sec^{-1} with a K_M of 0.12 mM and a K_i of 2.8 mM. OPAA hydrolyzes paraoxon at 1.94 sec^{-1} with a K_M of 4.1 mM. The maximum paraoxon concentration used in the assay for OPH was 2.0 mM. This is well above the K_M and below the solubility of paraoxon. The maximum paraoxon concentration used in the assay for OPAA was 9.0 mM. This is also above the K_M and below the solubility of paraoxon.

Demeton-S is the most commonly used analog of the nerve agents VX and RVX due to its P-S bond, similar chemical structure and kinetics (12) (Figure 1.1). The hydrolytic rate of demeton-S by OPH is 2.2 sec^{-1} and a K_M of 2.9 mM, while OPAA had no detectable catalytic activity for demeton-S even when allowed to react overnight at 22°C . It is important to note here that the demeton-S solubility limit, without addition of organic solvent, is 9.5 mM. Increasing amounts of organic solvent will inhibit the enzyme, thus it is beneficial to limit its use. While it is important to have substrate concentration well above the K_M , many of the OP compounds have limited solubility in the aqueous buffers required for enzymatic assays, and so saturating levels may not be reached. This is a limitation of the demeton-S hydrolysis assay.

Discussion

The chemical warfare nerve agents are obviously dangerous, difficult to work with, and availability is limited to small quantities and to select civilian and military installations. Thus, utilizing DFP and demeton-S as surrogates in research allows the

chemical warfare agents to be replaced with less toxic analogs. DFP is a smaller molecule than paraoxon and is used as the analog to the nerve agents sarin and soman because of its P-F bond. When the P-F bond is hydrolyzed, either enzymatically or chemically, a fluoride ion is released. This is monitored using a fluoride electrode in this study, but typically is monitored using GC-MS with the chemical agents. Demeton-S is a larger substrate with a P-S bond that is similar to the VX and RVX nerve agents. Hydrolysis of the P-S bond of these substrates produces a free thiol, which is not directly spectrophotometrically detectable; however, further reaction of the thiol with 2-DTP produces 2-thiodipyridine that absorbs at 343 nm.

The importance of enzyme kinetics as it relates to application purposes can be understood as follows (Figure 2.2). Substrate range I (I) is indicative of low substrate conditions, such as vascular OP concentrations, and substrate range II (II) is indicative of high substrate concentration, such as instances of pesticide or CWA spills, resulting in environmental or CMA contamination. Enzyme A has a greater k_{cat} and K_M than enzyme B. In substrate range II, a large k_{cat} would be desirable for detoxification/decontamination, as it is more likely that the enzyme will be saturated and so operating at maximum velocity. In contrast, an enzyme with a low K_M would be preferred in those cases which fall into substrate range I. Even though enzyme B has a lower maximum velocity, it has a faster rate in this substrate range and an enzyme with a low K_M would be preferred in a circumstance where substrate concentrations are likely to be low. Although the turnover numbers for DFP of the enzymes are similar, the K_M

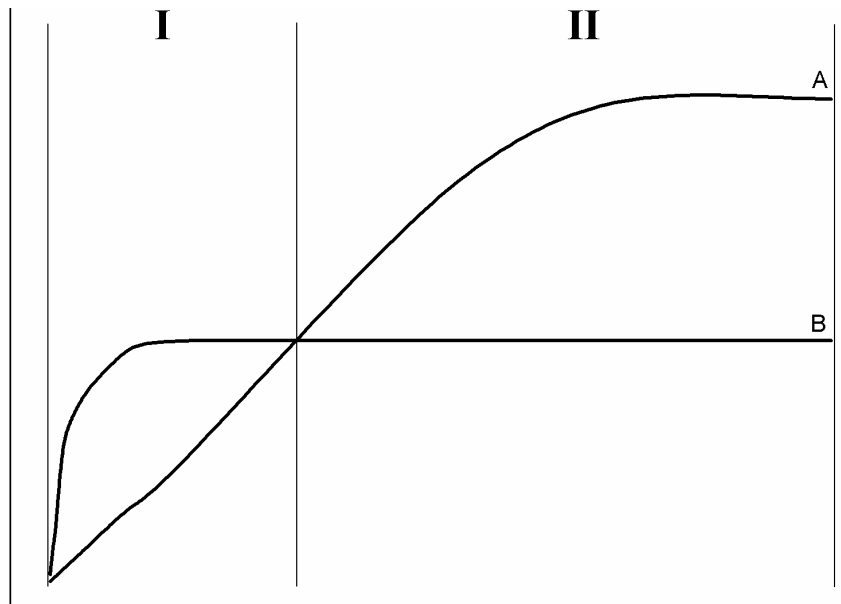


Figure 2.2: Substrate Saturation Curves. I) low [S], II) high [S], A) Enzyme with high k_{cat} and high K_M , B) Enzyme with low k_{cat} and low K_M .

for OPAA is, 15.3 ± 3.9 mM compared to OPH's 2.8 ± 0.5 mM. As a result, OPH's substrate specificity is correspondingly higher, $1.34 \times 10^6 \text{ M}^{-1} \text{ sec}^{-1}$ for OPH and $2.48 \times 10^5 \text{ M}^{-1} \text{ sec}^{-1}$ for OPAA. This limits OPAA's utility as an enzymatic bioremediation/detoxification tool, particularly for in vivo use, because the amount of OPAA needed to alleviate any toxicity would be great.

When selecting between OPH and OPAA for vascular defense, consideration must be given to the likely OP concentrations in the vascular system. For example, LD₅₀s for paraoxon, DFP and demeton-S in mice (IP) are 0.33, 4.2 and 7.0 mg/kg, respectively. Extrapolating these LD₅₀s for human (human IP LD₅₀s are not available) requires the following assumptions; 1) a 70 kg body weight, 2) a corresponding 5 L vascular blood volume, 3) that these values represent the effective dose of nerve agent and 4) all OP appears in the blood stream. With these assumptions, the intravascular concentration of 1 LD₅₀ of paraoxon, DFP and demeton-S can be estimated to be 0.017, 0.32 and 0.38 mM, respectively. These vascular concentrations are well below the K_Ms for the enzymes, suggesting that OPH has the advantage for all substrates tested (Table 2.4). The chemical warfare agents have even lower LD₅₀s and so would have correspondingly lower vascular concentration levels. For those circumstances where the OP concentrations are low, such as vascular defense, the K_M becomes arguably the most important selection criteria. In addition, OPH's utility with paraoxon would indicate it to be a suitable candidate for decontamination of P-O bond pesticides. OPH is more efficient with this substrate by approximately 5 orders of magnitude. The P-S bond substrates, which include VX, RVX as well as many pesticides, can only be remediated

Table 2.4: Intravascular OP Levels.

| | LD ₅₀ ^a (mg/kg) | [Vascular] (mM) | % of OPH's K _M | % of OPAA's K _M |
|-----------|--|--------------------|------------------------------|-------------------------------|
| Paraoxon | 0.33 | 0.017 | 12.9 | 0.42 |
| DFP | 4.2 | 0.32 | 11.4 | 2.1 |
| Demeton-S | 7 | 0.38 | 17.4 | NA |

^a Mouse IP

by OPH. Not only does OPH hydrolyze a broad range of substrates, such as P-O, P-S, and P-F, compared to OPAA's single P-F and P-O substrate utility, it hydrolyzes DFP and paraoxon more efficiently. For these reasons, OPH was determined to be the most suitable enzyme for a variety of bioremediation applications, and so will be the focus of further study.

CHAPTER III

RATIONAL DESIGN OF OPH FOR TARGETED ENZYME EFFICACY

The three-dimensional structure of Zn^{2+}/Zn^{2+} -OPH with a bound substrate analog, diethyl 4-methylbenzylphosphonate, has enabled the description of the active site as three distinct binding pockets considered responsible for the proper orientation of substrates (80). These binding pockets have been designated as the small, large, and leaving group subsites. The small subsite is predominantly defined by the side chains of Gly-60, Ile-106, Leu-303, Cys-59, Ser-61 and Ser-308. The pocket for the large subsite is largely formed by the side chains His-254, His-257, Leu-271, and Met-317. The residues that are primarily located around the leaving group subsite are Trp-131, Phe-132, Phe-306, and Tyr-309. These residues are depicted in Figure 1.9. The orientation of the inhibitor bound within the active site of OPH is illustrated in Figure 3.1 (109). It has been proposed that the large hydrophobic end of the substrates interact with residues in the large and leaving group pocket during cleavage, and that modification of the residues in this region can alter the specificity of OPH toward some of the more recalcitrant substrates, improving their rates of hydrolysis (11, 18, 85).

As previously discussed (see Chapter II), the rational design of protein structure and function is a powerful approach to test both general theories in protein chemistry, as well as specific theories for the redesign of a given protein. In either case, creation of a new function requires that all necessary interactions are understood and provided. The design approach is therefore a way to test the limits of completeness of understanding

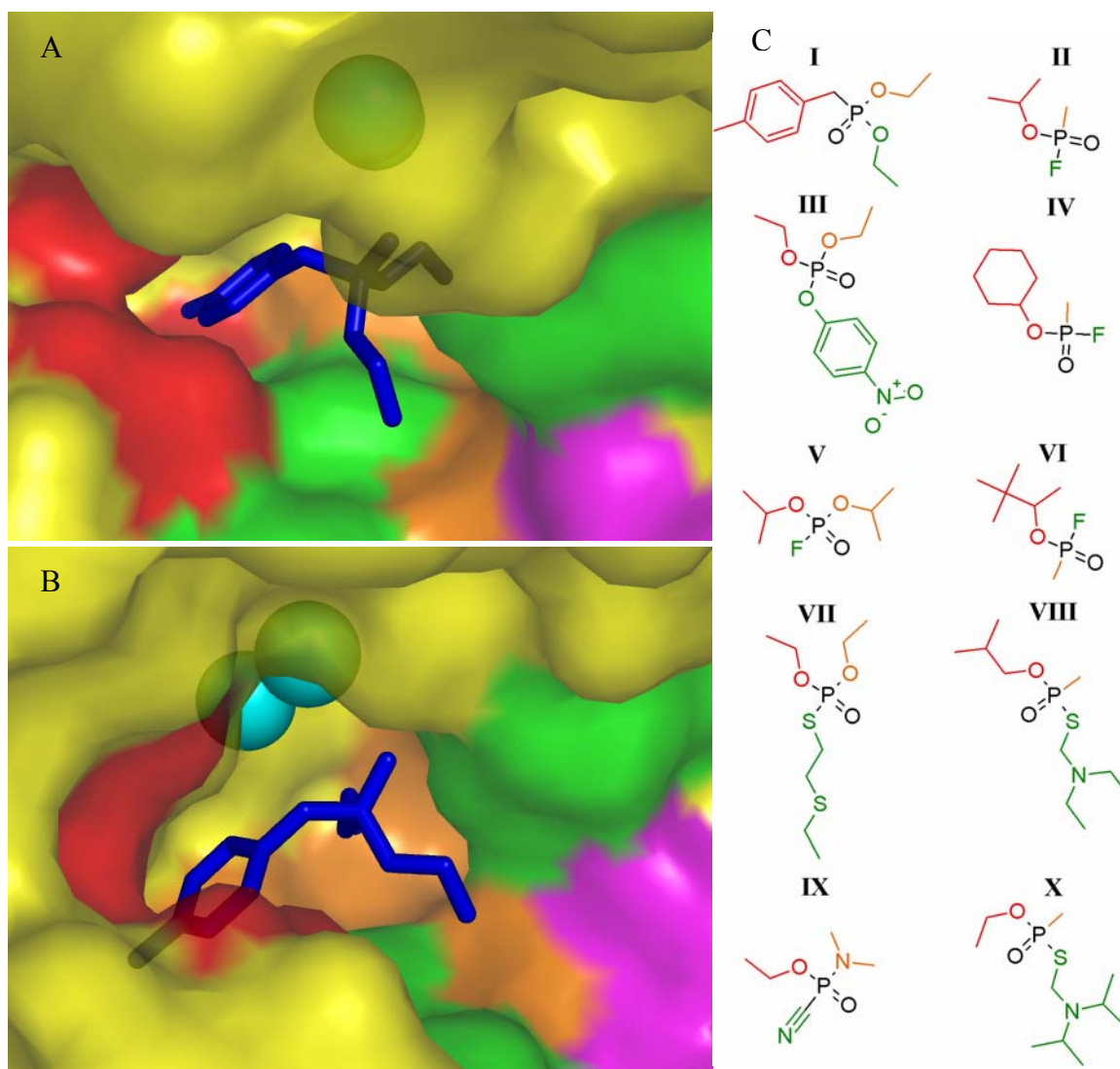


Figure 3.1: Molecular Description of the Active Site of OPH. Cyan spheres represent Zn^{2+} , and the diethyl 4-methylbenzylphosphonate inhibitor is represented in blue. The green surface represents the leaving group pocket, the red surface represents the large pocket, and the orange surface represents the small pocket. The purple surface is contributed by the adjacent subunit. A: View into large pocket. B: View into small pocket. C. The substrates are depicted with the colors corresponding to the pocket in which the functional group resides when productively docked. The chemical warfare agents are chiral at the phosphorus and the large and small pocket functional groups can be reversed. I: Diethyl 4-methylbenzylphosphonate. II: Sarin. III: Paraoxon. IV: Cyclosarin. V: DFP. VI: Soman. VII: Demeton-S. VIII: RVX. IX: Tabun. X: VX.

experimentally. Typically, the experiments are devised in a progressive fashion, such that the simplest possible variants are tried first, followed by iterative additions until the desired result is achieved. At the center of the design approach is the “design cycle,” in which theory and experiment alternate. Given the wealth of information regarding the structural and mechanistic information on OPH, rational design of the active site of OPH has been useful in improving hydrolysis rates for certain substrates. For example, wild type OPH has demonstrated hydrolysis of the phosphonofluoridates, sarin and soman (48). Sarin and soman, however, are stereoisomeric and OPH hydrolyzes each member of an isomeric set with a different efficacy. Sarin and soman are chiral at the phosphorus center, with the methyl substituent docking in the small pocket and the *o*-isopropyl substituent of sarin and the *o*-pinacolyl of soman docking in the large pocket of the OPH active site. (Soman has an additional chiral center at the C2 atom and, therefore, has four stereoisomers: $[R_pR_c]$, $[S_pR_c]$, $[R_pS_c]$, and $[S_pS_c]$, see Figure 3.2.) The hydrolysis is more efficient when the larger substituent is in the large pocket and the methyl substituent is in the small pocket, which is evidenced by the increased efficiency with the less toxic R_p isomers. Building on the crystallographic description of the active site, rationally designed mutants were created to reverse the stereoselectivity of these chiral substrates (110). As an example of the effective use of rational design, it was hypothesized that increasing the small pocket size and reducing the large pocket size would reverse the stereoselectivity of OPH. Three mutations of OPH were designed to do just that by changing the histidine at 254 to a tyrosine, thus decreasing the large

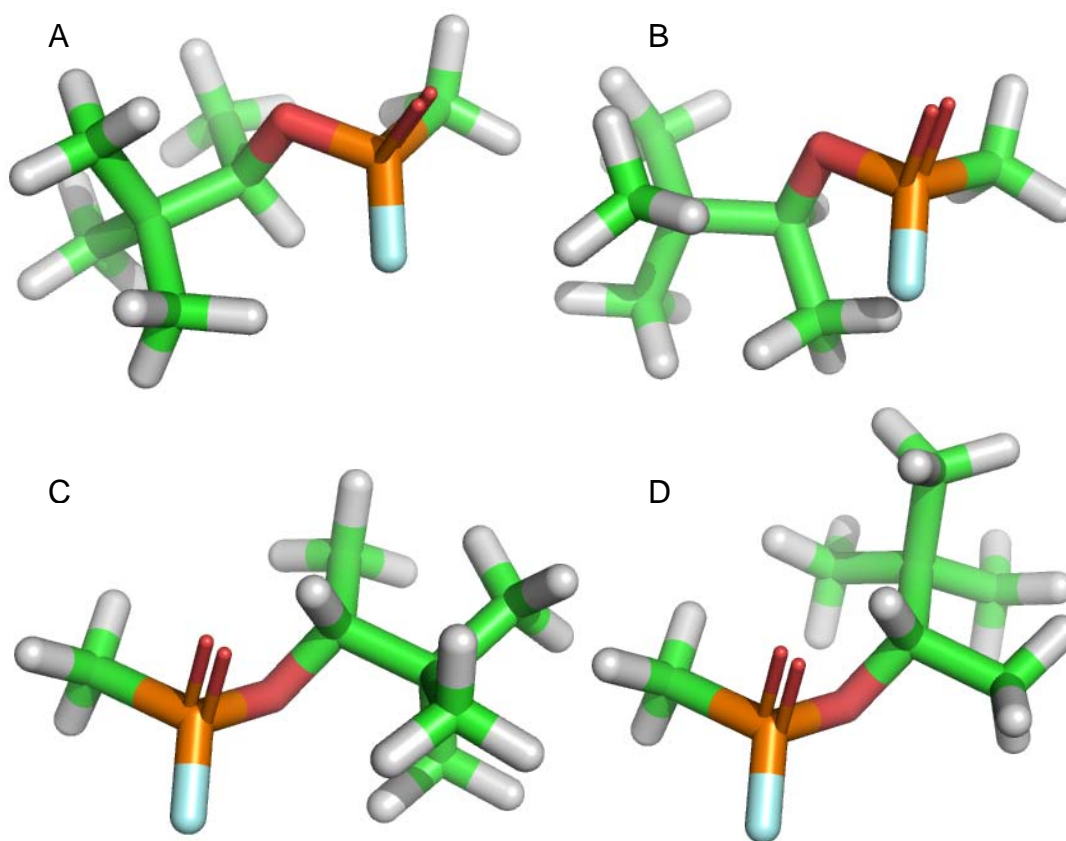


Figure 3.2: Stereoisomers of Soman. A) R_PR_C Soman B) R_PS_C Soman C) S_PR_C Soman D) S_PS_C Soman.

pocket size, and changing the phenylalanine at 132 and the isoleucine at 106 to alanines, increasing the small pocket size. As predicted, this variant demonstrated an increase of 6.6-fold in the catalytic efficiency toward the sarin S_P isomer analog and 75-fold for the S_PS_C soman isomer analog, not only demonstrating that OPH can be rationally designed to improve and target its OP degrading potential, but also validating the conceptual understanding of the role of the pockets in substrate selectivity (Table 3.1).

The studies reported here utilized a similar approach to redesign the active site of OPH for enhanced hydrolysis of VX. VX is the most toxic of chemical weapons in the United States arsenal, with an LD₅₀ of 0.008 mg/kg, and remains a large component of the United States chemical weapons stockpile at 8,000 metric tons. RVX, an isomer of VX, is a major component of the Russian arsenal. In considering the general phosphotriester (P-O), phosphorofluoridate (P-F), and phosphorothioate (P-S) substrates, the P-S bond is hydrolyzed the slowest by any of the OP degrading enzymes, including OPH (Table 2.1). VX and RVX are phosphonothioates with large aliphatic leaving groups and enzymes that do hydrolyze this class of compounds generally do so poorly, as can be seen by the reported k_{cat} for OPH of 0.3 sec⁻¹ with VX. The sulfur of the P-S bond is larger than the oxygen or fluorine of the P-O and P-F bond substrates and the pK_a of the P-S leaving group is high. The low electronegativity of the sulfur makes the phosphorus a weak electrophile, thus reducing the capacity of nucleophilic attack and bond hydrolysis. These characteristics contribute to the hydrolytic inefficiency of these substrates compared to the P-O and P-F substrates. Similar kinetic constraints exist for

Table 3.1 OPH Stereoselectivity with Chiral Substrates. (110).

| | | Wild Type | Variant |
|--------------|-------------------------------|----------------------|----------------------|
| | | k_{cat}/K_M | k_{cat}/K_M |
| Sarin Analog | R _P | 8.2×10^6 | 9.0×10^4 |
| | S _P | 4.1×10^5 | 2.7×10^6 |
| Soman Analog | R _P R _C | 1.6×10^5 | 2.8×10^2 |
| | R _P S _C | 1.2×10^4 | 5.6×10^1 |
| | S _P R _C | 3.8×10^2 | 9.2×10^3 |
| | S _P S _C | 1.6×10^1 | 1.2×10^3 |

other phosphorothioates, such as demeton-S (Table 2.3). In order to consider an enzymatic approach to detoxification of the P-S compounds, there is a need to increase the enzymatic efficiency with this substrate.

A set of OPH variants have previously been reported which improve the catalytic efficiency of OPH with the P-S substrate demeton-S as well as VX or RVX. These variants targeted histidine residues at 254 and 257, and included H254R, H257L, H254S and the double mutant H254R/H257L. H254 and H257 are large pocket constituents and the kinetic characterization of these variants support a role for this region in the enhanced catalysis of the target P-S substrates (11). Over two hundred variants of OPH have been created and described kinetically, most of which were designed to enhance activity against certain substrates or probe the mechanism of activity and/or stability (11, 106, 107, 109, 111-118). Over 75 of these published mutants involve residues H254, H257 or F306, and of the two hundred only five reported significantly improved kinetic characteristics of demeton-S hydrolysis. Each of these five variants with enhanced P-S bond hydrolysis had a mutation at either H254 or H257 (Table 3.2). The single mutants H254R, H254S and H257L all had improved kinetic characteristics with demeton-S and the double mutant H254R/H257L had a 31-fold increase in k_{cat}/K_M for demeton-S (11). It was proposed that the serine at 254 increased the flexibility of OPH in the accommodation of its P-S substrates and that the charged guanidinium group of an arginine at 254 stabilized the transition state of demeton-S more efficiently than the native histidine (119). A leucine at 257 increased the apparent binding affinity of OPH

Table 3.2: OPH Variants with Improved Demeton-S Activity.

| Mutation | k_{cat} (sec^{-1}) | K_{M} (mM) | $k_{\text{cat}}/K_{\text{M}}$ ($\text{M}^{-1}\text{sec}^{-1}$) |
|--------------------------|---|------------------------|---|
| WT ^a | 4.2 ± 0.1 | 4.8 ± 0.2 | 8.7E+02 |
| H254R/H257L ^a | 68 ± 5 | 2.5 ± 0.5 | 2.7E+04 |
| H254R/T352A ^b | 20 | 3.5 | 5.6E+03 |
| H254R ^a | 16 ± 0.7 | 4.4 ± 0.4 | 3.6E+03 |
| H257L ^a | 3.3 ± 0.05 | 1.9 ± 0.9 | 1.7E+03 |
| H254S ^c | 0.6 ± 0.1 | 0.033 ± 0.003 | 1.8E+04 |

^a (11)^b (118)^c (119)

for demeton-S, explained as an interaction between the 257L side chain with the hydrophobic counterpart on the substrate (119).

Because there is detailed knowledge of the structure and function of OPH, including active site structure and mechanism, rational design methods were employed in the redesign of OPH to address the catalytic inefficiency of the enzyme with the phosphorothioate substrates. Reiterating the design cycle by considering the improvements reported with the previous modifications, this study has expanded the available enzymes targeting the hydrolysis of demeton-S and VX. These second generation design variants include the H254L, H254S/H257L, H254S/F306L and H257L/F306L mutants (Table 3.3). These variants were made to improve phosphorothioate hydrolysis.

Materials and Methods

Materials. Paraoxon and demeton-S were purchased from ChemService (West Chester, PA). All other chemicals were purchased from Sigma–Aldrich (St. Louis, MO). The pUC19 plasmids containing the wild type (pOP419) or variant OPH genes was used as the template, and the mutations were introduced with the QuickChange™ site-directed mutagenesis kit from Stratagene (LaJolla, CA) (106). Non-homologous, non-overlapping primers were synthesized by Integrated DNA Technologies, Inc. (Coralville, IA) and used for the mutagenesis reactions (Table 3.4).

Construction of OPH Mutants. The pOP419-H254L mutant was created in the pOP419 plasmid with the H254L primers, using the QuickChange protocol (106). The pOP419-H254S/H257L mutant was created using the pOP419-H254S gene, previously

Table 3.3: Design Rational for the Variants.

| | |
|-------------|---|
| H254L | Increase the large pocket size and introduce a hydrophobic region to interact with the hydrophobic substrate leaving group |
| H254S/H257L | H254S and H257L mutations produce an increase in hydrophobicity of the large pocket to potentially combine the improved demeton-S kinetics of the individual variants |
| H254S/F306L | Combine the improved demeton-S binding affinity of the H254S and increase the size of the leaving group pocket to accommodate the larger sulfur atom |
| H257L/F306L | Increase the size of the active site to accommodate the larger sulfur atom |

Table 3.4: Mutagenic Primers. Altered bases are underlined.

| | |
|-------------|---|
| H254S/H257L | 5' CGC ACT <u>G</u> AG CGG GAT <u>G</u> GA GTC TAG ACC G 3' |
| | 3' GCG TGA <u>C</u> TC GCC CTA <u>C</u> CT CAG ATC TGG C 5' |
| F306L | 5' GGT GAC ATA GCT CGA <u>A</u> AG CCC G 3' |
| | 3' CCA CTG TAT CGA GCT <u>T</u> TC GGG C 5' |
| H254L | 5' CGC ACT GTG CGG GAT <u>G</u> AG GTC TAG ACC G 3' |
| | 3' GCG TGA CAC GCC CTA <u>C</u> TC CAG ATC TGG C 5' |

created, with the H254S/H257L primers (119). The pOP419-H254S/F306L mutant was created using the pOP419-H254S gene with the F306L primers. The pOP419-H257L/F306L mutant was created using the pOP419-H257L gene with the F306L primers. The mutated plasmids were sequenced to ensure the fidelity of the PCR reactions. The electrophoretic separation and analysis was performed by the Gene Technology Laboratory of Texas A&M University, the data was analyzed with DNASTAR Molecular Biology software (Madison, WI).

Purification of OPH. The wild type pOP419 or a variant OPH gene was transformed into competent *E. coli* DH5 α cells, prepared using a CaCl₂ method (106). A single colony was used to inoculate four 5 mL cultures of LB broth containing 50 μ g/mL of ampicillin, which were allowed to grow overnight at 37°C in a tube roller. The overnight cultures were used to inoculate four 1.0 L Fernbach flasks of Difco Terrific Broth (BD, Sparks, MD) media containing 1.0 mM CoCl₂ and 50 μ g/mL ampicillin (107). The cobalt-supplemented growth medium was incubated at 30°C and 180-200 rpm. After 20 hours of incubation, 50 μ g/mL ampicillin was added to each flask. The cells were harvested by centrifugation 40 hours after inoculation and lysed by sonication with five 60 second pulses at 4 °C with a model W-225R ultrasonic (Heat System Ultrasonics, Inc.), and OPH was purified according to published procedures (84). In brief, following lyses, centrifugation was utilized to pellet the cell debris and allow separation of the soluble cytoplasmic fraction as the supernatant. The nucleic acids were removed by slowly adding streptomycin sulfate (SS) to 1 % (w/v) and stirring at 4°C for 15 minutes, followed by centrifugation at 22,770 x g for 40 minutes. Solid ammonium

sulfate (AS) was added to the supernatant to 45 % saturation, stirred for at least 4 hours and again centrifuged for 70 minutes at 22,770 x g, to collect the pellet. The pellet was resuspended in K_2HPO_4/KH_2PO_4 buffer (10 mM potassium phosphate buffer, pH 6.7, 50 μ M $CoCl_2$) and dialyzed for at least 6 hours at 4°C with two fresh 2 L buffer exchanges. The dialyzed resuspension was loaded onto a 5.0 x 150 cm ion exchange column containing Sephadex SP sepharose (SP). OPH was eluted with a 0 to 0.5 M KCl gradient over 400 ml at a flow rate of 3.0 mL/min and collected as 6 ml fractions. Ten μ l of each fraction was analyzed using a 10% sodium dodecyl sulfate-polyacrylamide gel. The fractions that contained OPH were visualized using Commassie stain, and were pooled and concentrated to between 10-20 ml. The OPH fractions were dialyzed in K_2HPO_4/KH_2PO_4 + KCl buffer (10 mM potassium phosphate buffer, pH 8.3, 50 μ M $CoCl_2$, 20 mM KCl) overnight at 4°C. This fraction was then loaded and separated at 4°C on a DEAE-Sephadex (DEAE) column equilibrated in the same buffer and eluted into 6 ml fractions. The purity of the protein was verified by SDS-PAGE and the protein concentration was determined spectrophotometrically at 280 nm with a Nanodrop ND-1000 Spectrophotometer and calculated using OPH's extinction coefficient of 58,000 $M^{-1} cm^{-1}$. OPH was stored at a concentration of no less than 1.0 mg/ml in 10 mM potassium phosphate buffer, pH 8.3, 50 μ M $CoCl_2$, 20 mM KCl at 4°C. Each enzyme was purified independently three times.

Determination of DFP Kinetics. The hydrolysis of DFP results in the release of free fluoride, which was monitored in a continuously stirred 2 ml reaction. The reaction buffer was 50 mM NH_4Cl , 100 mM NaCl and 0.1 mM $MnCl_2$, pH 8.5. A standard curve

was established with known concentrations of fluoride ranging from 10 to 10,000 μM and plotted as signal in millivolts vs. $\log[\text{F}^-]$. This was fit to the equation $y = a + b \log[\text{F}^-]$, in which $[\text{F}^-]$ was the concentration of fluoride in μM , a was the signal at 0 μM F^- , b was the change signal (mV)/change in $\log[\text{F}^-]$, and y was the signal (mV), the plot representing signal as a function of fluoride concentration. DFP was dissolved into isopropanol at each concentration for the substrate saturation assay and was added at a constant volume to start the reaction. Fluoride release was monitored over three minutes using an Orion 96-09 ionplus fluoride specific electrode (Thermo Electron Corporation). Each reaction was prepared individually with 1860 μl of reaction buffer and 100 μl of appropriately diluted enzyme, which was defined as the amount of enzyme which resulted in a linear change in $[\text{F}^-]$ over the course of the 2-3 minute reaction interval. Forty μl of the isopropanol diluted DFP was added to the stirred mixture to initiate the reaction.

The $[\text{F}^-]$ vs. time was plotted and the linear portion of the graph was used to calculate a velocity. The k_{cat} , K_{M} and $k_{\text{cat}}/K_{\text{M}}$ of the wild type OPH enzyme from *B. diminuta* and its variants were determined from the Michaelis Menton equation (Equation 1) where V_o is the initial velocity, V_{max} is the maximum velocity, $[\text{S}]$ is the substrate concentration and K_{M} is the substrate concentration at $\frac{1}{2} V_{\text{max}}$.

The kinetic parameters, K_{M} , and k_{cat} , were determined from Equation 1 fit to the plot of the velocity vs. DFP concentration. The K_{M} of the enzymes demonstrated significant variation and the proper DFP concentration saturation range was determined

empirically for each enzyme preparation. The reported kinetic values represent the average of three assays from each of three independent purifications.

Determination of Paraoxon Kinetics. The hydrolysis of paraoxon releases *p*-nitrophenol, which can be detected spectrophotometrically at 405 nm ($\epsilon = 17,000 \text{ M}^{-1} \text{ cm}^{-1}$). The paraoxon assay was performed in 1 ml total volume in 20 mM CHES, pH 9.0 as a substrate saturation experiment in a Ultrospec 3300 pro UV/Vis Spectrophotometer. To obtain the saturation curve, the velocities at each substrate concentration must be linear over the initial course of the reaction. The appropriate dilution of pure enzyme, which produced a linear response over one minute, was determined empirically. In order to obtain an accurate K_M the substrate concentration must saturate the enzyme and since the K_{MS} of the enzymes can vary dramatically, the paraoxon concentration saturation range was determined empirically for each enzyme. The data was fit to Equation 1 obtained from the plot of the reaction velocity as a function paraoxon concentration to obtain the kinetic parameters, K_M , and k_{cat} . The reported kinetic values represent the average of three assays from each of three independent purifications.

Determination of Demeton-S Kinetics. The hydrolysis of demeton-S releases a product with a free thiol which reacts with 2,2'-dithiodipyridine (2-DTP, $\epsilon_{343} = 7060 \text{ M}^{-1} \text{ cm}^{-1}$). The demeton-S assay was performed similarly to the substrate saturation experiments in tripart buffer (50 mM MES, 25 mM N-ethylmorpholine, 25 mM diethanolamine) pH 8.0 with 1% methanol and 1 mM 2-DTP as a substrate saturation experiment in a Ultrospec 3300 pro UV/Vis Spectrophotometer in 1 ml total volume. To obtain the saturation curve the velocities at saturating substrate must be linear over the

course of the reaction. An appropriate amount of pure enzyme was used to produce a linear reading in a spectrophotometer over one minute at maximum velocity. As described previously, to obtain a K_M the substrate concentration must saturate the enzyme; since the K_{MS} of the enzymes vary, the proper demeton-S concentration range must be found empirically. The data was fit to Equation 1 obtained from the plot of the reaction velocity as a function demeton-S concentration to obtain the kinetic parameters, K_M and k_{cat} . The kinetic parameters with demeton-S show that the maximum substrate concentration used in the assay, 8 mM, is above the K_M of the enzymes showing hydrolysis of demeton-S, at least 2.1-fold, but the solubility of demeton-S prevented the complete saturation of the enzyme in some cases. This can be a limitation of the demeton-S hydrolysis assay. The reported kinetic values represent the average of three assays from each of three independent purifications.

OPH Modeling. The structural minimization of variant enzymes was performed using the Build Mutants tool of the Accelrys Discovery Studio 1.7. A CHARMM force field was applied to the Zn^{2+} containing 1DPM PDB wild type OPH crystal structure with the (diethyl-4-methylbenzylphosphate inhibitor and all residues within 800 pm of the substituted residues were minimized (81). Docking simulation of OP compounds within the active site of OPH was performed using the CDOCKER tool of the Accelrys Discovery Studio 1.7. The OP compounds were docked into a 1,500 pm radius of the active site and the fifty poses with least docking energies reviewed.

Results

The native OPH and selected variant proteins were purified to homogeneity. The kinetic comparison of the OPH variants was performed with three substrates, paraoxon (P-O bond hydrolysis), demeton-S (P-S bond hydrolysis) and DFP (P-F bond hydrolysis) to determine the rate of the three bond types, phosphotriesters, phosphorofluoridate, and phosphorothioates (Table 3.5).

The phosphotriester, paraoxon (P-O bond), is the preferred substrate of wild type OPH, and it is hydrolyzed with a catalytic efficiency of $6.46 \times 10^7 \text{ M}^{-1} \text{ sec}^{-1}$ ($7751 \text{ sec}^{-1} k_{\text{cat}}$). All mutations resulted in enzymes which exhibited a decreased k_{cat} with paraoxon relative to the WT OPH. This is expected, as wild type OPH hydrolyzes paraoxon at near diffusion limited rates and so the rate is not able to increase by any significant amount. The single-substituted enzyme, H254L, had a rate of hydrolysis which was 63% that of the WT enzyme, and the double mutations, H254S/H257L, H254S/F306L and H257L/F306L, exhibited decreases of approximately 90% to 95% in their hydrolysis rates with this substrate. The K_M values for H254L, H254S/F306L and H257L/F306L were not significantly different from WT. In comparison, the K_M of H254S/H257L for paraoxon was significantly lower than that of the WT enzyme.

DFP is a smaller substrate than paraoxon and serves as the analog to the nerve agents sarin and soman because of its phosphorofluoridate bond. When the P-F bond is broken by either enzymatic or chemical hydrolysis, a fluoride ion is released. The solubility limit of DFP permitted substrate saturation assays up to 87 mM DFP. The WT OPH, with a k_{cat} of 3748 sec^{-1} and a K_M of 2.8 mM, had a higher rate of hydrolysis with

Table 3.5 Kinetic Values of the OPH Variants.

| | paraoxon ^a | demeton-S ^a | DFP ^a |
|--|------------------------|------------------------|------------------------|
| WT OPH | | | |
| k_{cat} (s ⁻¹) | 7751 ± 1427 | 2.2 ± 1.0 | 3748 ± 370 |
| K_{M} (mM) | 0.12 ± 0.01 | 2.9 ± 0.5 | 2.8 ± 0.5 |
| $k_{\text{cat}}/K_{\text{M}}$ (M ⁻¹ s ⁻¹) | 6.46 x 10 ⁷ | 7.50 x 10 ² | 1.34 x 10 ⁶ |
| H254L | | | |
| k_{cat} (s ⁻¹) | 4896 ± 3 | 1.92 ± 0.25 | 2768 ± 301 |
| K_{M} (mM) | 0.18 ± 0.05 | 2.10 ± 0.06 | 2.6 ± 1.2 |
| $k_{\text{cat}}/K_{\text{M}}$ (M ⁻¹ s ⁻¹) | 2.77 x 10 ⁷ | 9.17 x 10 ² | 1.06 x 10 ⁶ |
| H254S/H257L | | | |
| k_{cat} (s ⁻¹) | 762 ± 78 | 78.5 ± 7.3 | 410 ± 103 |
| K_{M} (mM) | 0.014 ± 0.003 | 3.78 ± 0.26 | 0.48 ± 0.12 |
| $k_{\text{cat}}/K_{\text{M}}$ (M ⁻¹ s ⁻¹) | 5.48 x 10 ⁷ | 2.08 x 10 ⁴ | 8.59 x 10 ⁵ |
| H254S/F306L | | | |
| k_{cat} (s ⁻¹) | 794 ± 410 | ND ^b | ND |
| K_{M} (mM) | 0.20 ± 0.08 | ND | ND |
| $k_{\text{cat}}/K_{\text{M}}$ (M ⁻¹ s ⁻¹) | 3.89 x 10 ⁶ | ND | ND |
| H257L/F306L | | | |
| k_{cat} (s ⁻¹) | 47.3 ± 17.9 | ND | ND |
| K_{M} (mM) | 0.090 ± 0.002 | ND | ND |
| $k_{\text{cat}}/K_{\text{M}}$ (M ⁻¹ s ⁻¹) | 5.23 x 10 ⁵ | ND | ND |

^a The kinetic values are the average of triplicate assays performed on each of three independent purifications for each enzyme.

^b ND: Not Detectable

DFP than any of the mutants. The H254L enzyme was the most similar to WT, retaining 74% of the catalytic rate of WT OPH, and a relatively unchanged K_M value. In comparison, the H254S/H257L k_{cat} was reduced to 11% and the K_M was reduced to 17% of the WT. The H254S/F306L and H257L/F306L mutants had no detected catalytic activity for DFP under the described assay conditions.

Demeton-S is the commonly used analog of the nerve agents VX and RVX due to its P-S bond. The hydrolytic rate of H254L for this substrate was unchanged relative to the wild type enzyme and the H254S/F306L and H257L/F306L mutants again had no catalytic activity for the substrate. The H254S/H257L was the only mutant that had an improvement in kinetics for a tested substrate, with a k_{cat} increase with demeton-S of 35.7-fold. This resulted in a specificity constant for demeton-S that is 28-fold higher for the H254S/H257L variant than for the WT.

Discussion

The Chemical Warfare Convention of 1997 set a standard by which all signatories would destroy their chemical weapon stockpiles, as defined by Schedule 1, by 2007 with no extension past 2012. The United States General Accounting Office has announced it does not expect Russia to reach 100% destruction until 2027, and the Pentagon announced in late 2006 that it expected that the disposal of the U.S. stockpile would not be completed until 2023. The United States nerve agent stockpile consists primarily of sarin and VX, which are being destroyed in the order of presumed public hazard with sarin followed by VX. (Sarin was deemed the greatest public hazard due to its high volatility and related dispersion.) Over 80% of the United States stockpile of

sarin has been destroyed (95, 96). There remains over 8,000 metric tons of VX to be destroyed.

Because VX is so toxic and access to it is limited, a surrogate is used in its place for testing for VXase capability. Demeton-S is a phosphorothioate like VX and RVX, where the P-S bond is broken during hydrolysis. The sizes of the substrates are similar, demeton-S is 258 g/mol and VX is 267 g/mol, and their leaving groups are aliphatic.

Demeton-S and the Active Site of OPH. A productive binding of substrate in the active site of OPH characterized by the location of the leaving group on the side of the phosphorus opposite the activated hydroxyl (Figure 3.3). This means that for a productive binding orientation the leaving group of a substrate will reside adjacent to the large or in the leaving group pocket. This orientation is required for hydrolysis, and the accompanying Sn2 replacement with an inversion of stereochemistry as described in Chapter I. When comparing enzymes, there are several docking scenarios that would be indicative of an improvement in kinetics. For example, an increase in the number of productive orientations found in the most favorable docked conformations would suggest enhanced catalysis. Alternatively, a decrease in the docking energies of the productive orientations would indicate that substrate binding is energetically more favorable. Finally, a decrease in productive bindings of the hydrolysis product or increase in hydrolysis product docking energies, would indicate that the residence of the hydrolysis product in the active site is more unfavorable. Each of these docking effects could explain an improvement in kinetics and conversely the opposite could explain a kinetic deterioration. The docking results of paraoxon and demeton-S with WT are

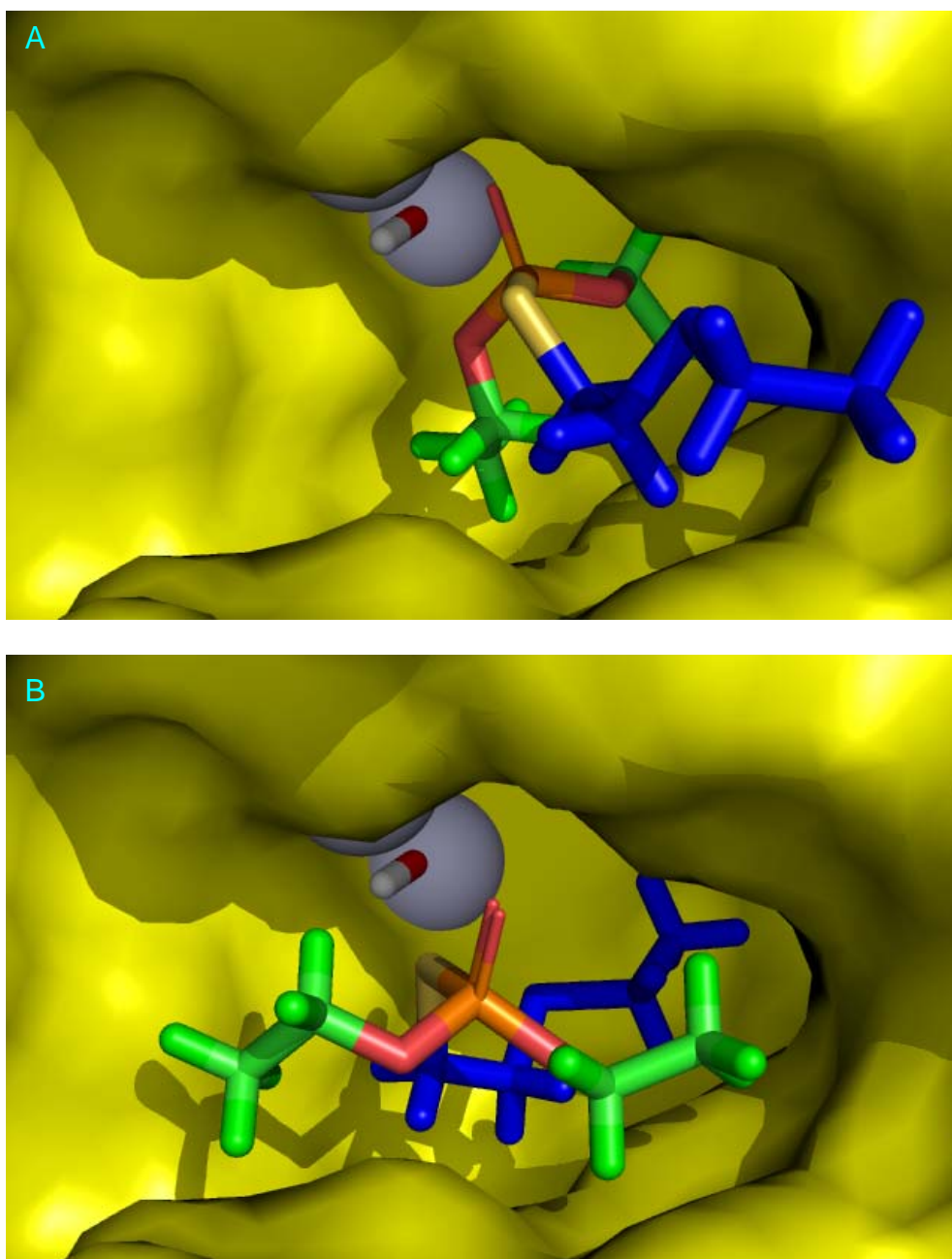


Figure 3.3: Representative Binding of Demeton-S into WT OPH. The demeton-S substrate is shown in sticks in each of the active sites. The Zn^{2+} atoms are displayed in silver spheres. Adjacent to the Zn^{2+} is the activated hydroxyl also shown in stick form. The leaving group is shown in blue with a yellow P-S sulfur. The two ethoxy groups are shown in green with red P-O oxygens. A) An example of a productive binding position in WT OPH with the leaving group of demeton-S opposite the activated hydroxyl from the phosphorus atom. B) A representative orientation in wild type Zn^{2+} with the leaving group positioned in the small pocket and the substrate in a nonproductive binding.

shown in Table 3.6. The angle formed by the hydroxyl, the phosphorus and the leaving group must be more than 110.3° and the distance from the hydroxyl to the phosphorus less than 500 pm to be defined as a productive binding. There are more productive poses with the paraoxon substrate than the demeton-S, which is reflected in the improved kinetics of WT with paraoxon.

Accommodation of Demeton-S in Active Site by Increase in Pocket Size. The sulfur of the P-S bond is approximately 40% larger (103 pm compared to 73 pm) than the oxygen of the P-O bond. The phenylalanine at 306 directly faces the oxygen of the P-O bond, and it was speculated for this design path that reducing the size of this residue should allot more space for accommodation of the sulfur in the active site (Figure 3.4). The F306L mutation was used in conjunction with the first generation H254S and the H257L, each of which supported improved kinetics for the demeton-S substrate. Unfortunately, the kinetic values were inferior to wild type in all cases; in fact, a complete loss of activity for demeton-S was observed. Although the hypothesis driving this mutation design, to better accommodate the larger sulfur moiety by increasing the size of the leaving group pocket, cannot be dismissed, these results indicate that residue 306 plays a critical role in maintenance of the active site for all the substrates that was not anticipated.

To better understand the role of 306 in the structure-function relations of this region, energy minimizations were performed. Using the 1DPM structure of the wild type OPH with the active site defined by diethyl-4-methylbenzylphosphate, Build Mutants tool of Discovery Studios was used to change the 306 residue to a leucine and

Table 3.6: WT Docking of Paraoxon and Demeton-S.

| Pose | Paraoxon | | | | Demeton-S | | | |
|------|----------------|---------|-------|----------|----------------|---------|-------|----------|
| | Binding Energy | Binding | Angle | Distance | Binding Energy | Binding | Angle | Distance |
| 1 | -37.2 | N | 66.6 | 3.0 | -40.9 | N | 15.6 | 5.0 |
| 2 | -37.0 | P | 131.8 | 3.3 | -40.9 | P | 139.3 | 3.3 |
| 3 | -37.0 | P | 131.4 | 3.3 | -40.8 | N | 17.0 | 5.0 |
| 4 | -36.8 | N | 82.8 | 3.2 | -39.6 | N | 91.0 | 4.3 |
| 5 | -36.8 | N | 82.5 | 3.2 | -38.7 | N | 89.8 | 4.2 |
| 6 | -36.6 | P | 143.4 | 3.4 | -38.4 | P | 144.7 | 3.1 |
| 7 | -36.1 | P | 140.7 | 3.4 | -38.0 | N | 83.3 | 3.7 |
| 8 | -35.4 | P | 121.9 | 3.5 | -37.8 | P | 145.4 | 3.4 |
| 9 | -34.1 | P | 128.2 | 3.3 | -37.7 | N | 55.7 | 3.6 |
| 10 | -32.0 | N | 59.3 | 7.6 | -37.6 | N | 75.1 | 3.6 |

P = Productive binding pose

N = Nonproductive binding pose

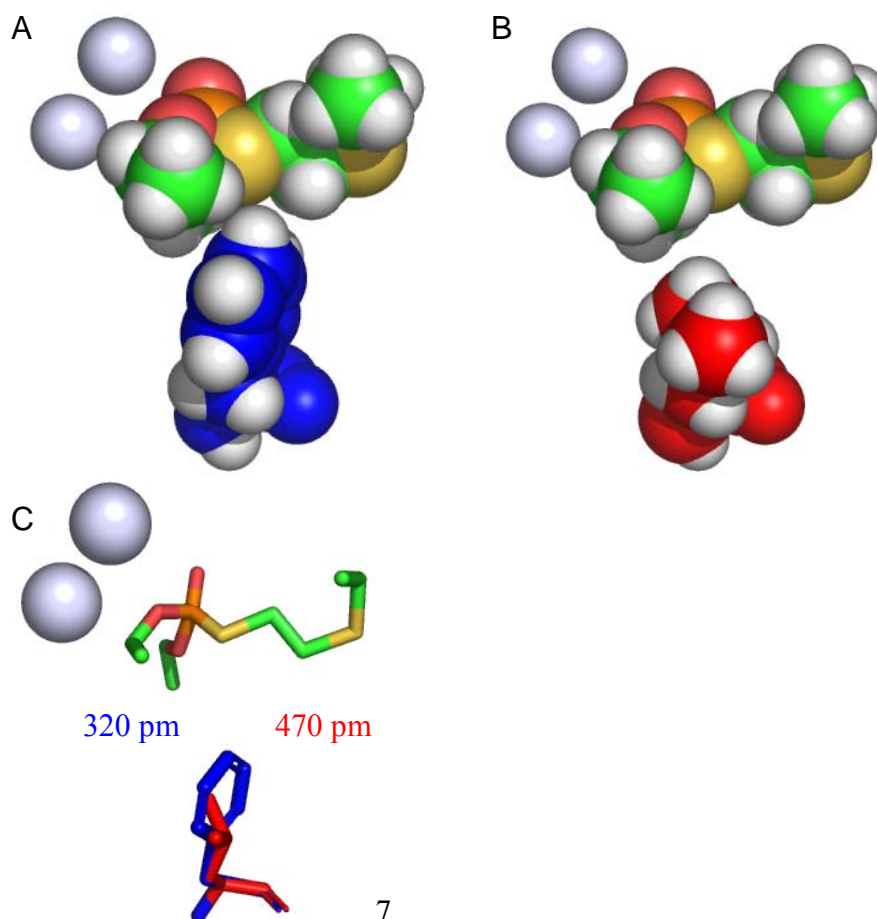


Figure 3.4: Cut Away of the Wild Type and the F306L OPH Variant Active Sites. This structure shows the 306 side chain, demeton-S (sphere colored by atom type) and the Zn^{2+} (the two silver spheres represent the Zn^{2+} in PDB 1DPM). The orientation was selected to illustrate the proximity of the sulfur of demeton-S (represented in yellow in the substrate spheres) to the 306 side chain. A) The Wild type structure with phenylalanine (in blue) at 306 of OPH. B) The F306L variant, with leucine (in red) at 306. C) Stick representation of wild type and variant. The distances shown are those between the demeton-S sulfur and the nearest hydrogen on the 306 residue.

the residues within a 0.8 nm radius were energy minimized. The resulting model suggested that elimination of a stacking interaction between the phenylalanine of 306 and the tyrosine at 309 results in an approximately 90° rotation of the tyrosine about the alpha and beta carbons. This new orientation partially occludes the active site, thus obstructing the binding of substrates (Figure 3.5). The opening to the active site, evaluated by the distance between the surface of the 254 residue to the surface of the 309 residue, decreases from 7.7 to 5.4 angstroms. The decrease in active site access can explain the observed decay of the kinetics of the F306L variants for all the substrates, as it is now more difficult, if not impossible, for the substrates to access the active site.

Although previously reported mutations at F306 were not tested with demeton-S, the paraoxonase activity loss was not reported to be as pronounced as that observed with the F306L mutants. However, in these previous studies the phenylalanine was replaced by a histidine or tyrosine, both residues that are capable of maintaining to some extent the stacking interaction with tyrosine 309, which is shown here to be critical for maintenance of the active site (117).

Effect of Single Mutations in the Large Pocket on P-S Substrate Hydrolysis.

Previously reported alterations at residues 254 and 257 have resulted in changes, and even improvements, in reaction kinetics with various substrates (Table 3.2). Replacing the native 254 histidine with an arginine maintained the hydrophilicity of the large pocket region and has been shown to increase the hydrolytic rate of the enzyme with the substrate demeton-S. A serine substitution at 254, which is less hydrophilic than arginine, lowered the K_M for demeton-S from the WT value of 4.8 mM to 0.033 mM.

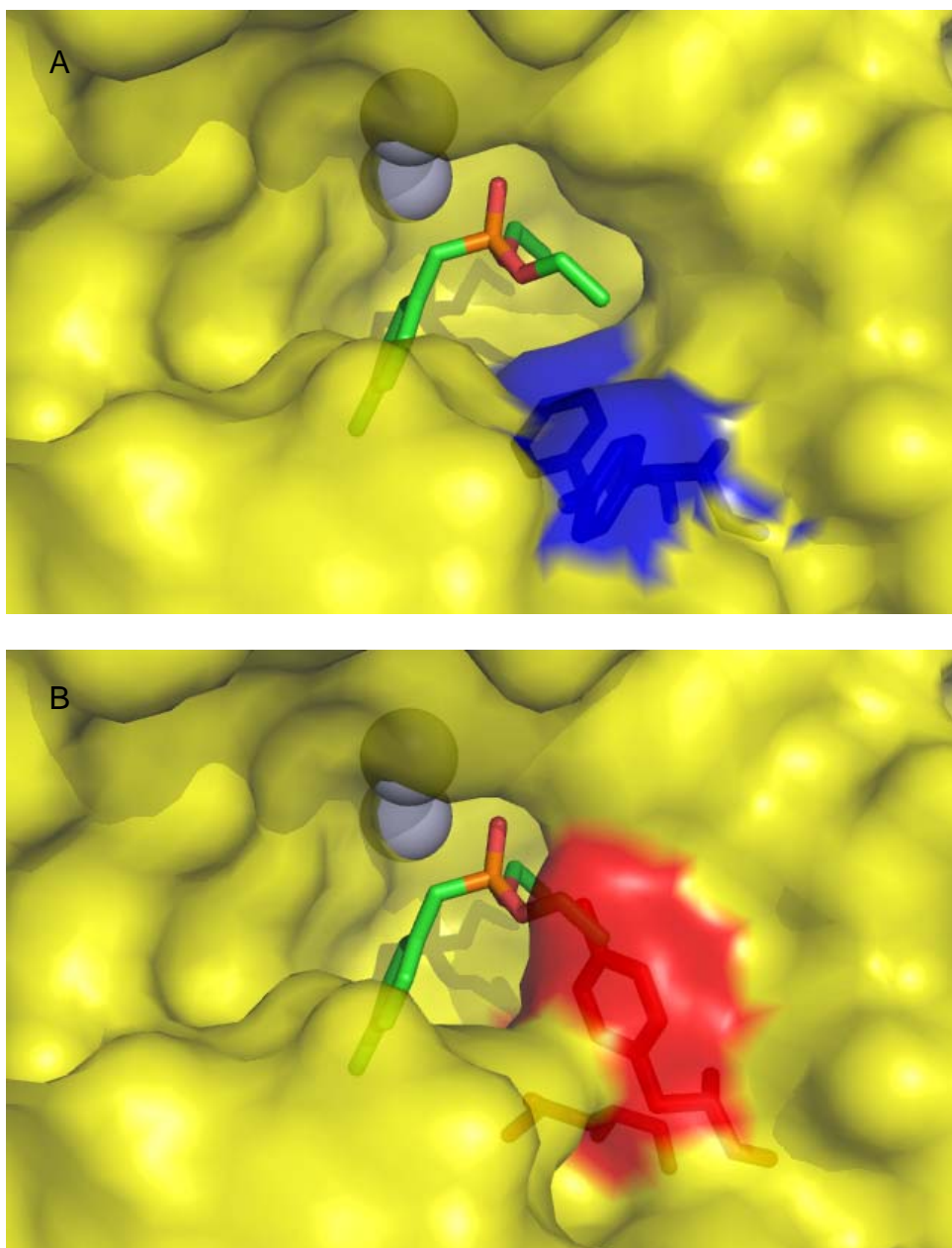


Figure 3.5: Energy Minimization of the F306L Variant. A) Wild type OPH with F306 and Y309 shown in blue sticks and surface. B) F306L OPH with L306 and Y309 shown in red sticks and surface. The blue surface is that contributed by the phenylalanine and tyrosine in the wild type OPH, while the red surface is that contributed by the leucine and tyrosine in the F306L variant. The methylbenzyl group of the inhibitor is behind the surface generated by L271 and M317. The F306L variant has the leaving group ethoxy group resides within the surface generated by T309. The active site is defined by the inhibitor found in the PDB 1DPM crystal structure and the silver spheres are the Zn²⁺ ions.

The leaving group of demeton-S, VX and RVX are large hydrophobic moieties. The hypothesis is that increasing the hydrophobicity of this region would allow the P-S substrates increased access to the active site. To test this hypothesis, the histidine at 254 was mutated to a leucine, increasing the hydrophobicity of the large pocket. As evaluated by modeling, the H254L active site (Figure 3.6) seems to be relatively unchanged from the wild type. This is consistent with the relatively small changes which were observed in the kinetics of this variant relative to WT (Table 3.5). The only obvious change visible is the designed hydrophobicity alteration of the active site surface, indicated by the blue shade at the surface of 254 in Figure 3.6. This indicates that the hydrophobicity of this region is not as directly related to the kinetics of the enzyme for a particular substrate as hypothesized. Although the H254 variant did not exhibit the large activity loss observed for the F306L mutations, it did not exhibit the desired kinetic improvement for demeton-S.

Synergistic Improvement in Hydrolysis Kinetics of Combined Mutations. The reported successful creation of mutations with enhanced demeton-S hydrolysis involving both 254 and 257 residues suggest that the leaving group of this substrate resides near the large pocket during hydrolysis (Table 3.2, Figure 3.1). The H254R and the H257L mutants demonstrated enhanced catalytic efficiency with the demeton-S substrate, 4.1-fold and 2.0-fold, respectively. When combined, the kinetics improved even further, with the H254R/H257L variant exhibiting a 31-fold increase in catalytic efficiency for demeton-S (11). The H254S created for these studies also demonstrated an improvement in the kinetics with demeton-S, 20.7-fold. To explore the potential for a

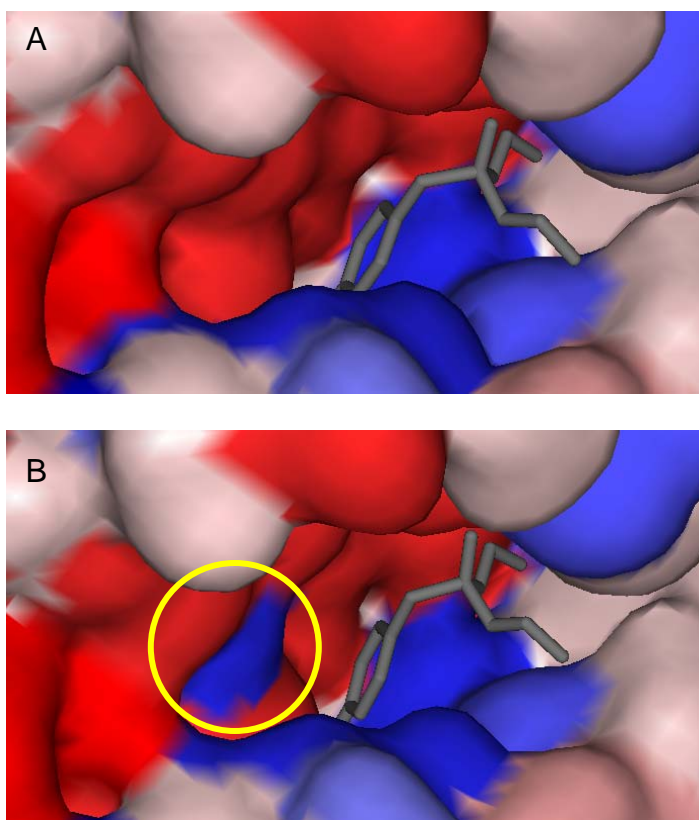
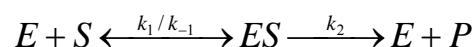


Figure 3.6: Hydrophobicity Change in the H254L Variant. The dark gray structure is the EBP inhibitor found in the active site of the 1DPM crystal structure. The yellow circle is the location of the H254L residue. A) Wild type (H254) OPH. B) Leucine at 254 of OPH. Red surface represents hydrophilic residues and blue surfaces represent hydrophobic residues.

synergistic relationship in this region, the H254S and H257L mutants were combined and indeed a 23.9-fold improvement in the kinetics was observed. The increase in k_{cat} from the WT 2.2 sec^{-1} to H254S/H257L's 78.5 sec^{-1} with demeton-S is responsible for the corresponding increase in catalytic efficiency. Based on the kinetic results, it was hypothesized that relative to the WT enzyme, there would be either an increase in the number of productive binding events or a decrease in the binding energy associated with the docking events within the H254S/H257L variant. Such an outcome would indicate that the substrate can more readily enter the active site and subsequently undergo hydrolysis. Alternatively, these results might also be explained by alterations in product release following hydrolysis. When hydrolysis occurs and the inversion in stereochemistry takes place, the two non-leaving group substituents, which in the case of demeton-S are two ethoxy groups, will generally face out of the active site while the hydroxyl group will face the inside of the active site. A decrease in the number of these productive hydrolysis product orientations or an increase in their docking energies would suggest that the diethyl phosphate product is energetically unfavorable in the active site.

To distinguish between these alternatives, docking studies were performed with the H254S/H257L variant. In those studies in which the docking of demeton-S was explored, there was neither an increase in the number of productive bindings nor was there any improvement in the predicted binding energies. This suggests that the enhanced catalysis observed with H254S/H257L was not directly related to substrate binding. However, when the diethyl phosphate hydrolysis product of demeton-S was docked in the enzymes' active sites, productive orientations were observed only for the

WT enzyme (Figure 3.7). For the WT, the top nine binding events were predicted to represent a productive orientation while none were observed with the H254S/H257L variant. This would indicate that the hydrolysis product in the variant is less stable, leading to an increase in the rate of product release. This can be visualized as an increase in the k_2 of the enzyme reaction;



where k_1 and k_{-1} are the entering and leaving of the substrate into the active site and k_2 is the chemistry and product leaving step. The maximum velocity is related to the concentration of total enzyme, $[E]_t = E + ES$, and the kinetic constant k_2 at saturating substrate concentrations, such that;

$$V_{\max} = k_2 [E]_t$$

and

$$k_{\text{cat}} = V_{\max}/[E]_t$$

Substituting $k_{\text{cat}} * [E]_t$ for V_{\max} ;

$$k_{\text{cat}} = k_2$$

This suggests that by enhancing product release, as is suggested by the diethyl phosphate docking, the k_2 and by analogy k_{cat} is expected to increase, which is exactly what is observed in the kinetic assays with demeton-S. These results support the

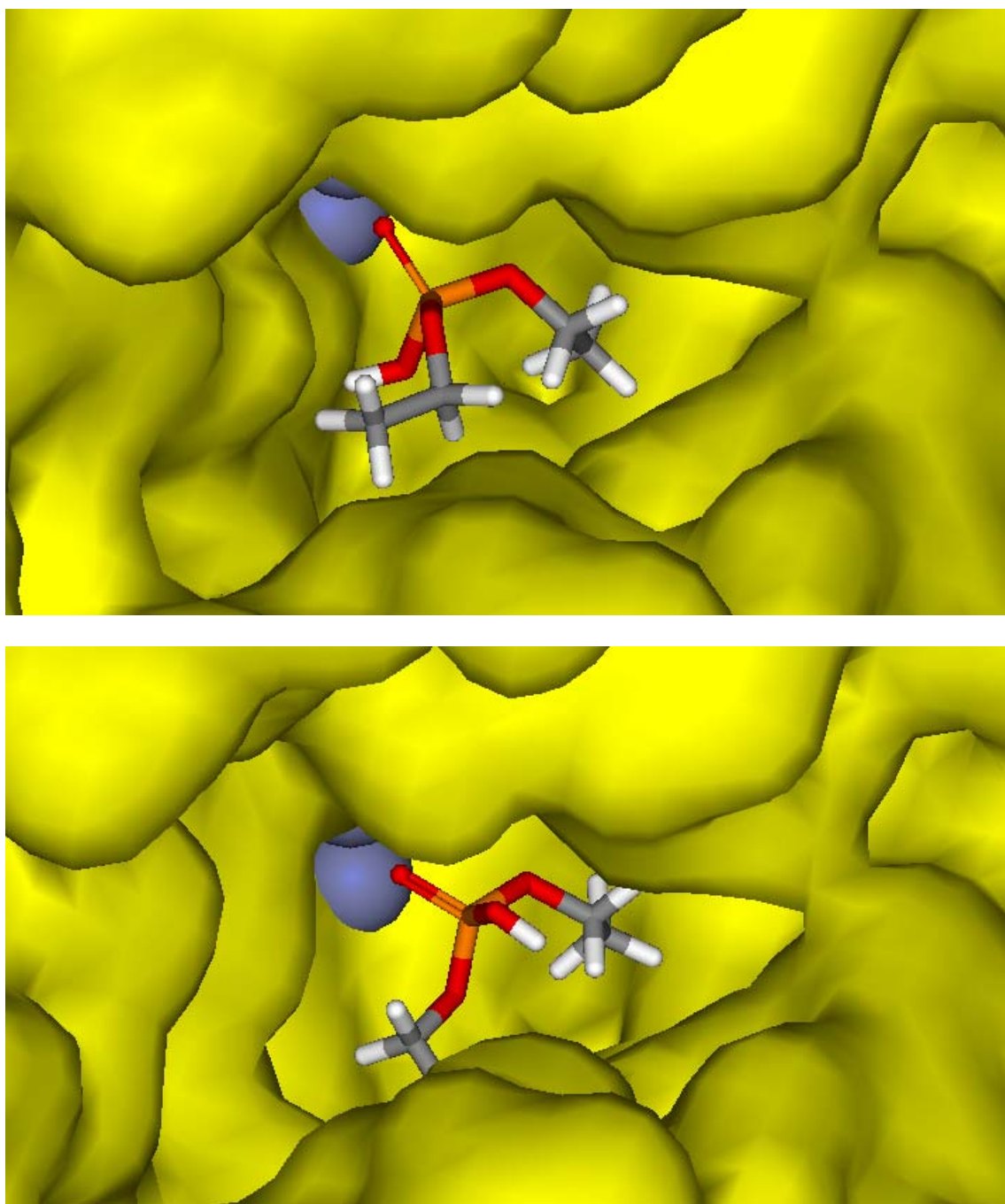


Figure 3.7: Representative Binding of the Demeton-S Hydrolysis Product into OPH. The demeton-S substrate is shown in sticks in each of the active sites. The Zn^{2+} atoms are displayed in silver spheres. A) An example of a productive binding position in wild type with the hydroxyl group towards the interior of the active site. B) A representative orientation in H254S/H257L with the hydroxyl group oriented facing out of the active site in a nonproductive binding.

hypothesis that change of the histidines at 254 and 257 to a serine and leucine, respectively, makes the residence of the demeton-S hydrolysis product in the active site less favorable, enhancing its rate of release which presents as an increase in k_{cat} .

Importance of Rational Design for Decontamination. Altering native enzymes is not without its limitations. Mutations can drastically reduce stability or prevent proper folding of the enzyme. Because of the iterative process of rational design, often many mutations must take place before the desired improvement results and, particularly with enzymes which hydrolyze a class of compounds, the enhancement of activity against a specific substrate often comes at the expense of others. Searching protein sequence space for improved catalyst requires either a high throughput approach, or a large body of information on which to base a rational approach. With its improved kinetics for the P-S bond, the H254S/H257L variant demonstrates both the importance and challenges of a rational approach in the re-design of enzymes. When demeton-S is docked in the OPH active site a significant percentage of the docking conformations orient the leaving group in the small pocket of the active site, which can be considered a nonproductive binding event and seven out of the top ten docking positions of demeton-S in wild type OPH have the leaving group facing or in the small pocket (Figure 3.3, Table 3.7). Some success in enhancing demeton-s hydrolysis was achieved in the design cycle reported here, but just as importantly, new information was gained about the active site of this enzyme, which will facilitate further enhancements. In order to properly align the demeton-S for productive binding a residue in the small pocket could be altered by

Table 3.7: Demeton-S Docking Energies and Positions.

| Demeton-S Pose | Docking energy Wild Type OPH | Leaving Group Position |
|-------------------|------------------------------|------------------------|
| 1 | -40.9 | Small Pocket |
| 2 | -40.9 | Productive |
| 3 | -40.8 | Small Pocket |
| 4 | -39.6 | Small Pocket |
| 5 | -38.7 | Small Pocket |
| 6 | -38.4 | Productive |
| 7 | -38.0 | Small Pocket |
| 8 | -37.8 | Productive |
| 9 | -37.7 | Small Pocket |
| 10 | -37.6 | Small Pocket |

introducing a larger residue to inhibit the leaving groups of large substrates from positioning in the small pocket.

CHAPTER IV

ANALYSIS OF THE IN VITRO PROTECTION OF ACETYLCHOLINESTERASE FROM INHIBITION BY OP NEUROTOXINS

When OP neurotoxins migrate into the brain and inhibit AChE, there is an accumulation of ACh in the synaptic junction. The resulting decrease in the termination of nerve impulses leads to a wide collection of cholinergic effects ultimately resulting in muscular dysfunction and nerve damage. Currently, the method of choice for the treatment of OP poisoning includes atropine, for removing the ACh from the muscarinic receptors, and oxime, for the regeneration of inhibited vascular AChE. Although this therapeutic approach can avoid permanent damage and be lifesaving, particularly at lower exposure levels, it does not affect the in vivo concentration of the OP. For this reason, there is a need to develop a post-exposure, therapeutic process which provides immediate protection and recovery from OP poisoning, while reducing vascular concentrations of the neurotoxic agents.

One of the considerations of OP neurosensitivity in mammalian species is the OP hydrolyzing capacity of indigenous, intravascular enzymes such as PON1. Evaluation of the protective effects of PON1 in human populations is complicated because the intravascular level of enzyme varies between individuals and PON1 has significant polymorphisms as well. Sequencing population variants of the human PON1 genes has identified two genetic polymorphisms, distinguished by amino acid substitutions at

positions 55 and 192, which play a role in OP sensitivity (*120, 121*). Pedigree analysis established the 192 polymorphism as concordant with the serum paraoxonase phenotypes, with the arginine 192 isoform hydrolyzing paraoxon more rapidly than the glutamine 192 isoform (*120, 122, 123*). This effect of the PON1 polymorphism is reversed for the hydrolysis of diazoxon, soman and especially sarin, with the serum of Glu192 homozygotes displaying almost 10-fold greater activity against sarin than the Arg192 homozygotes. Similar results have been reported for polymorphisms at amino acid 55. These PON1 polymorphisms, L55M and Q192R, affect OP hydrolysis activity. PON1 activity in blood serum from 55M homozygotes was reduced more than 50% with paraoxon compared to either the 55L homozygote or the LM heterozygote (*66*). In an occupational study, individuals homozygous for the M variant had the lowest AChE activity after OP exposure, which indicated that they were most susceptible to OP compounds (*124*). These studies indicate that there is a therapeutic role for PON1 in endemic resistance to OP neurotoxins and suggested that the use of efficient OP hydrolases from other biological sources could serve as an effective intravascular scavenger.

In general, the use of enzyme-based catalytic bioscavengers would be advantageous because lower concentrations of enzyme would be required in the intravascular system due to their higher catalytic activity compared to traditional non-enzymatic treatments. The lower concentrations of protein in circulation would be sufficient to detoxify relatively high concentrations of nerve agent, with the extent of protection predicted by the rate of reaction of the scavenger with a given nerve agent. In

fact, the half time for reaction of a nerve agent with a biological scavenger can be calculated using some conservative kinetic assumptions. Based on toxicity estimates in humans, the expected concentration of a nerve agent in the blood at an LD₅₀ dose would be approximately 8×10^{-7} M (125). The bimolecular rate constant for reaction of soman with AChE is $\sim 9 \times 10^7$ M⁻¹ min⁻¹ (126). If a scavenger were present in the blood at a concentration of 1 mg/ml (1×10^{-5} M), then the rate constant for reaction of scavenger with toxicant would be pseudo first order with respect to substrate, and the $t_{1/2}$ for the reduction of toxicant would be $\sim 3-7 \times 10^{-4}$ min. Under those conditions, which assume adequate mixing and the retention of the bioscavenger and the toxicant in the bloodstream, the concentration of toxicant would be reduced to 1/1000th of its initial concentration within 10 half lives of the enzyme catalysis ($2-4 \times 10^{-3}$ min). Where actual measurements have been made of the rate of reduction in the concentration of soman in guinea pigs in the absence of an exogenous scavenger, the concentration of a 2 x LD₅₀ dose of soman in circulation was reduced by 1000-fold in about 1.5 minutes (127). These results support the contention that the presence of a bioscavenger in circulation at the time of exposure would provide significant prophylactic protection. The reduction in OP neurotoxin concentration to a physiologically insignificant level (with no measurable inhibition of AChE) would be very rapid, and would occur in less than one circulation time at most concentrations of OP that might be encountered. The need to administer, repetitively, a host of pharmacologically active drugs with a short duration of action at a precise time following exposure is all but eliminated if a scavenger is used.

With the appropriate administration of various bioscavenger(s), such an approach could afford protection against all of the current threat agents, including those that induce rapid aging of AChE and are refractory to treatment by the current atropine and oxime treatment regime. The fast rates of reactions, relatively low K_M , and ease of production of the bacterial enzymes encourage the investigation of their potential as post-exposure, therapeutic or pre-exposure prophylactic antagonists against OP poisoning. The kinetic efficiencies of any potential therapeutic enzyme must be considered relative to realistic exposure concentrations and the nature of the neurotoxins. As has been previously discussed, substrate saturating (~millimolar) conditions are not likely to occur intravascularly, and when the concentration of available substrate is at or below the K_M of the enzyme, the catalyzed reaction becomes second order or pseudo first order with respect to substrate and k_{cat}/K_M , the second order rate constant, is indicative of the hydrolysis rate. The high toxicity of OP compounds sets a requirement for protection to be provided at relatively low OP vascular concentrations; for example, the lethal concentration of VX in vivo can be as low as 2 μM . This is well below the K_M of any hydrolyzing enzyme (~10 to 200 μM) for the OP substrates, especially the chemical warfare agents such as VX. In order to address these issues, an in vitro protocol for rapidly evaluating the efficacy of enzymes and drugs to protect AChE was developed.

The protection assay used in these studies focused on the extent to which 2-PAM, OPH and OPAA alone or in combinations can prophylactically prevent or therapeutically alleviate AChE inhibition. Since the site of action of oximes is the

inhibited AChE, it has been included in the test compounds, while atropine, with a muscarinic receptor site of action, was excluded from consideration. With the addition of OP hydrolyzing enzyme and the reaction of oximes with acetylthiocholine (ASCh), a multi-phased unwieldy reaction equation is generated (Figure 4.1). The activity of AChE is monitored spectrophotometrically using the hydrolytic product of the substrate ASCh, thiocholine, reacting with 5,5'-Dithio-bis-2-nitrobenzoic acid, leaving a compound that absorbs at 405 nm as depicted sequentially in reactions I and VII. Depending on the OP and/or oxime, there is the potential for other reaction products to contribute to the spectrophotometric signal, thus complicating the analysis. For example, 2-PAM also reacts with ASCh to produce thiocholine (reaction IV), and the enzymatic hydrolysis of paraoxon (reaction V) and demeton-S produces *p*-nitrophenol and a free thiol, respectively, both of which are monitored at 405 nm. In order to ensure the spectrophotometric signal analysis only considers the inhibition of AChE, it is necessary to remove any remaining OP or oxime prior to analyzing for remaining AChE activity. By working at OP concentrations that are just sufficient for complete AChE inhibition, the effectiveness of any added protectant can be evaluated by the amount of AChE activity that is protected. The potential to protect AChE with OP hydrolyzing enzymes is significant, as this adds a route to eliminate the OP, complimenting any regeneration of inhibited AChE that can be achieved by 2-PAM. Because of the complexity of the AChE reaction depicted in Figure 4.1 this method was developed, to allow for the efficacy prediction of in vivo treatment of OP compounds.

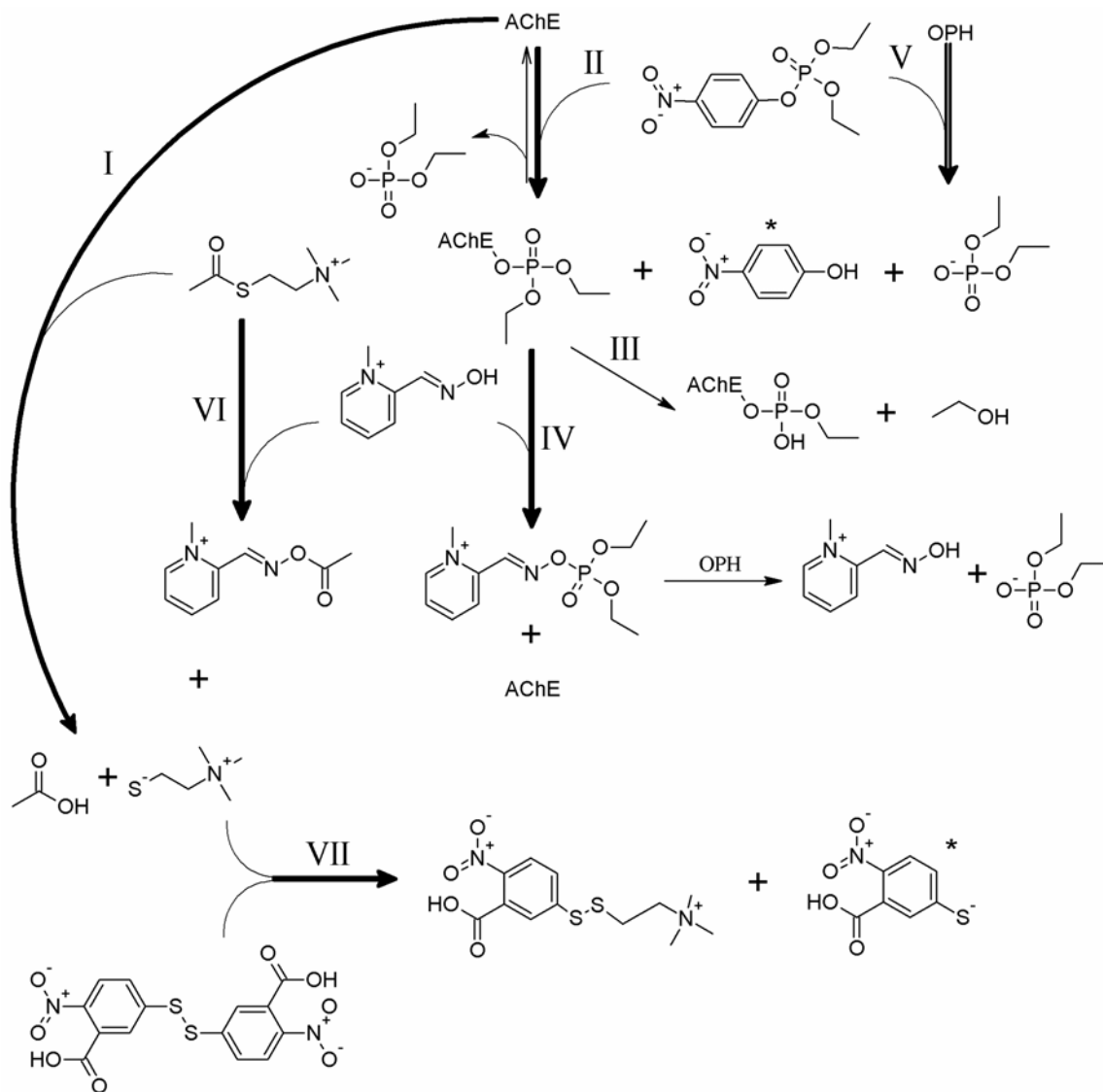


Figure 4.1: Reaction Scheme of Acetylcholinesterase Inhibition, Reactivation and Protection. OPH, 2-PAM and paraoxon are used in the example. I) AChE reaction with ASCh, II) AChE inhibition by paraoxon, III) AChE ageing, IV) AChE reactivation by 2-PAM, V) OPH reaction with paraoxon, VI) Oxime reaction with ASCh, VII) DTNB reaction with S⁻. The “*” indicates a photometrically detectable metabolite.

Materials and Methods

Materials. Paraoxon, DFP and demeton-S were purchased from ChemService (West Chester, PA). OPAA was a generous gift from the laboratory of T.C. Cheng, US Army Edgewood Chemical & Biological Center, Aberdeen Proving Ground, MD 21010-5423, USA and stored at -70°C in 1 μM DTT. All other chemicals were purchased from Sigma–Aldrich (St. Louis, MO). Electric eel AChE from Sigma was shipped as a lyophilized powder in 1000 unit increments.

AChE Inhibition by OP's. The cholinergic potency (AChE Inhibition levels) for each new vial of AChE had to be determined empirically for each of the OP compounds of interest. The commercial acetylcholinesterase product was resuspended to a protein concentration of 1 mg/ml (~1000 units) in 0.1 M potassium phosphate buffer, pH 7.4 and allowed to hydrate for 24 hours. To effect inhibition, the AChE suspension was incubated for 24 hours at a protein concentration of 0.1 mg/ml over a suitable concentration range for each of the selected OPs. Following the inhibition period, a Biorad P-6 microspin column was used to separate the AChE and excess inhibitor. To determine remaining AChE activity, the eluent, which contained the AChE fraction, was further diluted to 0.033 mg/ml and assayed. For these studies, acetylthiocholine (ASCh) was used as the substrate at a final concentration of 1 mM and the reaction was monitored at 405 nm with 1 mM 5,5'-dithio-bis-2-nitrobenzoic acid (DTNB). The concentration of each of the OP neurotoxins selected for use in the protection studies corresponded to that concentration which resulted in >95% inhibition of AChE. This

concentration had to be empirically determined for each vial of AChE in order to accommodate variations in the commercial enzyme activities.

Protection of AChE Activity by Monoxime. A stock solution of 2-pralidoxime (2-PAM) was prepared by resuspending the commercial preparation in 0.1 M potassium phosphate buffer, pH 7.4, to 10 mM. A concentration range of 2-PAM was prepared by dilution in 0.1 M potassium phosphate buffer, pH 7.4, and added to the AChE preparation at the same time as the OP inhibitor. The OP and AChE concentrations were kept constant. The activity of AChE without OP neurotoxin provided the activity control, while AChE plus OP neurotoxin without 2-PAM was the inhibition baseline control. Following the 24 hour inhibition period, a Biorad P-6 microspin column was used to separate the AChE from the excess inhibitor and 2-PAM. The column storage buffer was eluted by centrifugation for 2 minutes at 1000 x g and the AChE activity/inhibition assay solution was added and similarly eluted. The remaining AChE activity was measured as described above.

Protection of AChE Enzyme. Each concentration range of bioscavenger enzymes, either OPH or OPAA, was prepared by dilution in 0.1 M potassium phosphate buffer, pH 7.4, and added to the AChE preparation at the same time as the OP inhibitor. The OP and AChE concentrations were held constant. AChE without OP was used as the AChE activity control, while AChE with OP but without bioscavenger enzyme provided the activity inhibition control. Following the 24 hour inhibition period, a Biorad P-6 microspin column was used as described previously to separate the AChE

from the excess inhibitor. The remaining AChE activity was measured as previously described.

Results

Enzymatic Protection of AChE from OP Inhibition. OPH and OPAA have their highest bioscavenger activities with paraoxon and DFP, respectively. The ability of these enzymes, with and without 2-PAM, were evaluated in an in vitro assay with paraoxon (a phosphotriester pesticide) and diisopropyl-fluoridate (DFP, a phosphonofluoridate surrogate for class G chemical warfare agents) to determine their efficacy in protecting AChE from inhibition. The concentration ranges for the OP compounds which inhibited 95% of the AChE and the protectant concentration ranges were determined empirically, and are shown in Table 4.1. The P_{50} is defined as the [protectant]/[inhibitor] molar ratio at which AChE has 50% of the activity of the no inhibitor control. As a stoichiometric protectant, one molecule of 2-PAM can reactivate one molecule of AChE and so is expected to have a relatively high P_{50} of one or greater. The P_{50} of 2-PAM with paraoxon and DFP was 1 and 10, respectively (Figure 4.2). In the context of this protection assay, this can be interpreted to mean that it takes one mole of 2-PAM for every mole of paraoxon to effectively protect 50% of the AChE from the inhibiting effects of paraoxon. Similarly, it requires 10 moles of 2-PAM to protect AChE from 50% inhibition by DFP. Although enzymatic bioscavengers have the potential for a much lower P_{50} due to its catalytic nature, in practice this will be related to the catalytic efficiency of the enzyme for the specific OP inhibitor of AChE (Table 4.2). For example, even though OPAA catalyzes the hydrolysis of paraoxon with a k_{cat}

Table 4.1: Concentration of Protectants (μM) and Inhibitors (μM) of AChE.

| Protectant | Paraoxon (0.2 - 0.4) | DFP (0.6 - 0.8) | Demeton-S (2.0) |
|-------------|--|---|---|
| 2-PAM | 0.02 - 8.0 | 0.3 - 160 | 0.1 - 80.0 |
| OPH | 3.5×10^{-10} - 7.0×10^{-3} | 5.3×10^{-5} - 7.0×10^{-2} | NP |
| OPAA | 8.2×10^{-3} - 1.6×10^1 | 6.0×10^{-5} - 5.0×10^0 | 3.4×10^{-1} - 7.0×10^{-0} |
| H254R/H257L | NP | NP | 2.0×10^{-4} - 2.0×10^{-1} |
| H254S/H257L | NP | NP | 5.4×10^{-4} - 5.4×10^{-1} |
| H254R/H257F | NP | NP | 2.4×10^{-4} - 2.4×10^{-1} |

NP = Not Performed

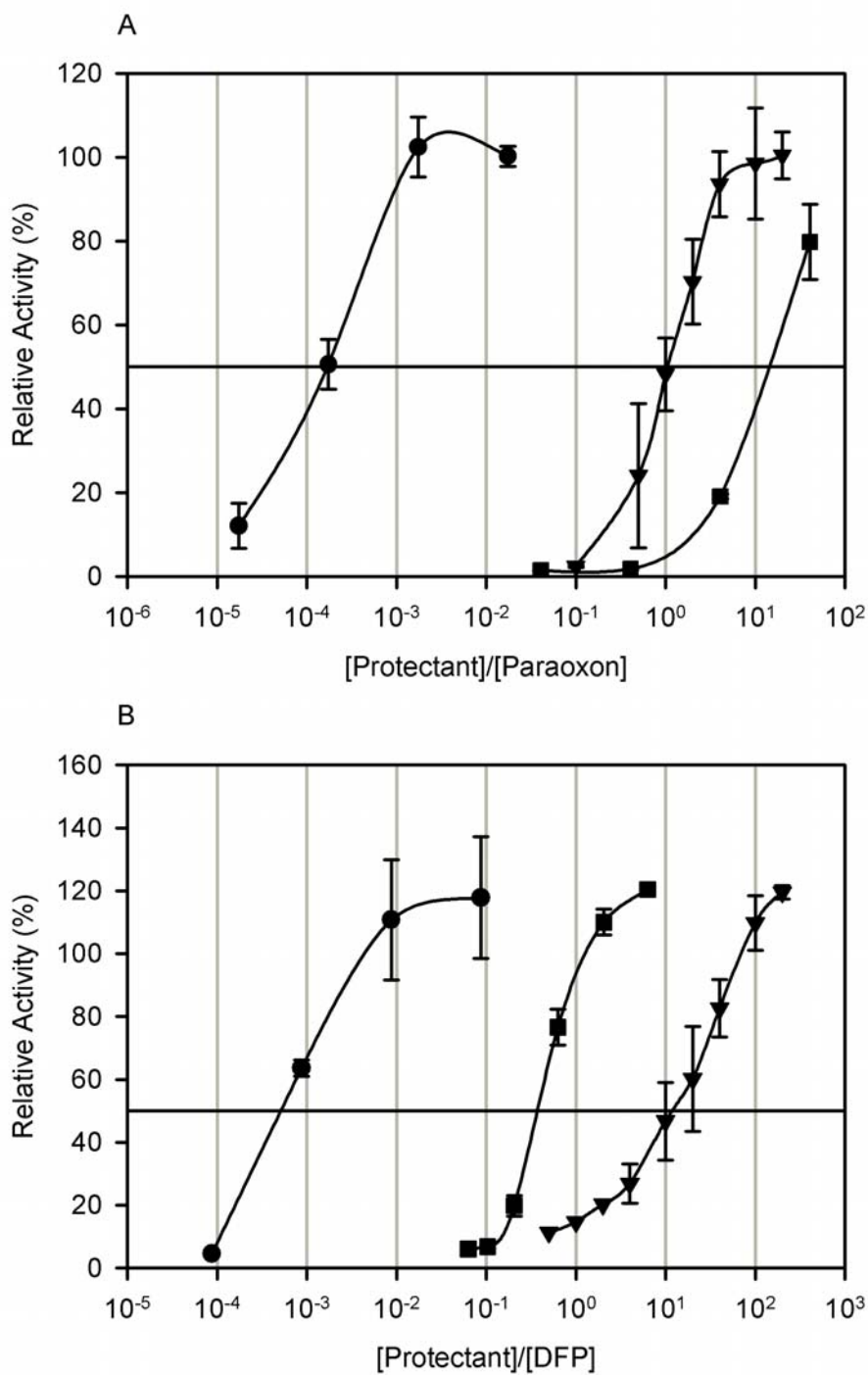


Figure 4.2: Counteracting AChE Inhibition. Protection of AChE from inhibition by (A) paraoxon and (B) DFP by (●) OPH, (■) OPAA and (▼) 2-PAM. The horizontal line represents the P₅₀, the ratio of protectant to inhibitor at which 50% of the AChE activity remains

Table 4.2. AChE Protective Index (P_{50}) of Enzymatic Bioscavengers.

| | Paraoxon | DFP |
|-------|----------|--------|
| 2-PAM | 1.0 | 10.0 |
| OPH | 0.0002 | 0.0005 |
| OPAA | 15.0 | 0.3 |

of almost 2.0 sec^{-1} (Table 2.3), it is twenty-fold less effective ($P_{50} = 15$) than even 2-PAM ($P_{50} = 1$) at protecting AChE against paraoxon (Figure 4.2). In contrast, OPH has a P_{50} of 2×10^{-4} , a 300,000 fold enhancement of protection as compared to OPAA.

The P_{50} values of OPH with paraoxon and DFP was determined to be 0.0002 and 0.0005, respectively, four and five logs more effective than the protection by 2-PAM alone. The P_{50} of OPAA with paraoxon and DFP was 15 and 0.3, respectively. The P_{50} values for the enzymes are proportional to their catalytic efficiencies (Figure 4.3). For example, even though the k_{cat} s of OPH and OPAA with DFP were within experimental error of each other, 3784 ± 370 and 3780 ± 560 , the P_{50} of OPH indicated it was approximately 600 times more effective than OPAA at protecting AChE against the inhibitory effects of DFP. There appears to be a good correlation between the P_{50} (Figure 4.3A) and enzyme specificity (Figure 4.3D). As has been previously discussed, at substrate concentrations well below the K_{M} s of the bioscavenger enzymes the second order rate kinetics become an important, if not the most important, predictor of efficacy. This can be seen in the comparison of Figure 4.3A and D, where the profile of the $k_{\text{cat}}/K_{\text{M}}$ values of the enzymes are inversely correlated with the P_{50} values.

OPH Variant Enzymes Designed for Enhanced Protection: The preceding studies used the native forms of OPH and OPAA for developing the AChE Protection Assay. However, enzymes (primarily OPH) have been modified to enhance their catalytic specificity, with some of the most important modifications targeting their capability to hydrolyze phosphorothioates (particularly the chemical warfare V-agents).

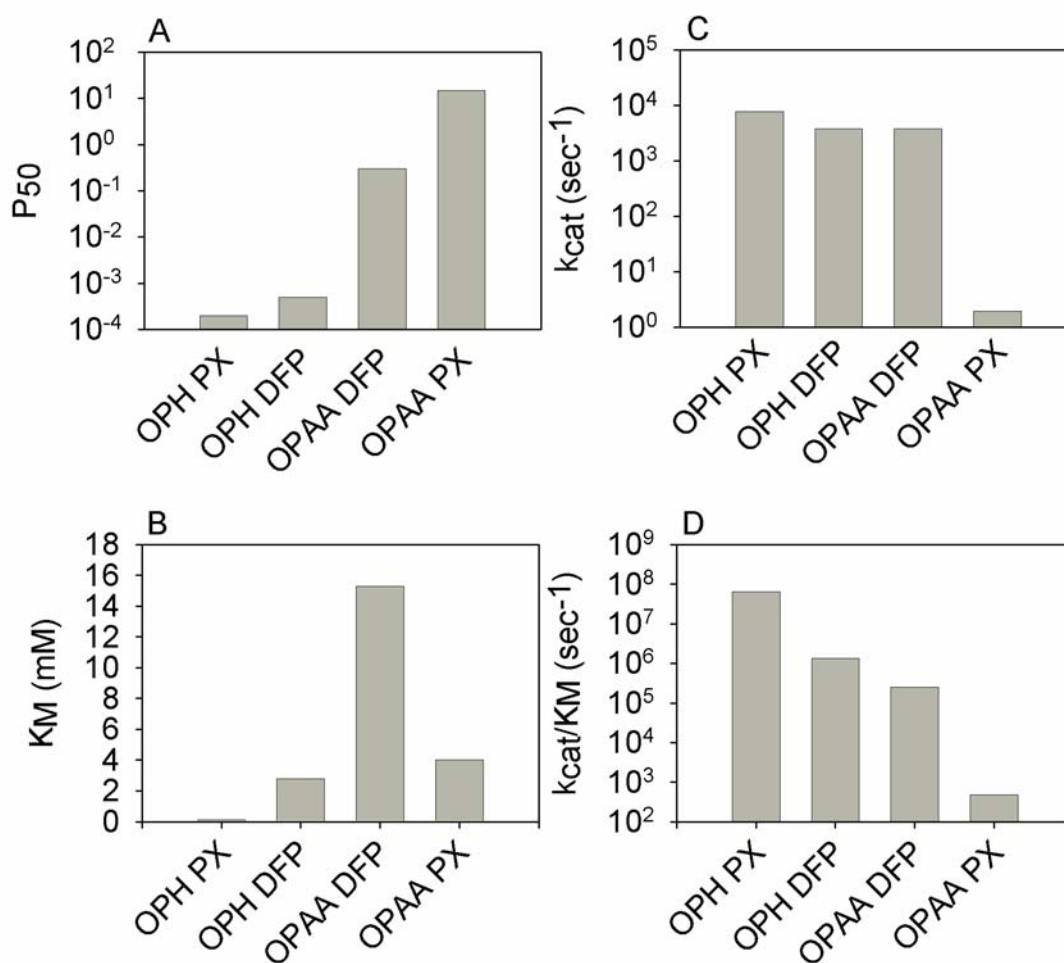


Figure 4.3: Comparison of the Protection Potential (P_{50}) and Kinetic Character of OPH and OPAA. The (A) P_{50} , [Protectant]/[Inhibitor] ratios of the enzymes, the (B) K_{MS} (mM), the (C) k_{cat} s (sec^{-1}) and the (D) k_{cat}/K_{MS} ($\text{M}^{-1} \text{sec}^{-1}$) for each enzyme with both paraoxon (PX) and DFP are compared.

Several variants of OPH have been created, including H254R/H257L (RL), H254R/H257F (RF), and H254S/H257L (SL), to improve the catalytic efficiency for the VX surrogate substrate demeton-S (see Chapter III). These are near active site mutations that have improved k_{cat} and K_{M} values for the P-S bond substrates. (OPAA does not have any detectable demeton-S activity, and so was not included in these studies.) The variant enzymes were evaluated to determine if the catalytic improvements were sufficient to improve protection of AChE against demeton-S over that provided by WT OPH (Figure 4.4). This is indeed the case as the P_{50} value for the wild type, RL, RF and SL are 0.2, 0.015, 0.006 and 0.010, respectively (Table 4.3). The variant enzymes demonstrated decreased P_{50} values with demeton-S by a factor of 13, 20, and 33 fold for RL, SL and RF, respectively. The protection curves of the variant enzymes are not significantly different from each other, as can be seen in Figure 4.5, however, the improvement of AChE protection over wild type OPH is approximately 100-fold, demonstrating that altering enzymes can improve protection performance (Figure 4.5). The RF enzyme appears to be an outlier in that its K_{M} is higher than that of the wild-type enzyme while the other two variants selected for this study had lower binding affinities. Furthermore, the enzyme specificity value ($k_{\text{cat}}/K_{\text{M}}$) is significantly lower for RL than the others. Nonetheless, its P_{50} index was virtually identical. It is conceivable that a larger than 2-fold difference in enzyme k_{cat} s is required to observe a change in P_{50} as evidenced by the variants' k_{cat} s and their respective indistinguishable P_{50} s.

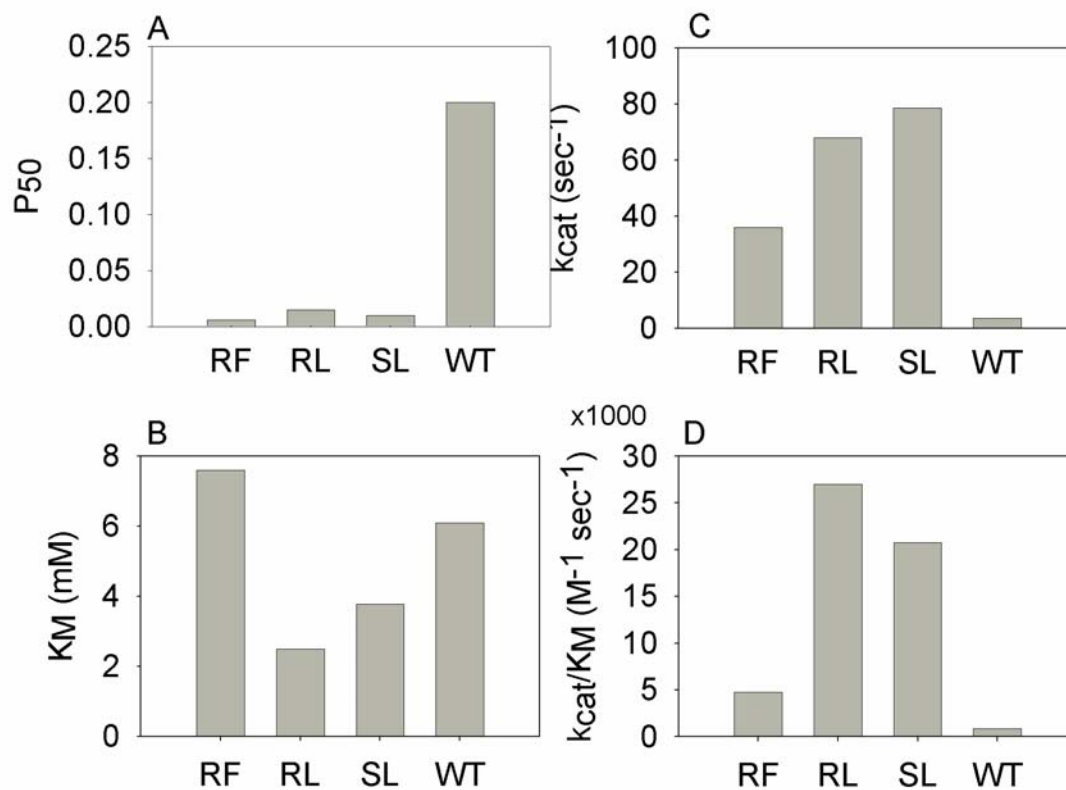


Figure 4.4: Comparison of the Protection Potential (P_{50}) and Kinetic Character of OPH Variants with the OP Compound, Demeton-S. The (A) [Protectant]/[Inhibitor] ratio of each enzyme, the (B) K_M (mM), the (C) k_{cat} (sec^{-1}) and the (D) k_{cat}/K_M ($\text{M}^{-1} \text{sec}^{-1}$) are shown for comparison.

Table 4.3. AChE Protective Index (P_{50}) of Enzymatic Bioscavengers with Demeton-S.

| | Demeton-S |
|-------|-----------|
| 2-PAM | 1.0 |
| OPH | 0.2 |
| RL | 0.015 |
| SL | 0.010 |
| RF | 0.006 |

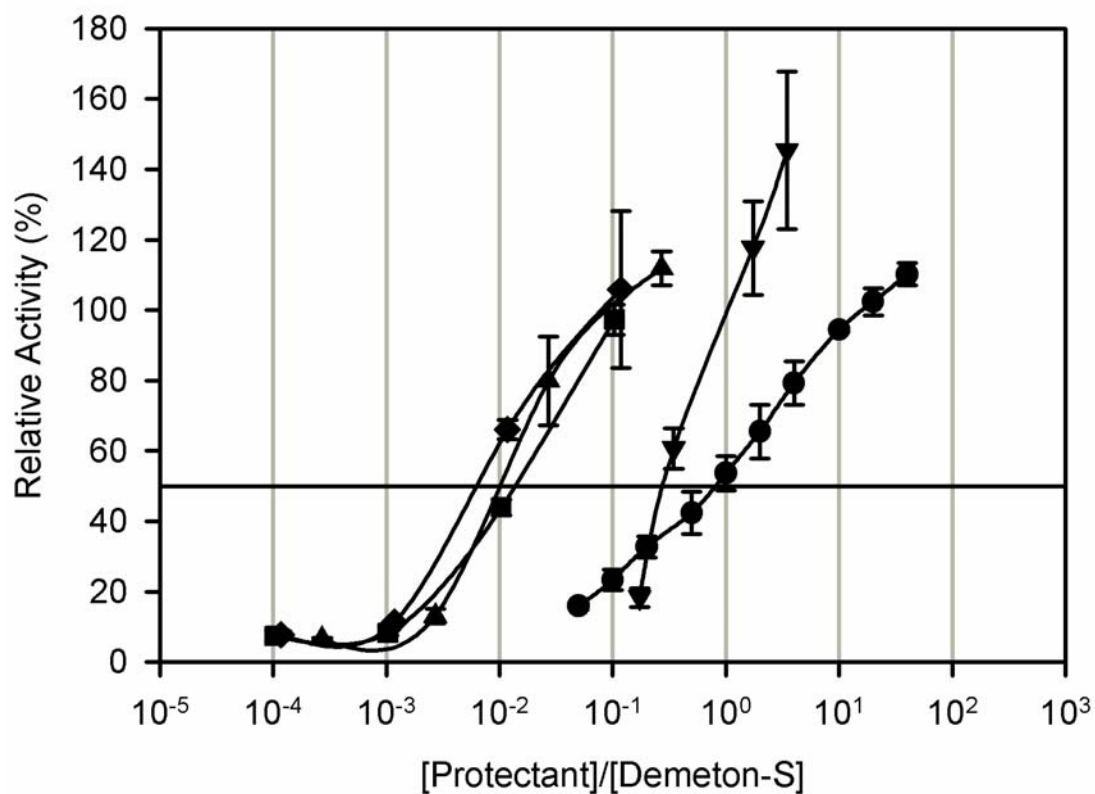


Figure 4.5: Counteracting AChE Inhibition by Demeton-S. Protection of AChE by (●) OPH wild type, (-) H254R/H257L, (■) H254R/H257F, (◆) H254S/H257L and (▼) 2-PAM is shown. The P_{50} is the ratio of protectant to inhibitor at which 50% of the AChE activity remains compared to a no inhibitor control.

Discussion

Based on the concentration of OP cholinergic neurotoxin that is required to provide 95% inhibition of AChE, the inhibitors can be ordered by their relative toxicity, from most toxic to least toxic, as follows: paraoxon (P-O bond) > DFP (P-F bond) > demeton-S (P-S bond) (Table 2.4). The protection ratio (P_{50}) values generally correlate with the k_{cat}/K_m values of each enzyme indicating the more catalytically efficient the enzyme, the better the protection ratio. With paraoxon and DFP, both 2-PAM and OPAA require an amount approaching or above stoichiometric levels to obtain an appreciable amount of AChE protection, with P_{50} 's ranging from 0.3 to 15. This is particularly noteworthy since OPAA has significant catalytic activity with DFP ($k_{\text{cat}} = 3780 \text{ sec}^{-1}$) but has very little protective value ($P_{50} = 0.3$). In contrast, OPH has a similar catalytic activity ($k_{\text{cat}} = 3784 \text{ sec}^{-1}$) with a protective ratio of 5×10^{-4} which is 600 fold more efficient. A notable characteristic which might contribute to this is that the K_M of OPAA and OPH for DFP are quite different ($K_M\text{-OPAA} = 15.3 \text{ mM}$; $K_M\text{-OPH} = 2.8 \text{ mM}$). This suggests that, particularly in those cases of similar catalytic rates, the substrate binding affinity plays a more formative role. In this scenario, 2-PAM and OPAA both function as a reactant. Each 2-PAM molecule reacts with a single inhibited AChE and is thus removed from further consideration as it decomposes to free AChE and phosphorylated oxime, which is no longer reactive with additional inhibited AChE. OPAA is behaving in a similarly stoichiometric fashion, with the P_{50} values suggesting that OPAA binds the OP, sequestering it and preventing AChE inhibition without evidence of catalysis. The OPAA hydrolysis reaction must be slow enough that it

functions as stoichiometric scavenger, requiring one molecule of OPAA to remove one molecule of OP. OPAA and 2-PAM function as reactants in a chemical reaction equation instead of functioning as catalysts being consumed in the reaction. As reactants, 2-PAM and OPAA require high molecular concentrations to drive the protection reaction, as it is second order. In contrast, OPH was able to provide the same levels of protection at far lower concentrations, resulting in P_{50} s of 0.0002 and 0.0005 for paraoxon and DFP, respectively.

With the phosphorothioate inhibitor demeton-S, the AChE protection afforded by wild type OPH approached a stoichiometric level ($P_{50} = 0.2$). However, this can be explained by the low catalytic efficiency rate ($k_{\text{cat}}/K_M = 759 \text{ M}^{-1} \text{ sec}^{-1}$) of the native enzyme toward demeton-S. Improvement in this is desired, as there are few alternative enzymes for P-S bond hydrolysis and there is a need for an efficient VXase. To address this, OPH variants were evaluated as protectants against the inhibitory effects of demeton-S, demonstrating that stoichiometric, catalytic protectants can be designed to provide enhanced protection from OP-induced inhibition of AChE. The variant enzymes decreased the P_{50} 's with demeton-S by as much as 33-fold. This demonstrates that enzymes with poor protection abilities can be altered to make their protection catalytically efficient instead of stoichiometric in nature. When these values are taken into account the OPAA protection from DFP is an outlier, with the k_{cat}/K_M predicting a lower P_{50} . While the overall protection trends inversely with the catalytic efficiency, these data suggest a critical role for K_M in protection. For example, the reported LCt_{50} s of racemic sarin and soman are 70 and 100 $\text{mg}/\text{min}/\text{m}^3$, respectively, and the LD_{50} of VX

is 0.04 mg/kg (128, 129). With the following assumptions, 1) respiration of 15 L/minute, 2) a 70 kg body weight, 3) 5 L vascular blood volume, 4) these values represent the effective dose of nerve agent and 5) that all OP appears in the blood stream, the intravascular concentration of a lethal dose of sarin, soman and VX can be estimated at 0.0015, 0.0016 and 0.0020 mM, respectively. Thus, the substrate binding affinity (K_M) is an incredibly important consideration for developing a vascular treatment.

The conventional treatment for exposure to G- and V-agents (not considered separately) involves the intramuscular injection of 2-PAM and atropine upon suspect of neurotoxin exposure. While this is useful in nerve agent poisoning mitigation, this treatment can have toxic effects of their own and are not always successful in treating extreme OP poisonings. The addition of catalytic bioscavengers such as OPH and OPAA to the exposure treatment procedures, have proven extremely effective at mitigating and even preventing the cholinergic effects of toxic OP exposures. . It has been shown that animal models have been dramatically protected against paraoxon and DFP exposure (130). In those studies, OPAA was able to protect mice against DFP concentrations 40-fold higher than the LD_{50} s, and OPH raised the LD_{50} for paraoxon from 400-800 LD_{50} . Both neurotoxin hydrolytic enzymes demonstrated protective effects by the AChE-inhibition protection ratio in vitro, but the protection afforded by OPAA was marginal for both paraoxon and DFP. OPH was far better for both AChE-inhibitors; however, the native enzyme was a very weak protector of demeton-S. (OPAA cannot hydrolyze the P-S bond of phosphorothioates like demeton-S and was not used in

these studies.) The protective effects of the enzymes as bioscavengers have been shown to be related to their kinetic constraints, with the $k_{\text{cat}}/K_{\text{MS}}$ of the enzymes for given substrates are indicative of their protective potential for those substrates. It is of interest to note that the concentration of inhibitor used in each case was well below the K_{MS} of the enzymes, in the micro-molar range. The K_{M} for a substrate, therefore, can be used as an indication of which hydrolytic enzyme should be used in a protective strategy. It is not to say that the k_{cat} of an enzyme is irrelevant in that range, it is that the K_{M} becomes more important as the reaction becomes second order with low substrate concentration. This was verified by demonstrating that genetically-engineered variants of OPH that had enhanced catalytic activities for demeton-S (up to a 36-fold higher P-O bond hydrolysis) also showed up to a 33-fold increase in protection ratios against demeton-S induced inhibition.

It should be noted that the chemical warfare agents are chiral in nature and the stereoisomers with a more potent inhibition of AChE are typically poorer substrates for the hydrolytic enzymes (73). While the substrates used in this study are achiral, the AChE-inhibition protection methodology described here could be easily applied to the evaluation of enzymes with the chemical warfare agents. However, this screening method cannot predict the bioscavenger immunogenicity or clearance rates of the therapeutics, which are important considerations with in vivo exposures. Enzymes can have varying rates of clearance from the vascular system and it is imagined that protection may decrease as the enzymes clear, requiring increased dosing levels. Human enzymes, such as PON1, are often predicted to have long residence times. So, although

OPH is much more efficient with P-O, P-F, and P-S substrates than PON1, OPH is a bacterial enzyme and is predicted to be more rapidly cleared and has a higher potential to be an allergen (131). The screening methods developed here can be used as an important precursor to in vivo pharmacokinetic studies that would be needed to evaluate clearance rates and immunogenicity.

While the low lethal concentrations of the chemical warfare agents indicate that the intravascular concentrations are expected to be well below the K_M values of the enzymes, conversely the OP concentrations for environmental clean up can be much higher and the enzyme reactions are more likely to be at saturating levels. So, for an environmental decontamination scenario, such as a pesticide spill, OPH and OPAA activities can be relatively similar (depending on the OP), but because of OPH's broad substrate utility it remains a more promising enzyme for decontamination applications. The type of application is important for the choice of enzyme and it is the conclusion here that OPH will make a more suitable enzyme for vascular therapy and bioremediation applications.

CHAPTER V

SUMMARY OF APPLICATIONS AND CONCLUSIONS

By December 2006, 19 percent of known chemical weapons stockpiles had been destroyed worldwide, falling far short of the total destruction goal of the CWC. Furthermore, only 40 percent of participating countries had passed the required legislation to outlaw chemical weapons production. Over 80 percent of the chemical weapons destroyed in the world since the treaty came into force in 2001 have been destroyed in the U.S. Nonetheless, the United States General Accounting Office has announced that it does not expect Russia to reach 100 percent destruction until 2027, nor the United States until 2014. Enzyme-based destruction of chemical warfare agents and related environmental issues, such as personal protection, secondary waste and neurotoxic agricultural pesticides, show promise as a supplement, and in some cases an alternative, to current chemical and incineration remediation methods. Several biotechnology utilizations have been initiated and are summarized as follows:

Dermal Protection with Enzyme Towelettes

Most studies of human pesticide exposure have monitored pesticide applicators (such as exterminators and farmers) and children in rural communities. The routes of exposure include inhalation and ingestion; however, these are usually less common than dermal exposure (*132-134*). For example, in a case study involving exterminators in New Jersey, 73 percent of the OP pesticide (chlorpyrifos) intake was through dermal exposure (*132*). Subsequent in vitro studies have evaluated the rate of dermal absorption

of OPs using a pigskin model (135). Within 1 hour of application only 15 percent of applied radiolabeled paraoxon remained on the skin surface or epidermis, approximately 41 percent had absorbed into the dermis and 15 percent had diffused through the skin into the receptor fluid. Within 24 hours 96 percent of the recovered paraoxon had reached the receptor fluid through the skin (135). Other OP's, such as the chemical warfare agent VX, are much more lipophilic and absorb into the skin even more rapidly, which suggests that any dermal protection or decontamination must occur prior to or rapidly after OP exposure.

OP hydrolyzing enzymes can play a protective role as a dermal barrier. As an example of the potential a personal protection application, OPH has been immobilized on cotton fabric in a collaboration with Lynntech (College Station, TX). Genetically modified OPH was attached to cotton fabric using a glutaraldehyde bridge between primary amines (136). When attached to the fabric at approximately $38 \mu\text{g}/\text{cm}^2$, the towellete was able to hydrolyze $21 \mu\text{g}/\text{min}/\text{cm}^2$ of paraoxon and $5.2 \mu\text{g}/\text{min}/\text{cm}^2$ of demeton-S. When used in vivo, large variation between the activity of the OPH towelletes presented as a challenge. The amount of paraoxon required to observe toxicity with dermal application was such that the towellete was overwhelmed and was unable to degrade enough OP in time to prevent toxicity. Despite these limitations the enzymatically active towelletes have potential to be used to decontaminate OP exposed skin or surfaces, thus eliminating the need for special disposal of the used self-decontaminating towelletes. With additional research these catalytically active fabrics

could be incorporated into the uniform of personnel, thus creating an active dermal barrier to OP exposure reducing the overall toxic response of the individual exposed.

Enhanced Enzyme Stability

For enzymes to be effective in various applications they must be incorporated into an appropriate delivery platform, and they must be cost effective for upscale use for commercial, medical or military requirements. The longer the enzyme can last in pre-application and/or field conditions, the lower the cost to maintain catalytic capacity. Shelf life stability of the enzyme can be optimized by considering storage methods, additive composition, and purity levels. The application purposes will vary, and the appropriate enzyme formulations will also vary. For example, direct intravascular enzyme injection will require a pure form of the enzyme. Conversely, if the enzymatic application involves surface treatment, such as enzymatic paint coatings, a less pure form of the enzyme could be used.

For this purpose, various purity fractions and buffer systems were evaluated for activity and storage stability of enzymatic solutions. These studies demonstrated that enzymatic solutions with purity less than 1 percent consistently outperformed the more pure fractions. In every instance, the stability of the activity decreases with purity of the enzyme preparation, ranging from months for the less pure enzyme fraction to less than one day for the most pure. Although additives, e.g. powdered milk, BSA and glycerol, were evaluated as stabilizers, in no instance did their contribution match that of a purity level of less than 1 percent. These less processed enzyme solutions accomplish three objectives, increased amount of activity, enhanced storage stability and lower cost when

compared to pure protein. In parallel studies, a Tris buffer system was the most supportive of enzymatic stability and was relatively inexpensive at \$1.56/L (research scale).

For long-term storage, lyophilization was used to extend the shelf life of the enzymatic preparations. Although this results in some variability in activity yield, the preparations demonstrated activity for up to 4 months after formulation.

Aerosol Fogging Decontamination

It has been possible to use lyophilized enzyme formulations in environmental applications, such as aerosol-based decontamination technology. Decontamination of an enclosed structure in which chemical warfare OP nerve agents may have moved into small crevasses and air ducts, or sensitive electronic equipment is difficult. The application of an enzymatic “fogging” technology was evaluated as a mechanism to address these challenges. In this approach, an aerosol fog mixes with airborne particulates, precipitates out of vapor phase, and deposits on surfaces. Fog-producing equipment is commercially available from Encapsulation Technologies (Richland, WA), which have a patented ultrasonic fogging apparatus and associated methods for aerosol based remediation and hazard mitigation of airborne contaminants (137). In collaboration with scientists at Pacific Northwest National Laboratories, the utility of an OPH-based remediation with the ET fogging technique was evaluated as a novel approach for the decontamination of an OP contaminated structure.

For development purposes, a Collison nebulizer was used to simulate the ET fogger. Although this system has a greatly reduced capacity for fog-generation as

compared to the ET transducer fogger (0.01 ml/cm^2 compared with 1 ml/cm^2), a surprising amount of decontamination was demonstrated. Even with the small amount of enzyme that accumulated on the contaminated surface due to the limited fog output, approximately 30 percent of the 1 g/m^2 paraoxon was degraded. The data obtained from these trials contributes to the fielding of an effective aerosol fog generator that can adequately decontaminate a fixed structure and allow for rapid recovery and reuse of sensitive equipment.

Conclusions

The current technology for OP decontamination involves the application of chemical neutralization or thermal destruction. Typically, chemical decontamination requires greater than stoichiometric amounts of decontaminant, thus necessitating large quantities of decontaminant. Enzyme-based countermeasures are becoming available to protect against and remediate OP contamination. Since OP hydrolyzing enzyme-based systems are catalytic, biodegradable, work under mild conditions, and often can provide benign alternatives to existing caustic or incineration processes. It was the goal of this work to explore the benefits and constraints of enzymes for personal and environmental applications.

The most promising of OP degrading enzymes, OPAA and OPH, have been extensively studied for their varying catalytic properties, and it has been observed that it is important to evaluate the kinetic parameters properly so that the best formulations can be developed. It has become clear the substrate concentration is a critical parameter and OPH was shown to outperform OPAA with all of the OP neurotoxins, including DFP.

For high OP concentrations, OPH is a superior enzyme because of its improved kinetics for P-O and P-S substrates. Furthermore, for low concentration DFP applications OPH is also superior as its second order rate constant is higher. Thus, OPH's kinetic parameters for the tested substrates make it more suited for use as a remediation tool.

The OP degrading enzymes have the lowest catalytic efficiency (k_{cat}/K_M) with the P-S bond substrates; however site-directed mutagenesis to the OPH enzyme greatly improved the catalytic rates for these substrates. Each of the OPH variants that have significantly improved P-S hydrolysis involved a residue change of amino acids at positions 254 or 257. While three of the mutations reported in this study were less effective with the target substrates, the H254S/H257L double mutant showed a 22-fold increase in catalytic activity for demeton-S. These predicted effects demonstrated that rational enzyme modification is a powerful tool in developing enzyme-based countermeasures to OP toxicity.

Because of the disruption of its role in nerve transmission, AChE is pivotal in OP intoxication. For these reasons, an *in vitro* method to directly evaluate and rapidly screen the protective effects of OP degrading enzymes was developed. It was found that the protection of AChE followed the second order rate constants of the protecting enzymes. The designed OPH variants exhibited enhanced AChE protection against the targeted toxicant, demeton-S, further demonstrating that enzyme modification can provide improved alternatives for OP mitigation.

Organophosphorus neurotoxins have ongoing and potential uses as agricultural pesticides and chemical warfare agents. This study aids in the development of OP

degrading enzymes for use against these OP compounds as bioremediation and anti-chemical warfare agent tools. It may be possible in the future to greatly reduce or eliminate the environmental hazard OP neurotoxins pose as these decontamination technologies are improved.

REFERENCES

1. de Clermont, P. (1854) Ueber die Darstellung einiger Aether, *Journal für Praktische Chemie* 63, 72-75, (Translated at WordLingo, http://www.wordlingo.com/en/products_services/wordlingo_translator.html).
2. Sidell, F. R. (1974) Soman and sarin: clinical manifestations and treatment of accidental poisoning by organophosphates, *Clinical Toxicology* 7, 1-17.
3. Sidell, F. R. (1997) Nerve agents, in *Medical Aspects of Chemical and Biological Warfare* (Army, O. o. T. S. G. U. S., Ed.), pp 129-179, Office of The Surgeon General, Borden Institute, Walter Reed Army Medical Center, Washington, DC.
4. Gharahbaghian, L., and Bey, T. (2003) Sarin and other nerve agents of the organophosphate class: properties, medical effects and management, *International Journal of Disaster Medicine* 2, 103-108.
5. Hay, R. (2000) Old dogs or new tricks: chemical warfare at the millennium, *Med Confl Surviv* 16, 37-41.
6. Reigart, J. R., and Roberts, J. R. (1999) *Recognition and Management of Pesticide Poisonings*, Fifth ed., U.S. Environmental Protection Agency, Washington, DC 20460.
7. Bey, T. A., Sullivan, J. B., and Walter, F. G. (2001) Organophosphates and carbamate insecticides, in *Clinical Environmental Health and Toxic Exposure* (Sullivan, J. B., and Krieger, G. R., Eds.), pp 1046-1057, Lippincott Williams & Wilkins, Philadelphia, PA.
8. Ragnarsdottir, K. V. (2000) Environmental fate and toxicology of organophosphate pesticides, *Journal of the Geological Society* 157, 859-876.
9. Freed, V. H., Chiou, C. T., and Schmedding, D. W. (1979) Degradation of selected organophosphate pesticides in water and soil, *Agriculture Food Chemistry* 27, 706-708.
10. DeLano, W. L. (2002) *The PyMOL Molecular Graphics System*, DeLano Scientific, San Carlos, CA, USA.
11. Di Sioudi, B., Grimsley, J. K., Lai, K., and Wild, J. R. (1999) Modification of near active site residues in Organophosphorus hydrolase reduces metal stoichiometry and alters substrate specificity, *Biochemistry* 38, 2866-2872.

12. Kolakowski, J. E., DeFrank, J. J., Harvey, S. P., Szafraniec, L. L., Beaudry, W. T., Lai, K., and Wild, J. R. (1997) Enzymatic hydrolysis of the chemical warfare agent VX and its neurotoxic analogues by organophosphorus hydrolase, *Biocatalysis and Biotransformation* 14, 297-312.
13. Munro, N. B., Talmage, S. S., Griffin, G. D., Waters, L. C., Watson, A. P., King, J. F., and Hauschild, V. (1999) The sources, fate, and toxicity of chemical warfare agent degradation, *Environ. Health Perspect* 107, 9933-9974.
14. Petrikovics, I., Cheng, T. C., Papahadjopoulos, D., Hong, K., Yin, R., DeFrank, J. J., Jaing, J., Song, Z. H., McGuinn, W. D., Sylvester, D., Pei, L., Madec, J., Tamulinas, C., Jaszberenyi, J. C., Barcza, T., and Way, J. L. (2000) Long circulating liposomes encapsulating organophosphorus acid anhydrolase in diisopropylfluorophosphate antagonism, *Toxicol Sci* 57, 16-21.
15. van der Schans, M. J., Lander, B. J., van der Wiel, H., Langenberg, J. P., and Benschop, H. P. (2003) Toxicokinetics of the nerve agent (□)-VX in anesthetized and atropinized hairless guinea pigs and marmosets after intravenous and percutaneous administration, *Toxicology and Applied Pharmacology* 191, 48-62.
16. Van Helden, H. P. M., Trap, H. C., Oostdijk, J. P., Kuijpers, W. C., Langenberg, J. P., and Benschop, H. P. (2003) Long-term, low-level exposure of guinea pigs and marmosets to sarin vapor in air: lowest observable effect level *Toxicology and Applied Pharmacology* 189, 170-079.
17. Benschop, H. P., Konings, C. A. G., Van Genderen, J., and De Jong, L. P. A. (1984) Isolation, *in Vitro* activity, and acute toxicity in mice of the four stereoisomers of soman, *Toxicol. Sci.* 4, 84-95.
18. Di Sioudi, B. D., Miller, C. E., Lai, K., Grimsley, J. K., and Wild, J. R. (1999) Rational design of Organophosphorus hydrolase for altered substrate specificities, *Chemico-Biological Interactions* 119-120, 221-223.
19. Atack, J. R., Perry, E. K., Bonham, J. R., and Perry, R. H. (1986) Molecular forms of acetylcholinesterase and butyrylcholinesterase in the aged human central nervous system, *Journal of Neurochemistry* 47, 263-277.
20. Wilson, B. W., Hooper, M. J., Hansen, M. E., and Neiberg, P. S. (1992) *Organophosphates: Chemistry, Fate and Effects*, Academic Press, San Diego, CA.
21. Gilman, A. G., Goodman, L. S., Rall, T. W., and Murad, F. (1990) *The Pharmacological Basis of Therapeutics*, 8th ed., Pergamon, New York, NY.

22. Ecobichon, D. J. (2001) Toxic effects of pesticides, in *Toxicology: The Basic Science of Poisons* (Klaassen, C. D., Ed.) 6th ed., pp 763-810, McGraw-Hill, New York, NY.
23. O'Callaghan, J. P. (2003) Neurotoxic esterase: not so toxic?, *Nature Genetics* 33, 437-438.
24. Johnson, M. K. (1987) Receptor or enzyme: The puzzle of NTE and organophosphate-induced delayed polyneuropathy, *Trends in Pharmacological Sciences* 8, 174-179.
25. O'Callaghan, J. P. (1994) A potential role for altered protein phosphorylation in the mediation of developmental neurotoxicity, *Neurotoxicology* 15, 29-40.
26. Jensen, K. F., Lapadula, D. M., Anderson, J. K., Haykal-Coates, N., and Abou-Donia, M. B. (1992) Anomalous phosphorylated neurofilament aggregations in central and peripheral axons of hens treated with tri-ortho-cresyl phosphate (TOCP). *Neuroscience Research* 33, 455-460.
27. Damodaran, T. V., Abdel-Rahman, A. A., Suliman, H. B., and Abou-Donia, M. B. (2002) Early differential elevation and persistence of phosphorylated cAMP-response element binding protein (p-CREB) in the central nervous system of hens treated with diisopropyl phosphorofluoridate, an OPIDN-causing compound, *Neurochemical Research* 27, 183-193.
28. Michaelson, D. M., Avissar, S., Kloog, Y., and M., S. (1979) Mechanism of acetylcholine release: possible involvement of presynaptic muscarinic receptors in regulation of acetylcholine release and protein phosphorylation, *PNAS* 76, 6336-6340.
29. Froede, H. C., and Wilson, I. B. (1971) *The Enzymes*, Vol. 5, Academic Press, New York and London.
30. Wilson, I. B. (1959) Molecular complementarity in antidotes for nerve gases, *Ann N Y Acad Sci* 81, 307-316.
31. Wong, L., Radic, Z., Bruggemann, R. J., Hosea, N., Berman, H. A., and Taylor, P. (2000) Mechanism of oxime reactivation of acetylcholinesterase analyzed by chirality and mutagenesis, *Biochemistry* 39, 5750-5757.
32. Lenz, D. E., Broomfield, C. A., Maxwell, D. M., and Cerasoli, D. M. (2001) *Nerve Agent Bioscavengers: Protection Against High- and Low-dose Organophosphorus Exposure*, CRC Press, Boca Raton, FL.

33. Russell, A. J., Berberich, J. A., Drevon, G. F., and Koepsel, R. R. (2003) Biomaterials for mediation of chemical and biological warfare agents, *Annual Review of Biomedical Engineering* 5, 1-27.
34. Jakubowski, H. (2000) Calcium-dependent human serum homocysteine thiolactone hydrolase, *Biological Chemistry* 275, 3957-3962.
35. Mazur, A. (1946) An enzyme in animal tissues capable of hydrolyzing the phosphorus-fluorine bond of alkyl fluorophosphates, *J. Biol. Chem.* 164, 271-289.
36. DeFrank, J. J., and White, W. E. (2002) *Phosphofluoridates: Biological Activity and Biodegradation*, Vol. 3N/2002, Springer Berlin / Heidelberg.
37. Simonian, A. L., Grimsley, J. K., Flounders, A. W., Schoeniger, J. S., Cheng, T. C., DeFrank, J. J., and Wild, J. R. (2001) Enzyme-based biosensor for the direct detection of fluorine-containing organophosphates, *Analytica Chimica Acta* 442, 15-23.
38. Cheng, T. C., Liu, L., Wang, B., Wu, J., DeFrank, J. J., Anderson, D. M., Rastogi, V. K., and Hamilton, A. B. (1997) Nucleotide sequence of a gene encoding an organophosphorus nerve agent degrading enzyme from *Alteromonas haloplanktis*, *Journal of Industrial Microbiology and Biotechnology* 18, 49-55.
39. Baillie, T. A., Moldeus, P., Mason, R. P., and Younes, M. (1993) *Enzymes Interacting with Organophosphorus Compounds*, Elsevier Scientific Publishers Ireland Ltd, Shannon.
40. Davies, H. G., Richter, R. J., Keifer, M., Broomfield, C. A., Sowalla, J., and Furlong, C. E. (1996) The effect of the human serum paraoxonase polymorphism is reversed with diazoxon, soman and sarin, *Nature Genetics* 14, 334-336.
41. Amitai, G., Gaidukov, L., Adani, R., Yishay, S., Yacov, G., Kushnir, M., Teitlboim, S., Lindenbaum, M., Bel, P., Khersonsky, O., Tawfik, D. S., and Meshulam, H. (2006) Enhanced stereoselective hydrolysis of toxic organophosphates by directly evolved variants of mammalian serum paraoxonase, *FEBS Journal* 273 1906-1919.
42. Hoskin, F. C. G. (1971) Diisopropylphosphorofluoridate and tabun: enzymatic hydrolysis and nerve function, *Science* 172, 1243-1245.
43. Hoskin, F. C. G., and Prusch, R. D. (1983) Characterization of a DFP-hydrolyzing enzyme in squid posterior salivary gland by use of soman, DFP and manganous ion, *Comparative Biochemistry and Physiology* 75C, 17-20.

44. Hartleib, J., Geschwindner, S., Scharff, E. I., and Ruterjans, H. (2001) Role of calcium ions in the structure and function of the di-isopropylfluorophosphatase from *Loligo vulgaris*, *Biochemistry* 353, 579-589.
45. Cheng, T. C., DeFrank, J. J., and Rastogi, V. K. (1999) *Alteromonas* prolidase for organophosphorus G-agent decontamination, *Chemico-Biological Interactions* 119-120, 155-462.
46. DeFrank, J. J., Beaudry, W. T., Cheng, T.-C., Harvey, S. P., Stroup, A. N., and Szafraniec, L. L. (1993) Screening of halophilic bacteria and *Alteromonas* species for organophosphorus hydrolyzing enzyme activity, *Chemico-Biological Interactions* 87, 141-148.
47. Ashani, Y., Rothschild, N., Segall, Y., Levanon, D., and Raveh, L. (1991) Prophylaxis against organophosphate poisoning by an enzyme hydrolysing organophosphorus compounds in mice, *Life Sciences* 49, 367-374.
48. Dumas, D. P., Durst, H. D., Landis, W. G., Raushel, F. M., and Wild, J. R. (1990) Inactivation of organophosphorus nerve agents by the phosphotriesterase from *Pseudomonas diminuta*, *Arch Biochem Biophys* 277, 155-159.
49. Rastogi, V. K., DeFrank, J. J., Cheng, T., and Wild, J. R. (1997) Enzymatic hydrolysis of Russian - VX by organophosphorus hydrolase, *Biochemical and Biophysical Research Communications* 241, 294-296.
50. Ashani, Y., Shapira, S., Levy, D., Wolfe, A. D., Doctor, B. P., and Raveh, L. (1991) Butyrylcholinesterase and acetylcholinesterase prophylaxis against soman poisoning in mice, *Biochem Pharmacol.* 41, 37-41.
51. Velan, B., Grosfeld, H., Kronman, C., Leitner, M., Gozes, Y., Lazar, A., Flashner, Y., Marcus, D., Cohen, S., and Shafferman, A. (1991) The effect of elimination of intersubunit disulfide bonds on the activity, assembly, and secretion of recombinant human acetylcholinesterase. Expression of acetylcholinesterase Cys-580----Ala mutant, *J. Biol. Chem.* 266, 23977-23984.
52. Kryger, G., Harel, M., Giles, K., Toker, L., Velan, B., Lazar, A., Kronman, C., Barak, D., Ariel, N., Shafferman, A., Silman, I., and Sussman, J. L. (2000) Structures of recombinant native and E202Q mutant human acetylcholinesterase complexed with the snake-venom toxin fasciculin-II, *Acta Crystallographica Section D* 56, 1385-1394.
53. Sussman, J. L., Harel, M., Frolow, F., Oefner, C., Goldman, A., Toker, L., and Silman, I. (1991) Atomic structure of acetylcholinesterase from *Torpedo californica*: a prototypic acetylcholine-binding protein, *Science* 253, 872-879.

54. Quinn, D. M. (1987) Acetylcholinesterase: enzyme structure, reaction dynamics, and virtual transition states, *Chem. Rev* 87, 955-979.
55. Harel, M., Quinn, D. M., Nair, H. K., Silman, I., and Sussman, J. L. (1996) The x-ray structure of a transition state analog complex reveals the molecular origins of the catalytic power and substrate specificity of acetylcholinesterase, *American Chemical Society* 118, 2340-2346.
56. Gentry, M. K., and Doctor, B. P. (1991) *Cholinesterases: Structure, Function, Mechanism, Genetics, and Cell Biology*, American Chemical Society, Washington, DC.
57. Grisaru, D., Sternfeld, M., Eldor, A., Glick, D., and Soreq, H. (1999) Structural roles of acetylcholinesterase variants in biology and pathology, *European Journal Biochemistry* 264, 672-686.
58. Paulus, J. M., Maigne, J., and Keyhani, E. (1981) Mouse megakaryocytes secrete acetylcholinesterase, *Blood* 58, 1100-1106.
59. Lev-Lehman, E., Deutsch, V., Eldor, A., and Soreq, H. (1997) Immature human megakaryocytes produce nuclear-associated acetylcholinesterase, *Blood* 89, 3644-3653.
60. Soreq, H., Patinkin, D., Lev-Lehman, E., Grifman, M., Ginzberg, D., and Zakut, H. (1994) Antisense oligonucleotide inhibition of acetylcholinesterase gene expression induces progenitor cell expansion and suppresses hematopoietic apoptosis *ex vivo*, *Proceedings of the National Academy of Sciences* 91, 7907-7911.
61. Nicolet, Y., Lockridge, O., Masson, P., Fontecilla-Camps, J. C., and Nachon, F. (2003) Crystal structure of human butyrylcholinesterase and of its complexes with substrate and products, *J Biological Chemistry* 278, 41141-41147.
62. Millard, C. B., Lockridge, O., and Broomfield, C. A. (1998) Organophosphorus acid anhydride hydrolase activity in human butyrylcholinesterase: synergy results in a somanase, *Biochemistry* 37, 237-247.
63. Patinkin, D., Lev-Lehman, E., Zakut, H., Eckstein, F., and Soreq, H. (1994) Antisense inhibition of butyrylcholinesterase gene expression predicts adverse hematopoietic consequences to cholinesterase inhibitors *Cellular and Molecular Neurobiology* 14, 459-473.
64. Lockridge, O., Blong, R. M., Masson, P., Froment, M. T., Millard, C. B., and Broomfield, C. A. (1997) A single amino acid substitution, Gly117His, confers

phosphotriesterase (organophosphorus acid anhydride hydrolase) activity on human butyrylcholinesterase, *Biochemistry* 28, 786-795.

65. Harel, M., Aharoni, A., Gaidukov, L., Brumshtein, B., Khersonsky, O., Meged, R., Dvir, H., Ravelli, R. B. G., McCarthy, A., Toker, L., Silman, I., Sussman, J. L., and Tawfik, D. S. (2004) Structure and evolution of the serum paraoxonase family of detoxifying and anti-atherosclerotic enzymes, *Nature Structural & Molecular Biology* 11, 412-419.
66. Mackness, B., Mackness, M. I., Arrol, S., Turkie, W., and Durrington, P. N. (1997) Effect of the molecular polymorphisms of human paraoxonase (PON1) on the rate of hydrolysis of paraoxon., *British Journal of Pharmacology* 122, 265-268.
67. Teiber, J. F., Draganov, D. I., and La Du, B. N. (2004) Purified human serum PON1 does not protect LDL against oxidation in the *in vitro* assays initiated with copper or AAPH, *Journal of Lipid Research* 45, 2260-2268.
68. Koepke, J., Scharff, E. I., Lücke, C., Rüterjans, H., and Fritzsche, G. (2002) Atomic resolution crystal structure of squid ganglion DFPase, *Acta Cryst. D* 58, 1757-1759.
69. Wang, F., Xiao, M., and Mu, S. (1993) Purification and properties of a diisopropyl-fluorophosphatase from squid *Todarodes pacificus steenstrup.*, *J Biochem Toxicol.* 8, 161-163.
70. Scharff, E. I., Lücke, C., Fritzsche, G., Koepke, J., Hartleib, J., Dierla, S., and Rüterjans, H. (2001) Crystallization and preliminary X-ray crystallographic analysis of DFPase from *Loligo vulgaris*, *Biological Crystallography* 57, 148-149.
71. Cheng, T. C., Harvey, S. P., and Stroup, A. N. (1993) Purification and properties of a highly active organophosphorus acid anhydrolase from *Alteromonas undina*, *Appl Environ Microbiol* 59, 3138-3140.
72. Cheng, T. C., Harvey, S. P., and Chen, G. L. (1996) Cloning and expression of a gene encoding a bacterial enzyme for decontamination of organophosphorus nerve agents and nucleotide sequence of the enzyme, *Appl Environ Microbiol* 62, 1636-1641.
73. Hill, C. M., Wu, F., Cheng, T. C., DeFrank, J. J., and Raushel, F. M. (2000) Substrate and stereochemical specificity of the organophosphorus acid anhydrolase from *Alteromonas sp. JD6.5* toward p-nitrophenyl phosphotriesters, *Bioorg Med Chem Lett* 10, 1285-1288.

74. DeFrank, J. J. (1991) Organophosphorus cholinesterase inhibitors: detoxification by microbial enzymes, *Application of Enzyme Biotechnology*, 165-180.
75. Harper, L. L., McDaniel, C. S., Miller, C. E., and Wild, J. R. (1988) Dissimilar plasmids isolated from *Pseudomonas diminuta* MG and *Flavobacterium* sp. contain identical opd genes, *Applied Environmental Microbiology* 54, 2586-2589.
76. McDaniel, C. S., Harper, L. L., and Wild, J. R. (1988) Cloning and sequencing of a plasmid-borne gene (opd) encoding a phosphotriesterase, *J Bacteriol* 170, 2306-2311.
77. Mulbry, W. W., Karns, J. S., Kearney, P. C., Nelson, J. O., McDaniel, C. S., and Wild, J. R. (1986) Identification of a plasmid-borne parathion hydrolase gene from *Flavobacterium* sp. by southern hybridization with opd from *Pseudomonas diminuta*, *Appl Environ Microbiol* 51, 926-930.
78. Dumas, D. P., Caldwell, R., Wild, J. R., and Raushel, F. M. (1989) Purification and properties of the phosphotriesterase from *Pseudomonas diminuta*, *J Biological Chemistry* 264, 19659-19665.
79. Grimsley, J. K., Scholtz, J. M., Pace, C. N., and Wild, J. R. (1997) Organophosphorus hydrolase is a remarkably stable enzyme that unfolds through a homodimeric intermediate, *Biochemistry* 36, 14366-14374.
80. Vanhooke, J. L., Benning, M. M., Raushel, F. M., and Holden, H. M. (1996) Three dimensional structure of the zinc-containing phosphotriesterase with the bound substrate analog diethyl 4-methylbenzylphosphonate, *Biochemistry*, 6020-6025.
81. Benning, M. M., Kuo, J. M., Raushel, F. M., and Holden, H. M. (1994) Three dimensional structure of phosphotriesterase: an enzyme capable of detoxifying organophosphate nerve agents, *Biochemistry* 33, 15001-15007.
82. Benning, M. M., Kuo, J. M., Raushel, F. M., and Holden, H. M. (1995) Three-dimensional structure of the binuclear metal center of phosphotriesterase, *Biochemistry* 34, 7973-7978.
83. Hong, S., Mullins, L. S., Shim, H., and Raushel, F. M. (1997) Mechanism-based inhibitors for the inactivation of the bacterial Phosphotriesterase, *Biochemistry* 36, 9022-9028.
84. Omburo, G. A., Kuo, J. M., Mullins, L. S., and Raushel, F. M. (1992) Characterization of the zinc binding site of bacterial Phosphotriesterase, *Journal of Biological Chemistry* 267, 13278-13283.

85. Grimsley, J., Calamini, B., Wild, J., and Mesecar, A. (2005) Structural and mutational studies of organophosphorus hydrolase reveal a cryptic and functional allosteric-binding site, *Archives of Biochemistry and Biophysics* 442, 169-179.
86. Benning, M. M., Hong, S. B., Raushel, F. M., and Holden, H. M. (2000) The binding of substrate analogs to phosphotriesterase, *Journal of Biological Chemistry* 75, 30556-30560.
87. Hong, S., and Raushel, F. M. (1996) Metal-substituted interactions facilitate the catalytic activity of the bacterial Phosphotriesterase, *Biochemistry* 35, 10904-10912.
88. Braue, E. H., Jr. (1999) Development of a reactive topical skin protectant, *Journal of Applied Toxicology* 19, S47-S53.
89. Romano, J. A., Jr., and Filbert, M. G. (1999) Historical overview of topical skin protectant development, *Journal of Applied Toxicology* 19, S39.
90. Shumpert, B., Watson, A., Rogers, G., Sorensen, J., Long, J., and Brooks, R. (1996) Planning Guidance for the Chemical Stockpile Emergency Preparedness Program, Oak Ridge National Laboratory, Oak Ridge, Tenn.
91. Macintyre, A. G., Christopher, G. W., Eitzen, E., Jr., Gum, R., Weir, S., DeAtley, C., Tonat, K., and Barbera, J. A. (2000) Weapons of mass destruction events with contaminated casualties: effective planning for health care facilities, *Journal of the American Medical Association* 283, 242-249.
92. Vogt, B. M., and Sorensen, J. H. (2002) How Clean is Safe? Improving the Effectiveness of Decontamination of Structures and People Following Chemical and Biological Incidents, (Program, U. S. D. o. E. C. a. B. N. S., Ed.), pp 1-115, Oak Ridge National Laboratory, Oak Ridge, Tenn.
93. Pei, L., Omburo, G. A., McGuinn, W. D., Petrikovics, I., Dave, K. I., Raushel, F. M., Wild, J. R., DeLoach, J. R., and Way, J. L. (1994) Encapsulation of phosphotriesterase within murine erythrocytes, *Toxicology and Applied Pharmacology* 124, 296-301.
94. Pei, L., Petrikovics, I., and Way, J. L. (1995) Antagonism of the lethal effects of paraoxon by carrier erythrocytes containing phosphotriesterases, *Fundamental and Applied Toxicology* 28, 209-214.
95. Siegel, J. (2006) Farewell to arms, *Bulletin of the Atomic Scientists* 62, 24-25.
96. United States Army Chemical Materials Agency, (2007) Agent Destruction Status.

97. Ember, L. R. (2006) A milestone of note, *Chemical and Engineering News* 84, 87-89.
98. Ember, L. R. (2007) Chemical arms treaty at 10, *Chemical and Engineering News* 85, 23-26.
99. National Homeland Security Research Center, (2005) *Compilation of Available Data on Building Decontamination Alternatives*, pp 1-197, Science Applications International Corporation, Reston, VA 20190.
100. Simcox, J., Fenske, R. A., Wolz, S. A., Lee, I. C., and Kalman, D. A. (1995) Pesticides in household dust and soil: exposure pathways for children of agricultural families., *Environ Health Perspect* 103, 1126-1134.
101. Horne, I., Sutherland, T. D., Harcourt, R. L., Russell, R. J., and Oakeshott, J. G. (2002) Identification of an opd (organophosphate degrading) gene in an *Agrobacterium* isolate, *Applied and Environmental Microbiology* 68, 3371-3376.
102. DeFrank, J. J., and Cheng, T. C. (1991) Purification and properties of an organophosphorus acid anhydrase from a halophilic bacterial isolate, *Journal of Bacteriology* 173, 1938-1943.
103. Cheng, T. C., and Calomiris, J. J. (1996) A cloned bacterial enzyme for nerve agent decontamination, *Enzyme and Microbial Technology* 18:597-601, 1996 18, 597-601.
104. Serdar, C. M., Gibson, D. T., Munnecke, D. M., and Lancaster, J. H. (1982) Plasmid involvement in parathion hydrolysis by *Pseudomonas diminuta*, *Appl. Environ. Microbiol.* 44, 246-249.
105. Dumas, D. P., Wild, J. R., and Raushel, F. M. (1989) Diisopropylfluorophosphate hydrolysis by a phosphotriesterase from *Pseudomonas diminuta*, *Biotechnology and Applied Biochemistry* 11, 235-243.
106. Lai, K., Dave, K. I., and Wild, J. R. (1994) Bimetallic binding motifs in organophosphorus hydrolase are important for catalysis and structural organization, *J. Biol. Chem.* 269, 16579-16584.
107. Kuo, J. M., and Raushel, F. M. (1994) Identification of the histidine ligands to the binuclear metal center of phosphotriesterase by site-directed mutagenesis, *Biochemistry* 33, 4265-4272.
108. Segel, I. H. (1993) Graphical Determination of K_M and V_{max} , in *Enzyme Kinetics* (John Wiley & Sons, I., Ed.), Wiley-Interscience, New York, NY.

109. Chen-Goodspeed, M., Sogorb, M. A., Wu, F., Hong, S. B., and Raushel, F. M. (2001) Structural determinants of the substrate and stereochemical specificity of phosphotriesterase, *Biochemistry* 40, 1325-1331.
110. Li, W. S., Lum, K. T., Chen-Goodspeed, M., Sogorb, M. A., and Raushel, F. M. (2001) Stereoselective detoxification of chiral sarin and soman analogues by phosphotriesterase, *Bioorganic & Medicinal Chemistry* 9, 2083-2091.
111. Cho, C. M. H., Mulchandani, A., and Chen, W. (2002) Bacterial cell surface display of organophosphorus hydrolase for selective screening of improved hydrolysis of organophosphate nerve agents, *Applied and Environmental Microbiology* 64, 2026-2030.
112. Cho, C. M. H., Mulchandani, A., and Chen, W. (2004) Altering the substrate specificity of organophosphorus hydrolase for enhanced hydrolysis of chlorpyrifos, *Applied and Environmental Microbiology* 70, 4681-4685.
113. Hill, C. M., Li, W. S., Thoden, J. B., Holden, H. M., and Raushel, F. M. (2003) Enhanced degradation of chemical warfare agents through molecular engineering of the phosphotriesterase active site, *Journal of American Chemical Society* 125, 8990-8991.
114. Kuo, J. M., Chae, M. C., and Raushel, F. M. (1997) Perturbations to the active site of phosphotriesterase, *Biochemistry* 36, 1982-1988.
115. Roodveldt, C., and Tawfik, D. S. (2005) Directed evolution of phosphotriesterase from *Pseudomonas diminuta* for heterologous expression in *Escherichia coli* results in stabilization of the metal-free state, *Protein Engineering, Design & Selection* 18, 51-58.
116. Watkins, L. M., Kuo, J. M., Chen-Goodspeed, M., and Raushel, F. M. (1997) A combinatorial library for the binuclear metal center of bacterial phosphotriesterase, *PROTEINS: Structure, Function, and Genetics* 29, 553-561.
117. Watkins, L. M., Mahoney, H. J., McCulloch, J. K., and Raushel, F. M. (1997) Augmented hydrolysis of diisopropyl fluorophosphate in engineered mutants of phosphotriesterase, *Biological Chemistry* 272, 25596-25601.
118. Yang, H., Carr, P. D., McLoughlin, S. Y., Liu, J. W., Horne, I., Qiu, X., Jeffries, C. M. J., Russell, R. J., Oakeshott, J. G., and Ollis, D. L. (2003) Evolution of an organophosphate-degrading enzyme: a comparison of natural and directed evolution, *Protein Engineering* 16, 135-145.

119. Lai, K. (1994) Modification and characterization of the neurotoxic substrate specificity of organophosphorus hydrolase, in *Toxicology*, p 103, Texas A&M University, College Station, TX.
120. Adkins, S., Gan, K. N., Mody, M., and La Du, B. N. (1993) Molecular basis for the polymorphic forms of human serum paraoxonase/arylesterase: glutamine or arginine at position 191, for the respective A or B allozymes, *Am. J. Hum. Genet.*, 52598-52608.
121. Furlong, C. E., Costa, L. G., Hassett, C., Richter, R. J., Sundstrom, J. A., Adler, D. A., Disteche, C. M., Omiecinski, C. J., Chapline, C., and Crabb, J. W. (1993) Human and rabbit paraoxonases: purification, cloning, sequencing, mapping and role of polymorphism in organophosphate detoxification, *Chem Biol Interact* 87, 35-48.
122. Humbert, R., Adler, D. A., Disteche, C. M., Hassett, C., Omiecinski, C. J., and Furlong, C. E. (1993) The molecular basis of the human serum paraoxonase activity polymorphism, *Nat. Genet.* 3, 73-76.
123. Smolen, A., Eckerson, H. W., Gan, K. N., Hailat, N., and La Du, B. N. (1991) Characteristics of the genetically determined allozymic forms of human serum paraoxonase/arylesterase, *Drug Metab. Dispos.* 19, 107-112.
124. Zheng, J., Zhou, Z. J., Zheng, G., Dai, X. F., Gu, X. A., (2005) Relationship between the polymorphism of carboxylic esterases and genetic susceptibility to organophosphates pesticides exposure, *Zhonghua Lao Dong Wei Sheng Zhi Ye Bing Za Zhi* 23, 83-86.
125. Lenz, D. E., Brimfield, A. A., and Cook, L. A. The development of immunoassays for detection of chemical warfare agents, in *Development and Applications of Immunoassays for Environmental Analysis* (Aga, D., and Thurman, E. M., Eds.), p 77, ACS Books, Washington, DC.
126. Hanke, D. W., and Overton, M. A. (1991) Phosphorylation kinetic constants and oxime-induced reactivation in acetylcholinesterase from fetal bovine serum, bovine caudate nucleus, and electric eel, *Toxicol Environ Health* 34, 141-156.
127. Langenberg, J. P., VanDijk, C., Sweeney, R. E., Maxwell, D. M., Dejong, L. P. A., and Benschop, H. P. (1997) Development of a physiologically based model for the toxicokinetics of C(+/-)P(+/-)-soman in the atropinized guinea pig, *Archives of Toxicology* 71, 320-331.
128. Munro, N. B., Ambrose, K. R., and Watson, A. P. (1994) Toxicity of the organophosphate chemical warfare agents GA, GB, and VX: implications for public protection, *Environ Health Perspect* 102, 18-38.

129. Försvarets Forskningsanstalt, Swedish Defence Research Establishment, (1992) *A FOA Briefing Book on Chemical Weapons*, Vol. S-172 90, FOA, Stockholm, Sweden.
130. Petrikovics, I., Wales, M. E., Jaszberenyi, J. C., Budai, M., Baskin, S. I., Szilasi, M., Logue, B. A., Chapela, P., and Wild, J. R., . (2007) Enzyme-based intravascular defense against organophosphorus neurotoxins: synergism of dendritic-enzyme complexes with 2-PAM and atropine, *Nanotoxicology* 1, 85-92.
131. Rochu, D., Chabriere, E., and Mason, P. (2007) Human paraoxonase: a promising approach for pre-treatment and therapy of organophosphorus poisoning, *Toxicology and Applied Pharmacology* 233, 47-59.
132. Fenske, R. A., and Elkner, K. P. (1990) Multi-route exposure assessment and biological monitoring of urban pesticide applicators during structural control treatments with chlorpyrifos, *Toxicol Ind Health*. 6, 349-371.
133. Lu, C., Knutson, D. E., Fisker-Andersen, J., and Fenske, R. A. (2001) Biological monitoring survey of organophosphorus pesticide exposure among preschool children in the Seattle metropolitan area, *Environmental Health Perspectives* 109, 299-303.
134. Perry, M. J., and Layde, P. M. (1998) Sources, routes, and frequency of pesticide exposure among farmers, *Journal of Occupational & Environmental Medicine* 40, 697-701.
135. Reifenrath, W. G., Hawkins, G. S., and Kurtz, M. S. (1991) Percutaneous penetration and skin retention of topically applied compounds: an *in vitro-in vivo* study, *Journal of Pharmaceutical Sciences* 80, 526-532.
136. Grimsley, J. K., Singh, W. P., Wild, J. R., and Giletto, A. (2001) A novel, enzyme-based method for the wound-surface removal and decontamination of organophosphorus nerve agents, in *ACS Symposium Series*, pp 35-49, American Chemical Society, Washington DC.
137. Berg, R. O., Robles, P., Rigby, W. F., and Albers, J. (1999) Method and Apparatus for Encapsulating Particulates, US.

VITA

Name: **Rory James Kern**

Address: NIH Fellowship (Toxicology of Environmental Contaminants
Training Grant, NIEHS T32 ES07273, 2003-2007)

Department Biochemistry & Biophysics
c/o of Dr. James Wild
Texas A&M University
College Station, TX 77843-2128
phone: (979) 845-9459
fax: (979) 845-9274
e-mail: rjk3307@yahoo.com

Education: B.S. (Biochemistry) Texas A&M University, 2001 GPA 3.086
Ph.D. (Toxicology) Texas A&M University, 2007 GPR: 3.75

Presentations

Enzyme Linked Towelettes for Protection From Dermal Organophosphate
Exposure: Toxicology Student Seminar (August 2004)
Enzymatic Bioaerosol Decontamination of Enclosed Structures: Toxicology
Student Seminar (August 2005)
Encapsulated Enzyme Bioscavengers Provide an Intravascular Defense Against
OP-Neurotoxins: Toxicology Student Seminars (August 2006)

Honors And Awards:

Distinguished Student (1996)
Sul Ross Scholarship (1996-1997)